let. - vol. 50 (2004) št. - no. 12

STROJNIŠKI VESTNIK 12

JOURNAL OF MECHANICAL ENGINEERING

strani - pages 567 - 640

ISSN 0039-2480 . Stroj V . STJVAX

cena 800 SIT

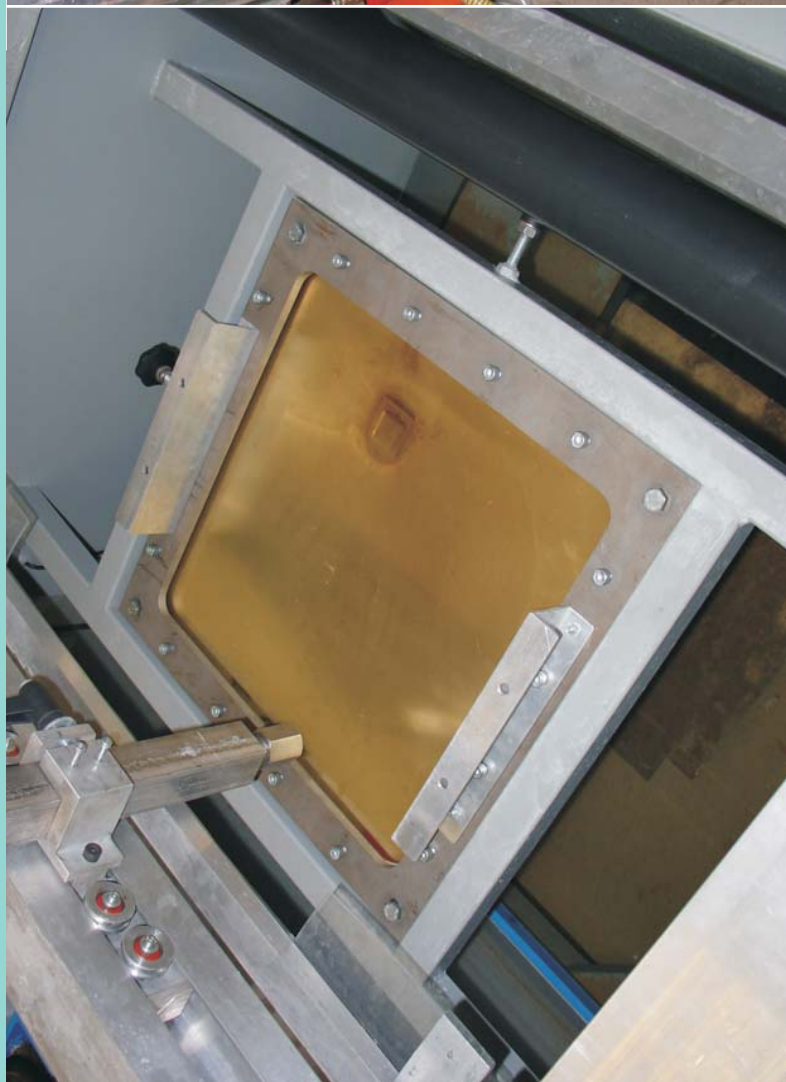

© Strojniški vestnik 50(2004)12, 567
Mesečnik
ISSN 0039-2480

© Journal of Mechanical Engineering 50(2004)12,567
Published monthly
ISSN 0039-2480

Vsebina
Contents

Strojniški vestnik - Journal of Mechanical Engineering
letnik - volume 50, (2004), številka - number 12

© Strojniški vestnik 50(2004)12,568-579
ISSN 0039-2480
UDK 621.9.02
Izvirni znanstveni članek (1.01)

© Journal of Mechanical Engineering 50(2004)12,568-579
ISSN 0039-2480
UDC 621.9.02
Original scientific paper (1.01)

Spremljanje obrabe rezalnega orodja z uporabo signalov krmilnega sistema

Monitoring Cutting-Tool Wear Using Signals from the Control System

Tihomir Mulc - Toma Udiljak - Franci Čuš - Matjaž Milfelner

Varnost in zanesljivost delovanja industrijskih obdelovalnih postopkov je pomemben pogoj za gospodarsko donosnost. Motnje v postopku, kakor so kolizija, preobremenitev, izpad in obraba orodja, niso popolnoma razumljive in povzročajo napake proizvodnega sistema. Da bi preprečili vpliv različnih motenj obdelovalnega postopka, npr. obrabo in lom orodja, posvečajo moderni tehnološki sistemi posebno pozornost napovedovanju stanja rezalnega orodja. Številne teorije o spremljanju skušajo klasificirati in pojasniti obrabo orodja, vendar še nobena ni dala zadovoljivih rezultatov, ki bi hkrati zagotovila prilagodljivo in preprosto obvladovanje postopka za sprejemljivo ceno. Brezzančna struktura modernega ali digitalnega krmiljenja odpira nove možnosti in perspektive v tem pogledu. V mnogih primerih kombinacija signalov digitalne opreme in internih podatkov krmilnega sistema stroja, skupaj z izpolnjenimi metodami analize signalov, lahko nadomesti zunanje sisteme za spremljanje. Vgradnje programskega modula za nadzor postopka v krmilni sistem stroja omogoča hitre reakcije, če se pojavijo motnje postopka, in sicer brez dodatnega povečanja računalniške opreme.Ta prispevek preučuje občutljivost signalov v nadzornem sistemu na postopke obrabe rezalnega orodja pri čelnem struženju.

(Ključne besede: nadzor stanj, sistemi krmilni, občutljivost signalov, struženje, obraba orodij)

The safety and reliability of operation of industrial manufacturing processes is a very important prerequisite for economic production. Process disturbances such as collision, overload, breakdown and tool wear are not yet fully understood, and cause production-system failures. In order to prevent the effects of excess wear or eventual tool breakdown, modern technological systems pay particular attention to predicting the condition of tool. Numerous theories of monitoring have tried to classify and explain tool wear, but none have given completely satisfactory results as yet, while at the same time ensuring flexible, simple and cost-effective process control. The open structure of modern digital control opens up new possibilities: in many cases the combination of digital plant signals and the internal data of the machine control system, along with advanced methods of signal analysis, can replace external control systems. The integration of a process-control software module into the machine control system allows fast reactions, should there be any process disturbances, without any additional hardware expansion. This paper studies the sensitivity of signals contained in the control system to the cutting-tool wear processes in face turning.

(Keywords: condition monitoring, control systems, sensitivity analysis, turning, tool wear)

0 UVOD

Obdelovalni stroji in proizvodni sistemi so nosila razvoja nove proizvodne opreme, to pomeni, da je stroj tehnična struktura, vsota mnogih tehnologij in je konstruiran z namenom, da preoblikuje material v funkcionalne izdelke, koristne za ljudi. V zadnjih letih so obdelovalni stroji in proizvodni sistemi doživeli velike spremembe, v največji meri zaradi razvoja informatike in prilagodljive avtomatizacije. Premik od klasičnih v smeri izpopolnjenih, hitrih,

0 INTRODUCTION

Machine tools and production systems are the generators of new production equipment, i.e., the machine is the technical structure, a collection of many technologies, designed with the aim of reshaping raw materials into functional units that are useful to people. Over recent years, machine tools and production systems have gone through dramatic changes caused, to a large extent, by the development of information technology and flexible automation.

prilagodljivih in zelo učinkovitih obdelovalnih celic je očiten. Na področju odrezovanja je v zadnjih letih obdelava z velikimi hitrostmi postala standard. Spremenila je odnos do strojne obdelave, rezalnih orodij in obdelovalnih strojev. Da bi dosegli velike hitrosti strojne obdelave, je potreben razvoj dinamičnih strojev lahke zgradbe in majhne mase, zgoščene izvedbe in velike togosti. V takih okoliščinah je namestitev motornega vretena obdelovalnega stroja z visokimi frekvencami vrtenja, hlajenjem s tekočino, z avtomatskim sistemom vpenjanja orodja (HSK - gnezdenje), podajalnimi zobniki z digitalnimi pogonskimi sistemi in hitrimi vodili postala standardna.

Krmiljenje obdelovalnih strojev z velikimi hitrostmi je zelo zahtevna naloga, ki terja močne in učinkovite sisteme za spremljanje in diagnosticiranje postopkov obdelave. Glavna pogoja za dobro izvajanje spremljanja postopka obdelave sta poznavanje postopka in izvajanje ustreznih ukrepov. Ker je postopek obdelave brezzančni sistem in ni popolnoma definiran, lahko pride do motenj v postopku, ki niso povsem razumljive in jih ni mogoče napovedati. Glavni parameter, ki povzroča nepričakovane motnje v sistemu obdelave in med samo obdelavo, je obraba rezalnega orodja [1], ki ga povzroča interakcija med orodjem, obdelovancem in obdelovalnimi razmerami. Raznolikost vhodnih parametrov, nenehni razvoj novih materialov, geometrijska oblika in novi materiali orodja pa tudi večja hitrost obdelave [2], s hkratnim uvajanjem vedno strožjih standardov glede varnosti, zapletejo spremljanje krmilnega postopka [3], tako da je spremljanje postopka obdelave ena najzahtevnejših nalog pri nadaljnjem razvoju obdelovalnih sistemov.

1 SISTEMI ZA SPREMLJANJE OBDELOVALNEGA POSTOPKA

Pri postopkih obdelave z odvzemanjem materiala se uporabljajo različne metode za spremljanje in nadzorovanje postopkov, vendar je glavni vir za spremljanje postopka signal zaznavala. Zaznavalo pretvori eno fizikalno vrednost v drugo (sila, akustična emisija, vibracije in električni signal) [4]. Vgrajena zaznavala morajo biti podprta z dodatno programsko opremo za analizo in sprejemanje signalov z ustreznim sistemom za ovrednotenje podatkov. Dodatna oprema mora biti prilagojena posameznemu stroju in obdelovalnim opravilom. S tehničnega vidika [5] je povezava zunanjih sistemov in krmilnega sistema stroja vedno povezana z določenimi težavami, tako da je mogoče pri uporabi klasičnih sistemov za spremljanje poudariti nekaj slabih strani:

- potrebne so dodatne naprave in zaznavala, ki morajo biti prilagojeni stroju,
- zunanji sistemi dajejo dobre rezultate šele po dobri pripravi,

The shift from classical towards sophisticated, fast, flexible and high-efficiency machining cells is obvious. In the field of material removal, over recent years, high-speed machining has become a standard process. It has changed attitudes towards machining, cutting tools and machine tools. In order to achieve high-speed machining, the development of dynamic machines with a light structure and low mass, a compact construction and high rigidity is required. As a result the installation of motor spindles with high rotation frequencies, liquid-cooled, with an automatic tool clamping system (HSK – nesting), feed gears equipped with digital drive systems and fast guides have become standard practise.

The control of high-speed machines is a very demanding task that requires powerful and efficient systems of process monitoring and diagnostics. The basic conditions for good management of machining monitoring include knowledge about the process state and the undertaking of adequate actions. Since the machining process is an open system and is not fully defined, process disturbances that are not completely understandable or predictable might be encountered. The main parameter generating unexpected disturbances in a machining system during machining is the process of cutting-tool wear [1], which is caused by the interaction between the tool, the work piece and the machining conditions. The diversity of input parameters, the constant development of new materials, new geometries and new tool materials, as well as higher machining speeds [2], with the simultaneous setting of increasingly strict standards regarding safety, complicate control process monitoring [3], so that process monitoring remains one of the most demanding tasks in further development of machining systems.

1 MACHINING-PROCESS MONITORING SYSTEMS

In material-removal processes different methods for monitoring and controlling processes are applied, but the main monitoring source is the signal obtained from the sensor. The sensor converts one physical value into another (force, sound emission, vibrations into electrical signal) [4]. Built-in sensors have to be supported by additional equipment for analysis and the reception of signals with an appropriate assessment system. Additional equipment needs to be adapted to the particular machine and the machining operations. From the technical point of view [5], the linking of external systems and the machine control system is always related to certain difficulties, so that some of the disadvantages can be highlighted when using conventional monitoring systems:

- additional devices and sensors are necessary, and they need to be adapted to the machine,
- external systems provide good exploitation results only after good preparation,

- ne uporabljajo se razpoložljivi podatki, ki jih vsebuje krmilje,
- vzdrževanje sistema za spremljanje in definiranje parametrov je pogosto zahtevno in zapleteno.

Ugotoviti je mogoče stanje sistema kadar se v merilnem signalu pojavi napaka. Vpliv na merilni signal naj ne bi bil samo teoretičen, ampak bi moral delovati na tok signalov z možnostjo ponovitve (obraba - sile, vibracije, zvočna emisija itn.). Žal ni vedno (če sploh kdaj) mogoče ugotoviti preproste povezave med stanjem sistema in signalom, toda iz različnih razlogov lahko pride do sprememb signala, tako da razlaga napak znatno vpliva na učinkovitost in zanesljivost sistema za spremljanje. Razvoj metod in sistemov zaznaval se nagiba k temu, da zagotovi največjo zanesljivost v večini pogojev obdelave in izboljšanje občutljivosti na opazovani pojav [6]. Glede zahtevane zanesljivosti sistema za spremljanje morajo zaznavala izpolniti različne potrebe glede zaznavanja stanja. Po eni strani je treba napake zaznati zelo hitro, po drugi strani pa morajo biti odločitve zelo zanesljive, da se popravijo izgube zaradi lažnih opozoril. Problemi analiz ropota in pogosto nasprotujoče si informacije o zaznavah pri analizi signalov so središče raziskav, kajti tudi najuspešnejša strategija odločanja je omejena, če vhodni podatki niso zadosti obsežni in zanesljivi.

Po prejšnjih izkušnjah se zdi, da metode analiziranja posameznih signalov ne morejo zagotoviti večjih izboljšav v sistemih za spremljanje postopkov, tako da so najnovejše raziskave usmerjene v razvoj večzaznavalnih sistemov z namenom, da bi dobili boljše, bolj zanesljive in varnejše podatke o stanju nadzorovanega postopka ali sistema. Uporaba izpopolnjenih tehnologij sprejemanja in analiziranja signalov, kakršni so ocenitev parametrov, nevronska mreža [8], prepoznavanje vzorcev, mehka logika pomenijo mogoče možne pripomočke, kadar je treba obdelovati dvoumne signale in šume. Torej tudi moderni brezzančni računalniški numerični krmilni sistem (RNK) ponuja nekaj možnosti za vzpostavitev preprostih in poceni sistemov za spremljanje, s katerimi ni težko ravnati.

2 ZGRADBA BREZZANČNIH KRMILNIH SISTEMOV

Nadzorna naprava znatno vpliva na zmogljivost obdelovalnih sistemov. Težnje pri razvijanju nadzornih sistemov so usmerjene k vzpostavitvi inteligentnega sistema z vgrajenimi moduli za prilagoditev dinamičnim spremembam okolja, možnostim vključitve novih uporabniških uporab in motnostim učenja iz postopka. Definicija brezzančnega RNK sistema je lahko raznolika, odvisno od izdelovalcev opreme in uporabnikov RNK obdelovalnih strojev. Tipični brezzančni RNK sistem

- available information contained in the control is not used,
- maintaining the monitoring system and defining the parameters is often demanding and complicated.

It is possible to identify the system condition when failure shows in the measuring signal. The influence of failure on the measuring signal should not only be theoretical, but should act on the signal flow with the possibility of reproduction (wear forces, vibrations, sound emission, etc.). Unfortunately, it is not always (if ever) possible to establish a simple link between the condition of the system and the signal, but signal changes can result due to various causes, so that the interpretation of failures significantly influences the efficiency and reliability of the monitoring system. The development of sensory methods and systems is led by the tendency to realize the maximum reliability in most machining conditions, and the improvement of sensitivity on the observed phenomenon [6]. Regarding the required reliability of the monitoring system, sensors have to satisfy various needs with regard to detection of the condition. On the one hand, failures need to be detected very quickly, and on the other hand, the decisions have to be trustworthy, so as to eliminate losses due to false alarms. The problems of noise analyses, and the often contradictory information of senses in signal analysis, represent the focus of research, since even the most successful strategy of decision-making is limited if the input information is not sufficiently extensive and reliable.

Based on previous experiences, it seems that the methods of analyzing particular signals cannot provide any major improvements to the monitoring system, so that the latest research is directed to the development of multi-sensory systems with the aim of obtaining better, more reliable and safer information on the condition of the monitored process or system. The application of advanced technologies of reception and analysis of signals, such as the assessment of parameters, neural networks [8], pattern recognition, fuzzy logic, represent possible tools regarding the need to process ambiguous signals and noises. This also means that a modern, open CNC control system offers some possibilities for establishing simple, inexpensive and easy-to-manage monitoring systems.

2 THE STRUCTURE OF OPEN CONTROL SYSTEMS

The controller significantly affects the capabilities of machining systems. The trends in developing control systems are directed towards establishing an intelligent system with integrated modules for adaptation to the dynamic environmental changes, the possibilities of integration of new users' applications, and the learning possibilities from the process. The definition of an open CNC system can vary, depending on the equipment manufacturers and the CNC machine tools' users. A typical CNC open

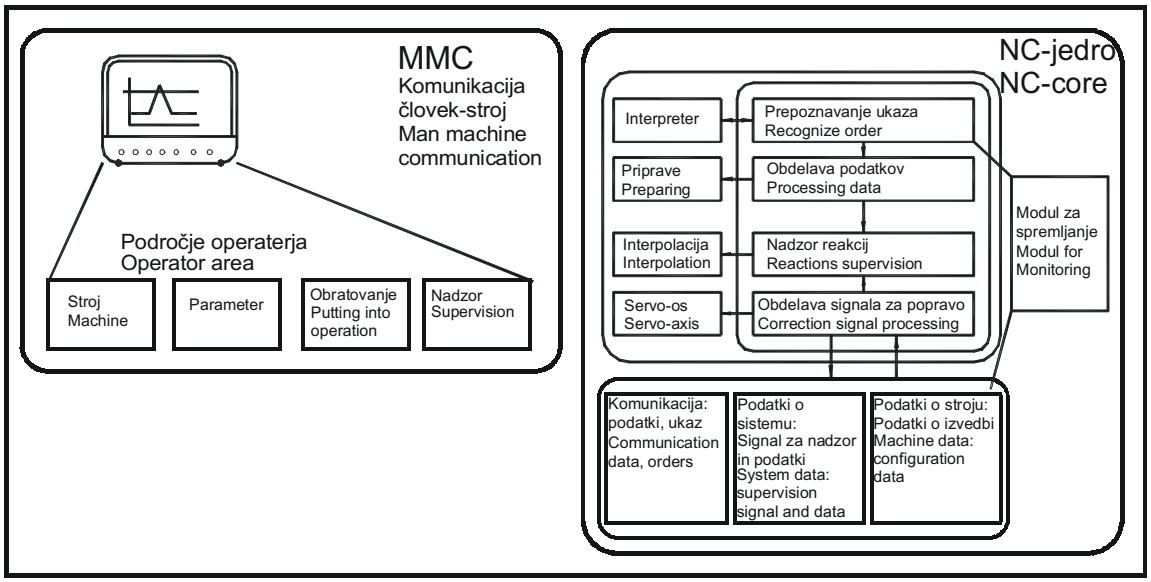

Sl. 1. *Zgradba brezzančnega nadzornega sistema (3)*
Fig. 1. *Structure of the open control system (3)*

ima standardne funkcije, ki se na splošno uporabljajo za vse obdelovalne stroje (sl. 1).

Odvisno od kinematike stroja in njegovih specifičnih karakteristik imajo lahko nekatere lastnosti različne opravilne algoritme, čeprav je splošna zgradba RNK ista. RNK sistem se dobi tako, da izberemo programske module iz standardne knjižnice in jih avtomatsko povežemo. Obstaja možnost, da razvijemo manjkajoče funkcije in jih dodamo standardni knjižnici. Tako je mogoče standardno knjižnico funkcij dopolniti s specifičnimi moduli za spremljanje orodja, da bi uporabnikom zagotovili nove možnosti na področju sprotnega spremljanja postopka obdelave glede na preprečitev kolizije, loma orodja, preobremenitve ter spremljanja obrabe orodja [7]. Programski modul, nameščen v krmilnem sistemu, zagotavlja tudi najhitrejšo reakcijo v primeru že znane motnje v postopku. Vendar je treba za vsak določen primer nadzirati občutljivost in uporabnost takih sistemov v različnih razmerah obravnave in temu ustrezno prilagoditi strategijo nadzora.

3 OPIS NAČRTOVANJA PREIZKUSOV

Cilj preizkusa je določiti občutljivost parametrov pogonskega sistema na obrabo proste ploskve orodja pri postopku finega struženja. Postopek določitve občutljivosti krmilnih signalov na obrabo orodja je razdeljen na dva dela:

- določitev stopnje obrabe proste ploskve orodja [9] in
- zbiranje podatkov med postopkom obdelave in njihovo nadaljnje analiziranje.

Občutljivost nadzornega signala na obrabo proste ploskve orodja je bila preizkušena na NK stružilni enoti, izvedeni za obdelavo vztrajnika. Glavni

system has standard functions that are used generally for all the machine tools, Figure 1.

Depending on the machine kinematics and its specific characteristics, some properties can have different operation algorithms, although the general CNC structure is the same. The CNC system is formed by selecting the software modules from the standard library and their automatic linking. There is the possibility of developing the missing functions and their being added to the standard library. Thus, a standard-functions library can be supplemented by specific modules for tool monitoring in order to provide the users with new possibilities in the field of online process monitoring with regard to avoiding collisions, breakdowns, overloads and the monitoring of tool wear [7]. The software module installed in the control system also provides the fastest reaction in the case of a known process disturbance. However, for every concrete case the sensitivity and applicability of such systems in various processing conditions need to be checked, and the supervision strategies need to be adapted accordingly.

3 DESCRIPTION OF THE PLANNING OF THE EXPERIMENT

The aim of the experiment was to determine the sensitivity of the drive-system parameters to tool-flank wear in the process of fine turning. The procedure for determining the sensitivity of control signals to tool wears is divided into two parts:

- determining the level of tool-flank wear [9],
- gathering the data during the machining process and its subsequent analysis.

The sensitivity of the control signal to tool-flank wear was tested on an NC turning unit, designed for flywheel machining. The main and feed drive

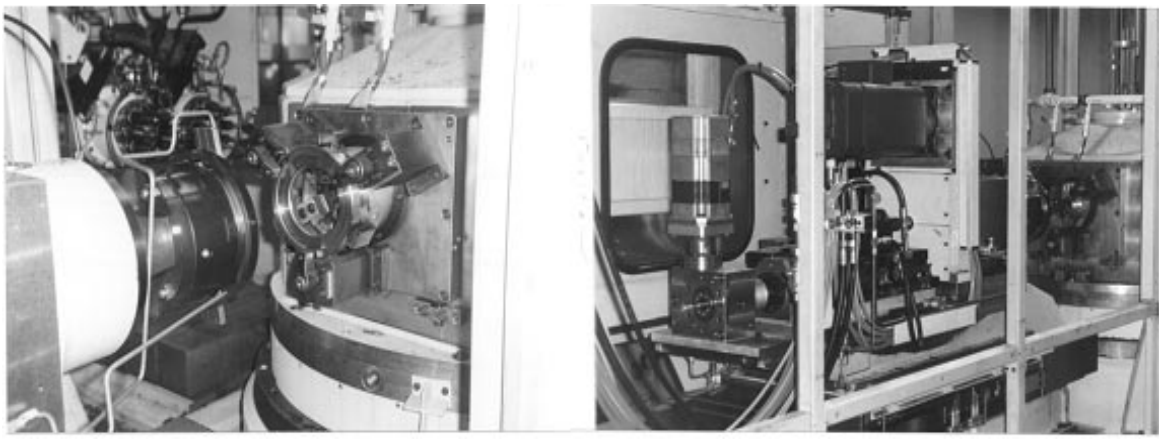

Sl. 2. *Enota za fino stru□enje (SAS-Zadar)*
Fig. 2. *Unit for fine turning (SAS-Zadar)*

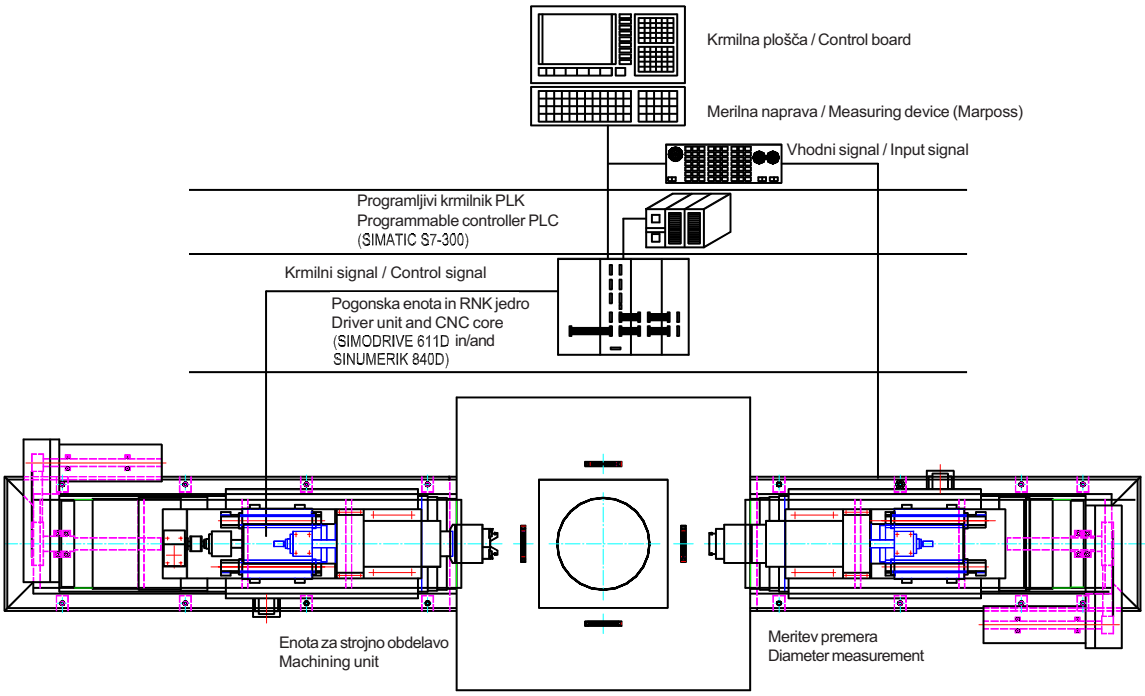

Sl. 3. *Specialni stroj za obdelavo vztrajnika (SAS - Zadar)*
Fig. 3. *Special machine for flywheel machining (SAS - Zadar)*

pogonski motorji in motorji za podajanje so bili digitalni, ponovljivost lege je bila v območju ±2µm.

Stružilna enota je bila nameščena v sklopu specialnega stroja, krmiljena s Siemensovim digitalnim krmilnim sistemom, Sinumerik 840D (sl. 3). Specialni stroj je obsegal štiri postaje, od katerih je bila ena opremljena z merilnim sistemom Marposs za merjenje poprej strojno obdelanega premera. Izmerjena vrednost je bila osnova za popravo geometrijskih parametrov rezalnih orodij. Na podlagi znanega razmerja med obrabo orodja in spremembo struženega premera [10] so bile hkrati shranjene popravne vrednosti, uporabljene za oceno obrabe proste ploskve orodja (sl. 4).

Preizkusni parametri so podani v preglednici 1. Rezalni parametri so bili definirani v skladu s podatki,

motors were digital, and the position repeatability was in the range of ±2µm.

The turning unit was fitted within the unit of special machine controlled by a Siemens digital control system, Sinumerik 840D, Figure 3. The special machine consisted of four stations, one of which was fitted with a Marposs measuring system for measuring the previously machined diameter. The measured value was the basis for the correction of the geometric parameters of cutting tools. At the same time, based on the known relation between the tool wear and the change of the turned diameter [10], stored correction values were used for an estimation of the tool-flank wear, Figure 4.

The experimental conditions are presented in Table 1. The cutting parameters were defined in

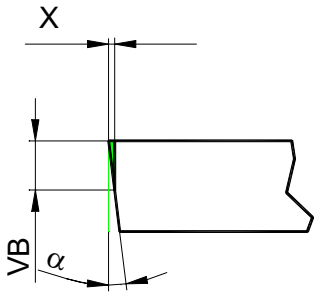

$$VB = X / tg\alpha$$

Sl. 4. *Geometrijska oblika rezalnega roba*
Fig. 4. *Geometry of cutting edge*

Preglednica 1. *Parametri struženja*
Table 1. *Turning conditions*

material obdelovanca workpiece material	16MnCr5
začetni premer d_0 mm start diameter d_0 [mm]	ϕ 115H8
končni premer d_1 mm final diameter d_1 [mm]	ϕ 115,7H6
vrtilna frekvenca n min^{-1} number of revolutions n [min^{-1}]	600
rezalna hitrost v_c m/min cutting speed v_c [m/min]	218
podajanje f mm feedrate f [mm]	0,15
dolžina rezanja l mm cutting length l [mm]	10
čas rezanja t s cutting time t [s]	7,2
hladilno sredstvo coolant	suha obdelava dry machining
rezalna ploščica (Sumitomo) insert type (Sumitomo)	SCMT 09T3 04N FP-T 110A

ki jih je priporočil proizvajalec, vendar je nesprejemljiva oblika odrezkov (neprekinjen odrezek) zahtevala spremembo rezalnih parametrov. Da bi dobili sprejemljivo obliko odrezka, smo povečali globino reza in uporabili suho obdelavo.

Med postopkom obdelave smo iz uporabniškega jedra NK zbrali podatke o toku, hitrosti in legi. Podatke smo zbrali s pomočjo PLK (Simatic 5). Podatke o krmilnem sistemu smo zbrali s programsko opremo, napisano v programskem jeziku Step5 (v PLK) (sl. 5). Podatke smo shranili v ustrezen podatkovni blok [11].

Začetek zapisovanja podatkov smo sprožili iz porabniškega programa NK z uporabo funkcije M(v tem preizkusu smo izbrali pomožno funkcijo M25). Podatki so bili zapisani prek vhodnih modulov v podatkovni blok v taktu PLK, in sicer hkrati za glavni in podajalni pogon. Tako je bilo mogoče podatke dalje analizirati, da bi našli popravo med obrabo orodja in ravnjo signala.

accordance with data recommended by the manufacturer, but an unacceptable chip form (continuous chip) demanded changes to the cutting data. In order to obtain an acceptable chip form the depth of cut was increased and dry machining was applied.

During the machining process, data on current, velocity and position were gathered from the NC users' core. The data were gathered by means of PLC (Simatic 5). The control system data were gathered by means of software written in the programming language Step5 (in PLC), Figure 5. The data were stored in the appropriate data block (DB) [11].

The start for data recording was activated from the users' NC program, using the M function (in this experiment the auxiliary function M25 was selected). The data were recorded through input modules into the data block (DB) in PLC tact, simultaneously for the main drive and the feed drive. Thus the recorded data could be subsequently analyzed to find a correlation between tool wear and signal level.

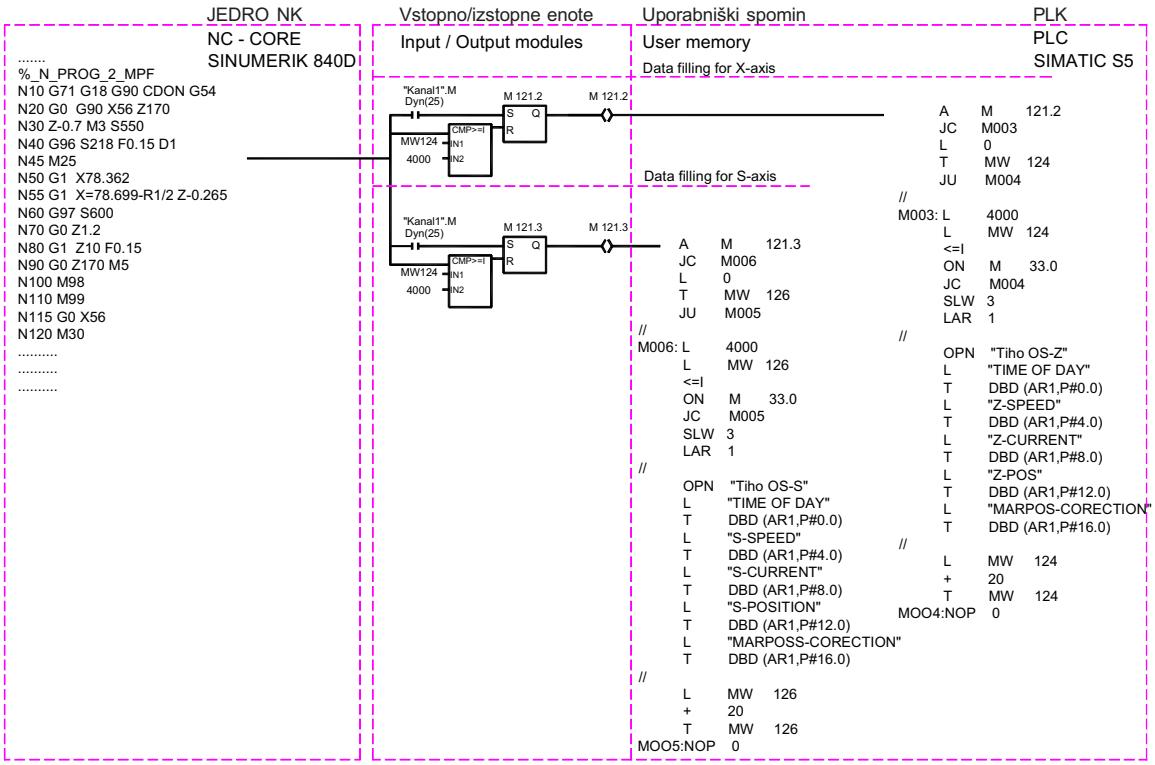

Sl. 5. *Zgradba toka signalov*
Fig. 5. *Structure of the signal flow*

4 REZULTATI ANALIZE

Podatki o popravah rezalnega orodja, ki so bile napravljene med delovanjem stroja brez strežbe (od začetka do takrat, ko je obraba orodja dosegla mejo) [12], smo shranili in omogočili še risanje krivulje, ki je prikazovala odvisnost obrabe proste ploskve od števila obdelanih kosov (sl. 6).

4 ANALYSIS OF THE RESULTS

The data on cutting-tool corrections that were applied during the unattended working of the machine (from the beginning, until the tool wear reached the limit) [12] were stored, and this allowed the drawing of a curve showing the dependence of flank wear on the number of machined workpieces, Figure 6.

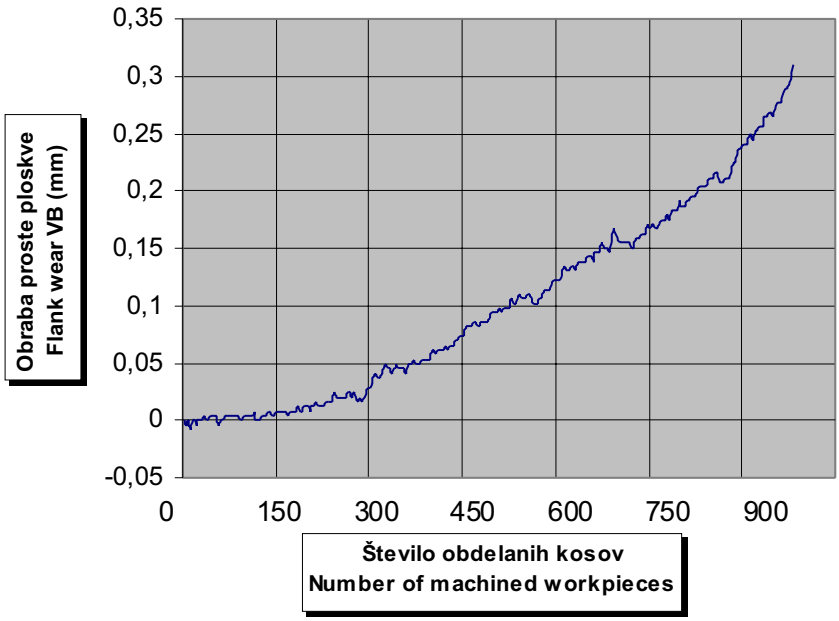

Sl. 6. *Krivulja obrabe orodja*
Fig. 6. *Tool-wear curve*

Preglednica 2. *Izmerjene vrednosti obrabe proste ploskve orodja pri različnih časih obdelave*
Table 2. *Measured values of tool-flank wear for various machining times*

Meritev # Measurement #	1	2	3	4	5	6
obraba proste ploskve VB, *mm* tool flank wear VB, *mm*	0	0,012	0,215	0,252	0,289	0,309
število obdelanih kosov the number of machined workpieces	1	186	861	921	974	981
čas obdelave, *min* machining time, *min*	0,12	22,3	103,3	110,5	116,8	117,7

Oblika krivulje jasno prikazuje, da se intenzivnost obrabe povečuje, čim bolj se doba trajanja orodja bliža koncu, kar smo pričakovali. Nadaljnja obdelava z izrabljenim orodjem bi pripeljala do loma orodja in izpada sistema. Preglednica 2 prikazuje vrednosti obrabe orodja pri različnem številu obdelovancev in ustreznem času obdelave.

Slika 7 prikazuje odvisnost toka glavnega in podajalnega motorja pri različnih vrednostih obrabe rezalnega orodja.

Zlahka opazimo pojavljanje signala z visoko frekvenco, kar pomeni, da uporaba nefiltriranih signalov za nadziranje obrabe orodja ne bi bila primerna [13]. Ena od možnosti za filtriranje signala je, da uporabimo površino pod krivuljo signala toka. Preglednica 3 prikazuje vrednosti področja pod krivuljo toka pri različnih vrednostih obrabe.

Pokazali smo, da obraba orodja najbolj vpliva na glavno vreteno, to je glavni pogon. Signal toka glavnega pogona se je povečal za približno 23% med povečanjem obrabe orodja od VB1 do VB6 (od 0 do 0,309 mm). To je znatno povečanje in bi lahko rabilo za presojanje stanja orodja. Krivulja, ki kaže odvisnost moči glavnega vretena v razmerju do obrabe orodja, je skoraj linearno sorazmerna (sl. 8). Ujema se z nekaterimi prejšnjimi raziskavami zlasti z [10], ki prinaša enačbo (1) kot matematični model, ki opisuje razmerje med močjo glavnega vretena in obrabo orodja:

The curve shape clearly illustrates that wear intensity is increasing as the tool life approaches its end, as expected. Further machining with a worn tool would result in tool breakage and system breakdown. Table 2 shows the tool-wear values for a different number of workpieces and the corresponding cutting times.

Figure 7 shows the dependence of the main- and feed-motor currents for different values of cutting-tool wear.

It is easy to observe the high-frequency signals, which implies that the use of unfiltered signals for tool-wear monitoring would not be appropriate [13]. One of the possibilities for signal filtering is to use the surface below the curve of the current signal. Table 3 shows the values of the area below the current curve for several tool-wear values.

It has been shown that tool wear mostly influences the main spindle, i.e., the main drive. The current signal of the main drive increased by approximately 23% during the increase of tool wear from VB1 to VB6 (from 0–0.309 mm). It is a significant increase, and could be used for judging the tool's condition. The curve showing the dependence of the main spindle power in relation to tool wear is almost linear, Figure 8. This is in accordance with some previous studies, in particular [10], which introduces Equation 1 as the mathematical model describing the relation between the main spindle power and the tool wear:

$$P = C \cdot VB + P_0 \qquad (1).$$

Preglednica 3. *Površine pod krivuljo toka v odvisnosti od velikosti obrabe rezalnega orodja*
Table 3. *Areas below the current curve depending on the level of cutting-tool wear*

Področje pod krivuljo toka Area bellow the current curve (%)	P-VB1	P-VB2	P-VB3	P-VB4	P-VB5	P-VB6
obraba proste ploskve Flank wear (mm)	0	0,012	0,215	0,252	0,289	0,309
vreteno S Spindle S	1823,61	2039,47	1914,77	2133,08	2169,7	2382,2
pogon osi X X axes drive	399,3	381,9	366,13	417,1	366,44	368,5

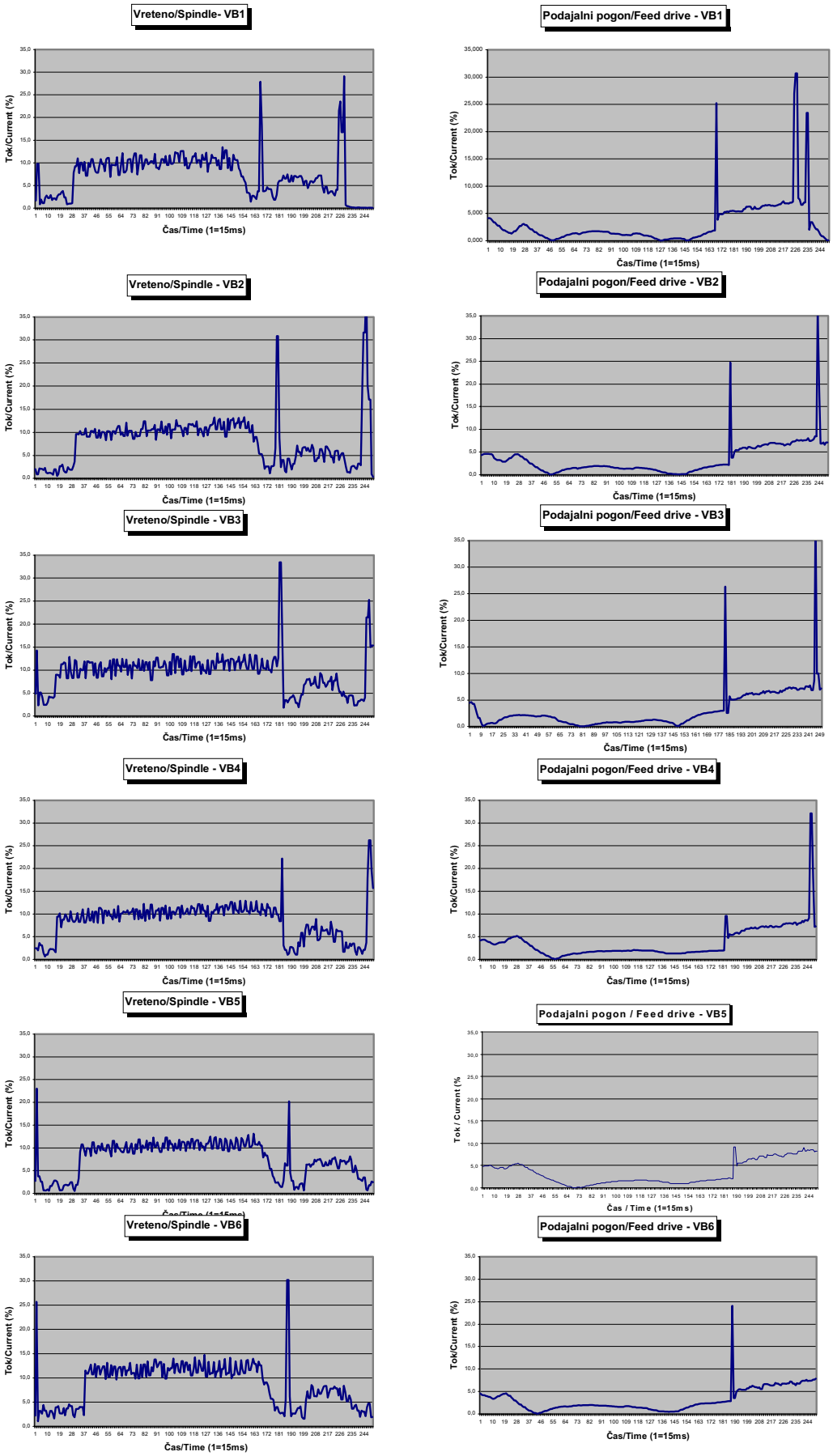

Sl. 7. *Krivulja signalov pogonov za glavno in podajalno os*
Fig. 7. *The curves of drive signals for the main and feed axes*

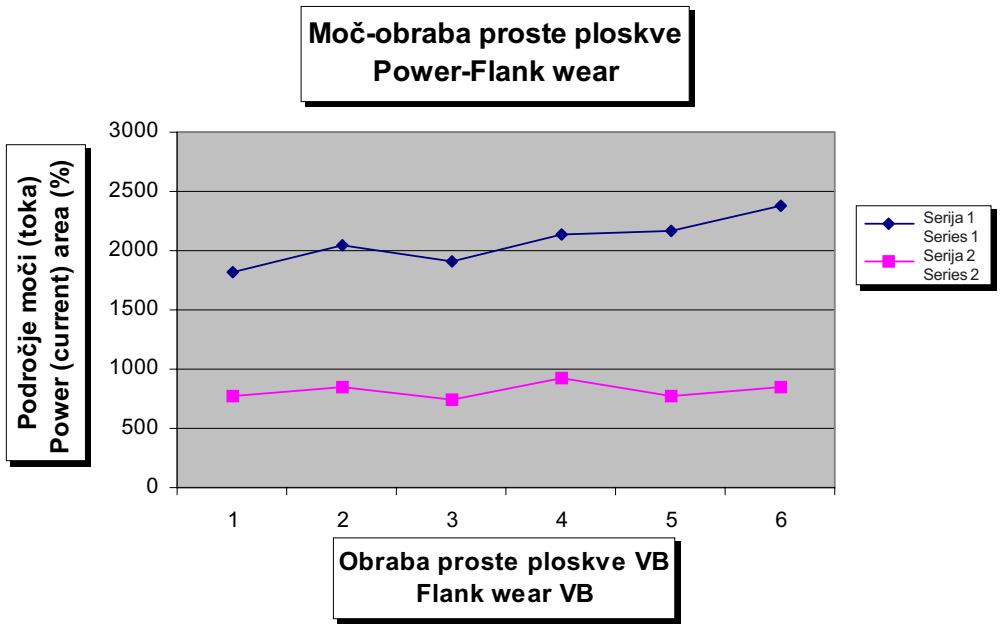

Sl. 8. *Odvisnost področja pod krivuljo toka glavnega motorja od obrabe orodja*
Fig. 8. *Dependence of the area below the main engine current curve on the flank wear*

Preizkusni rezultati potrjujejo, da signal motorja podajalnega gibanja ni primeren za določanje stanja orodja pri finem struženju. Ker je delež moči, potreben, da premaga trenje in mehanske izgube v podajalnem pogonu, zelo velik, ni mogoče izločiti spremembe moči v podajalnem pogonu, ki je posledica povečanja obrabe orodja. Potrebne so nadaljnje raziskave, da bi vzpostavili točno definirane meje za uporabo signala podajalnega pogona.

5 NADALJNJE RAZISKAVE IZBOLJŠANJA PODATKOVNE BAZE

Programski modul, vgrajen v nadzorno enoto, ponuja gospodarno rešitev v nasprotju z zunanjim zaznavnim sistemom. Pogonski sistem ne deluje neposredno na izvršilni del orodja, ampak je povezan s postopkom obdelave prek mehanskih komponent. Glavni vplivi motenj sistema prenosa so:

- trenje pri mirovanju in drsno trenje verige pogona, pri čemer je nelinearno obnašanje odvisno od hitrosti gibanja in stanja mirovanja,
- pospeševanje, ki pomeni obremenitev sistema,
- prazna razdalja, ki jo povzroči sprememba smeri verige pogona.

Kar se tiče vrednosti motenj, jih je lahko analizirati in ločiti od osnovnega signala med obdelavo signala, tako da ostanejo samo signali postopka. Upoštevati je treba naslednje vplive:

- vpliv pospeška zaradi vztrajnosti v postopku pospeševanja,
- vplivi trenja v premikajočih se oseh, vretenu, vodilih ali trenje zaradi vrtenja,
- vpliv drž anja pri mirovanju in prazna razdalja pri spremembi smeri.

The experimental results confirm that the feed drive signal is not suitable for judging the tool condition during fine turning. Because the share of power necessary to prevent friction and mechanical loses in the feed drive is very high, it is not possible to isolate the power changes in the feed drive that are the consequence of an increase in tool wear. Further investigations are necessary in order to establish closely defined limits for the application of the feed drive signal.

5 FURTHER RESEARCH ON IMPROVING THE INFORMATION BASE

A software module integrated into the control offers, in contrast to an external sensory system, an economical solution. The drive system does not act directly on the executive part of the tool, but is connected with the machining process through mechanical components. The main disturbance influences of the transmitting systems include:

- the resting and sliding friction of the drive chain, with non-linear behavior depending on the movement velocity, and the state of rest,
- acceleration that changes system load,
- the clearance caused by the change of direction in the drive chain.

Considering the values of disturbance, this needs to be analyzed and separated from the basic signal during signal processing, so that only the processing signals remain. The following effects have to be taken into account:

- the acceleration effect via inertia in the acceleration process,
- friction effects in moving axes, spindles, guides or rotation friction,
- holding effects in standstill and clearance in the change of direction.

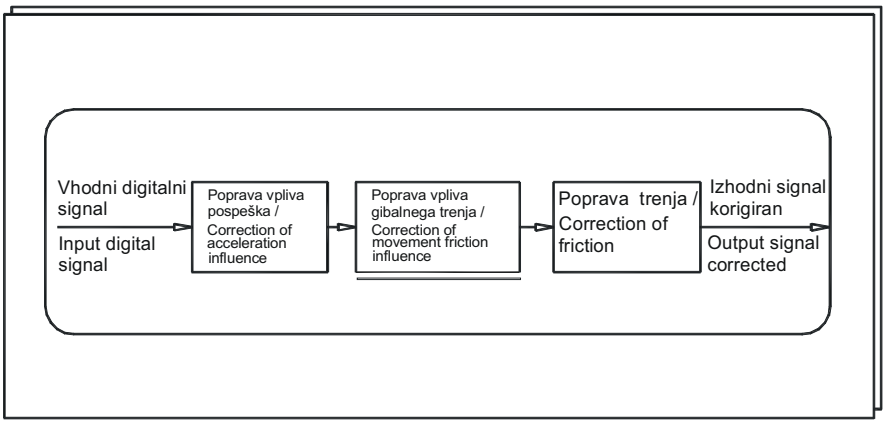

Sl. 9. *Odvisnost toka glavnega motorja in raven obrabe*
Fig. 9. *Dependence of the main engine current and the level of wear*

Slika 9 podaja pregled popravnih veličin, ki se izločijo že v prototipu iz vpliva signalne motnje, kar naredi dober signal.

Nadaljnjo obdelavo tako dobljenih zelo dobrih signalov lahko opravimo z izpolnjenimi tehnologijami umetne inteligence, nevronskih mrež in prepoznavanjem vzorcev [14]. Ker za delovanje nevronskih mrež niso potrebni jasno definirani algoritmi niti teorija, ker imajo možnost pridobiti znanje prek niza primerov, so zelo primerni za delo s podatki o obrabi orodja [15] in napovedovanje preostale dobe trajanja orodja. Zmožnost nevronskih mrež, da ustvarijo zanesljive kazalnike obrabe orodja, je strogo odvisna od zgradbe mreže kakor tudi od pogojev možnosti učenja mreže.

6 SKLEP

Brzzančno krmiljenje z digitalnim sistemom pogona odpira nove možnosti in perspektive na področju sprotnega spremljanja obdelovalnih sistemov. V mnogih primerih lahko spremljanje orodij prek nadzornega sistema zamenja običajne zunanje sisteme spremljanja. S kombinacijo digitalnih sistemov pogona z dodatnimi podatki iz nadzornega sistema, z metodami izločevanja karakteristik iz signala in izpopolnjenimi tehnologijami obdelave podatkov dobimo veliko zanesljivost in varnost analize signala. Prav tako spremljanje obdelovalnega postopka prek programsko vgrajenih NK modulov jedru omogoča hitre reakcije na znane motnje postopka, in sicer brez dodatnih omejitev strojne opreme na sistemu. Tako je mogoče razviti praktične skupine postopkovnih modulov, ki so glede strojne opreme neodvisni in odprti, to je preobličljivi. Uporabnost teh sistemov je v glavnem omejena z občutljivostjo glede na opazovani pojav, ki mora biti vnaprej definirana. Raven nadzornega sistema z razvitim najmanjšim številom dodatnih funkcij spremljanja poenostavi povezavo med človekom in strojem, tako da postane

Figure 9 offers an overview of the corrective magnitudes that are already eliminated in the prototype from the disturbance signal influence, thus generating a good signal, Figure 9.

Further processing of the thus obtained valuable signals can be carried out by sophisticated technologies of artificial intelligence, neural networks, and pattern recognition [14]. Since no clearly defined algorithms or theory are necessary for the operation of neural networks, because they have the possibility to acquire knowledge through a series of examples, they are very suitable for working with data on tool wear [15] and predictions of the remaining tool life. The possibility of neural networks creating reliable indicators of tool wear depends strictly on the network structure, as well as on the conditions of the learning possibilities of the network

6 CONCLUSION

Open control with a digital drive system opens up new possibilities and prospects in online monitoring of machining systems. In many cases the monitoring of tools via a control system can replace conventional, external monitoring systems. By a combination of digital drive systems with additional information from the control system, methods of isolating the characteristic features from the signal and sophisticated data processing technologies, high reliability and the safety of signal analysis is achieved. Also, supervising the machining process through software-integrated modules in the NC core allows fast reactions to known processing disturbances, with no additional hardware restrictions on the system. In this way, practical sets of processing monitoring modules can be developed, hardware-independent and open, i.e., reconfigurative. The applicability of such systems is mainly limited by sensitivity in relation to the observed phenomenon, which has to be pre-defined. The control system platform with a developed minimum number of additional monitoring functions, simplifies the man-machine

sprejemljiva za operaterja stroja. Nadaljnji razvoj teh sistemov in metoda izločevanja karakterističnih lastnosti s hkratno uporabo tehnologij umetne inteligence pomenijo znaten korak naprej k uresničitvi preprostega, zanesljivega, uporabniško prijaznega načina spremljanja rezalnih orodij in postopkov.

connection, and makes it acceptable to the operator. The further development of such systems, and the method of isolating characteristic features, at the same time applying the technologies of artificial intelligence, present a significant step towards realizing a simple, reliable, user-friendly way of monitoring cutting tools and processes.

7 LITERATURA
7 REFERENCES

[1] Udiljak, T. (1996) Contribution to development of the methods for research on tool life and monitoring of tool wear (in Croatian), dissertation, *University of Zagreb*.

[2] Shulz, H. (1996) Hochgeschwindigkeitsbearbeitung, *Carl Hanser Verlag*, Munich Vienna.

[3] Isermann, R. (1994) Überwachung und Fehlerdiagnose, *VDI-Verlag*, Düsseldorf.

[4] Milfelner, M., F.Čuš (2003) Simulation of cutting forces in ball-end milling. *Robotics and Computer Integrated Manufuring*, Vol. 19 (1/2), 99-106.

[5] Koning, W., F Klocke (1997) Fertigungsverfahren 1, *Springer-Verlag Berlin, Heidelberg New York*.

[6] Cuppini, D., G. D'Errico, G. Rutelli (1990) Tool wear monitoring based on cutting power measurement, *Wear,* 139, 303-311.

[7] Kopač, J., S. Šali (2001) Tool wear monitoring during the turning process, *Journal of Materials Processing Technology,* Vol. 113, (1/3), special issue "5th APCMP, Seoul, Korea", 312-316.

[8] Novaković, B., D. Majetić, M. Široki (1997) Artificial neural networks (in Croatian), *Školska knjiga Zagreb*, Zagreb.

[9] Srinivasa, P., T.N. Nagabhushana, P.K. Ramakrishna Rao (2002) Flank wear estimation in face milling based on radial basis function neural networks, *International Journal of Advanced Manufacturing Technology,* 20 (4), 241-247.

[10] Zdenković, R. (1965) Metal cutting (in Croatian), *University of Zagreb, FSB*.

[11] Zimmermann, H.J. (1965) Neuro+Fuzzy, *VDI-Verlag*, Düsseldorf.

[12] ISO International Standard: Tool life testing with single point turning tools, Stockholm, 1997.

[13] Srinivasa Pai, P., T.N. Nagabhushana, P.K. Ramakrishna Rao (2000) Tool wear estimation using resource allocation network, *International Journal of Machine Tools and Manufacture*, 41(5), 673–685.

[14] Damodarasamy, S., S. Raman (1993) An inexpensive system for classifying tool wear states using pattern recognition, *Wear*, 170,149-160.

[15] Li, X.(2), S. Dong (2), P.K. Venuvinod(1) (2000) Hybrid learning for tool wear monitoring, *International Journal of Advanced Manufacturing Technology*, 16(5), 303-307, ISSN: 1433-3051.

Naslova avtorjev: Tihomir Mulc
doc.dr. Toma Udiljak
Sveučilište u Zagrebu
Fakultet strojarstva i brodogradnje
Ivana Lučića 5
10 002 Zagreb
toma.udiljak@fsb.hr

prof. dr. Franci Čuš
dr. Matjaž Milfelner
Univerza v Mariboru
Fakulteta za strojništvo
Smetanova 17
2000 Maribor
matjaz.milfelner@uni-mb.si
franc.cus@uni-mb.si

Authors' Addresses: Tihomir Mulc
Doc.Dr. Toma Udiljak
University of Zagreb
Faculty of Mechanical Eng. and
Naval Architecture
Ivana Lučića 5
10 002 Zagreb, Croatia
toma.udiljak@fsb.hr

Prof. Dr. Franci Čuš
Dr. Matjaž Milfelner
University of Maribor
Faculty of Mechanical Eng.
Smetanova 17
SI-2000 Maribor, Slovenia
matjaz.milfelner@uni-mb.si
franc.cus@uni-mb.si

Prejeto: 21.4.2004
Received:

Sprejeto: 2.12.2004
Accepted:

Odprto za diskusijo: 1 leto
Open for discussion: 1 year

© Strojniški vestnik 50(2004)12,580-593
ISSN 0039-2480
UDK 678.033:534
Pregledni znanstveni članek (1.02)

© Journal of Mechanical Engineering 50(2004)12,580-593
ISSN 0039-2480
UDC 678.033:534
Preview scientific paper (1.02)

Analiza zvočnih lastnosti kompozitnih materialov

An Analysis of the Acoustic Properties of Composite Materials

Samo Šali - Uroš Žnidarič - Janez Kopač

Da bi izdelovalcu okrovov zvočnikov olajšali izbiro optimalnega materiala, smo testirali različne vrste plastičnih materialov, oplemenitenih z drobno mletimi lesnimi delci, ter jih primerjali z aluminijem, MDF (srednje gosti komopziti), polistirenom drugega izdelovalca zvočnikov (JVC) in ABS (akrilonitril – butadien – stiren). Vsi preizkušani materiali so bili v obliki plošč z izmerami 150×150 mm, njihova debelina pa je bila 2 mm. Ker so bile v ospredju testov zvočne lastnosti materialov, smo merili njihov relativni zvočni upor, relativno dušenje zvočne radiacije in faktor viskoznega dušenja. Prvi dve veličini sta izpeljani iz gostote in relativnega modula elastičnosti, ki ju lahko dobimo iz meritev frekvenčnega odziva prosto vpetih preizkušancev. Rezultati kažejo, da se s pravilno izbiro drobno mletih lesnih delcev in plastične osnove lahko približamo materialu MDF, ki velja za zelo dobro izbiro pri izdelavi okrova zvočnika.

(Ključne besede: materiali kompozitni, lastnosti akustične, analize modalne, metode preskušanja)

To help select the best material for loudspeaker boxes, we tested various types of polymer materials that are filled with fine, ground wood particles. In addition, we compared these materials with aluminium, MDF (medium-density fiberboard), polystyrene from another producer of loudspeaker boxes (JVC), and ABS (acrylnitril – butadiene – styrene). All the specimens were in the shape of square plates with dimensions 150×150 mm and the thickness 2 mm. Because the analysis was focused on the acoustic properties of the materials, we measured their relative sound-wave resistance, the relative damping of the sound radiation and the viscous-damping factor. The first two parameters are derived from the density and the relative modulus of elasticity, which can be obtained from measurements of the frequency response for free-supported specimens. The results show that a careful selection of fine, ground wood particles and polymer can give a satisfactory approximation to MDF, which is known as one of the best choices for the production of loudspeaker boxes.

(Keywords: composite materials, acoustic properties, modal analysis, testing methods)

0 UVOD

Modalna analiza tankih štirikotnih plošč je razmeroma dobro raziskano področje ([1] do [4]). Poleg vpetja in oblike preizkušancev na njihovo modalno obnašanje vsekakor vpliva tudi gradivo. Modalno obnašanje objekta pomeni amplitudo, dušenje in gibalne oblike pri posameznih frekvencah nihanja tega predmeta. Primerjava zvočnih lastnosti različnih materialov pomeni torej primerjavo modalnega obnašanja preizkušancev z enako obliko in vpetjem, pri čemer je spremenljivka vrsta materiala. V našem primeru smo za določanje zvočnih lastnosti preizkušancev uporabili metodo za prosto vpete, izotropne, tanke štirikotne plošče.

0 INTRODUCTION

The modal analysis of thin, square-shaped plates is relatively well investigated ([1] to [4]). Besides the specimens' shape and the type of support, their modal behaviour depends on the choice of material. The modal behaviour of an object means the amplitude, the damping and the modal shapes at certain frequencies of vibration (oscillation) for this object. A comparison of the acoustic properties of different materials is therefore a comparison of specimens with equal shape and the some type of support, where the only variable is the material. In our case, for a definition of the acoustic properties of the specimens, a method for free-supported, isotropic and thin square-shaped plates was

Podoben postopek je že bil uspešno uporabljen pri meritvah zvočnih lastnosti izrazito izotropnega (ortotropnega) materiala, tj. lesa [5]. Zato predpostavljamo, da morebitna izotropnost preizkušanih materialov ni vplivala na kakovost analize, kar pa bo še podrobneje razloženo. Cilj raziskave je bila metoda za merjenje zvočnih lastnosti kvadratastih tankih plošč ter kriterij za določanje zvočne kakovosti različnih plastičnih materialov z lesnimi vključki, ki so namenjeni za velikoserijsko proizvodnjo brizganih okrovov za srednje kakovostne zvočnike za poslušanje glasbe.

Akustične lastnosti materialov ne moremo definirati enopomensko. Za primer: med najboljše materiale za zvočne plošče lesenih glasbil uvrščamo smreko, medtem ko se ta in podobne vrste lesa sploh ne uporabljajo pri gradnji okrovov za zvočnike. Razlog je seveda v različnosti namena, ki ga imata zvočna plošča glasbila in okrov zvočnika.

Modul elastičnosti E in gostota ρ sta edini veličini, ki določata zvočni upor Z in dušenje zvočnega sevanja ϑ trdnih teles [6]:

applied. A similar approach was already applied during measurements of the acoustic properties of an extremely non-isotropic (orthotropic) material – wood [5]. It is assumed, therefore, that the probable non-isotropy of the tested materials did not affect the analysis, which will be explained in more detail later. The aim of this research was to devise method for measuring the acoustic properties of thin, square-shaped plates and a criterion for determining the acoustic quality of different polymer materials with wood particles. These materials are intended for the large-scale production of middle-quality loudspeaker boxes using injection-moulding technology.

The acoustic properties of materials cannot be defined simply. For example, the best choice for the sound boards of wooden instruments is spruce, whereas this and similar types of wood are not used in the production of loudspeaker boxes. The reason for this lies in the different requirements of a sound board and a loudspeaker box.

The modulus of elasticity E and the density ρ are the only two variables that denote the sound-wave resistance Z and the damping of the sound radiation ϑ of solids [6]:

$$Z = \sqrt{\rho \cdot E} \tag{1}$$

$$\vartheta = \frac{\sqrt{E/\rho}}{\rho} \tag{2}.$$

Razlike v E in ρ se izražajo tudi v spremembi dinamičnega Youngovega modula. Ta modul izraža razmerje togosti in specifične teže preizkušanca. Togost in gostota se lahko primerjata z E in ρ. Slika 1

Variations in E and ρ will also result in changes to the dynamic Young's modulus. This modulus is defined as the ratio of the stiffness to the specific gravity of the specimens. The stiffness and the density can be compared to E

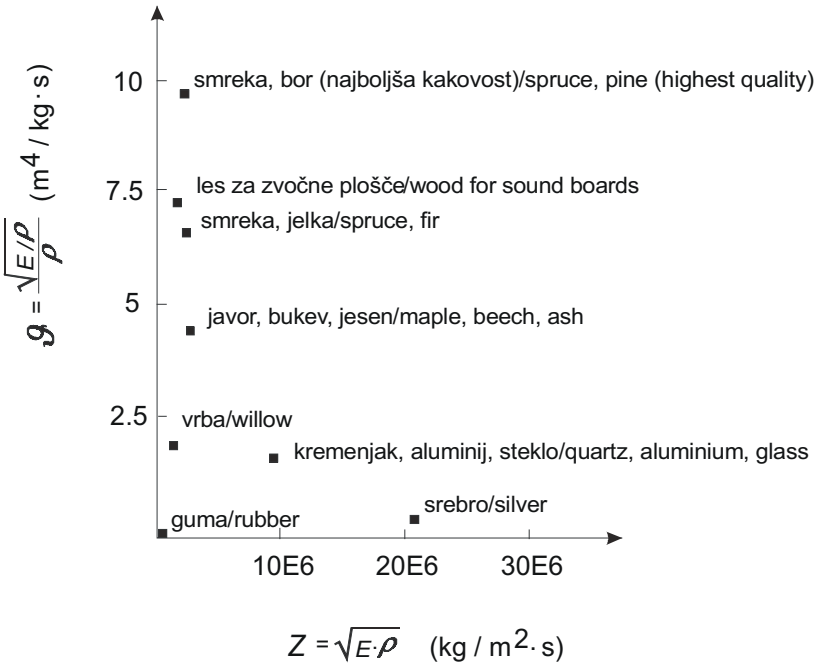

Sl. 1. *Odvisnost dušenja zvočnga sevanja (ϑ) od zvočnega upora (Z) za različne vrste lesa in druga gradiva [6]*

Fig. 1. *Dependence of radiation damping (ϑ) on sound wave resistance (Z) for several types of wood and other materials [6]*

prikazuje odvisnost dušenja zvočnega sevanja od zvočnega upora za različne vrste lesa in nekatera druga gradiva.

Prikazane odvisnosti potrjujejo, da sta pri zvočnih ploščah glasbil zaželena majhen zvočni upor in veliko dušenje zvočnega sevanja. Z drugimi besedami, večji dinamični Youngov modul zvočne plošče je ugodnejši.

Zvočna plošča glasbila mora namreč čim več prejete energije spremeniti v zvočno energijo, izgube zaradi notranjega trenja morajo zato biti čim manjše. Z drugimi besedami, pri čim manjšem faktorju viskoznega dušenja (definicija sledi) mora biti dušenje zvočnega sevanja za zvočne plošče glasbil čim večje. Faktor viskoznega dušenja δ lahko izračunamo na podlagi faktorja kakovosti Q iz enačbe, ki velja za malo dušene sisteme [7]:

and ρ, respectively. Figure 1 shows the dependence of the damping of sound radiation on the sound-wave resistance for different wood species and other materials.

The presented relations confirm that in the sound boards of musical instruments, low sound-wave resistance and high damping of the sound radiation are desirable. In other words, a high rather than a low dynamic Young's modulus of the sound boards is preferred.

The wooden resonant boards of musical instruments should translate most of the input energy into sound radiation. Therefore, losses due to internal friction are not desired. In other words, the factor of viscous damping (definition follows) should be as low as possible, and the damping of the sound radiation should be as high as possible. The viscous-damping factor δ can be calculated from the expression for the quality factor Q, which applies to low-damped systems [7]:

$$Q \cong \frac{1}{2\delta} \cong \frac{f_{0d}}{f_2 - f_1} \qquad (3),$$

kjer je f_{0d} lastna frekvenca modalnega načina, f_1 in f_2 pa pomenita frekvenci, kjer je amplituda frekvenčnega vrha enaka $P/\sqrt{2}$ (sl. 2).

Za primer resonančne frekvence s slike 2, ki pomeni lastni modalni način, je faktor viskoznega dušenja premo sorazmeren koeficientu viskoznega dušenja b in obratno sorazmeren zmnožku modalne mase m in modalne togosti k [7]:

where f_{0d} is the natural frequency, and f_1 and f_2 are frequencies where the amplitude is $P/\sqrt{2}$ (see Figure 2).

In the case of the resonant frequency, which is presented in Figure 2, and which presumably indicates a natural mode, the factor of viscous damping is proportional to the coefficient of viscous damping b, and inversely proportional to the product of the modal mass m and the stiffness k [7]:

$$\delta = \frac{b}{2\sqrt{k \cdot m}} \qquad (4).$$

Podobno razmišljanje velja pri izbiri optimalnega materiala za okrove zvočnikov, namenjenih za poslušanje glasbe. V tem primeru mora okrov preprečevati pojav izrazitih resonanc in odmevov, ki nastanejo zaradi izvira zvoka – vibracij membrane zvočnika. To je logično, saj želimo predvajati le signal, ki prihaja iz elektronskih komponent v mebrano zvočnika, in to brez dodatnih negativnih vplivov, ki bi se utegnili pojaviti zaradi prisotnosti okrova. Po drugi strani okrov zvočnika ne sme imeti pretiranih dušilnih lastnosti, saj bi to pomenilo prevelike izgube zvočne

A similar way of thinking is applied when the selection of the best material for loudspeaker boxes is considered. In this case the box of a loudspeaker has to prevent the phenomenon of distinctive resonances and echoes that appear due to a sound source – vibrations of the loudspeaker diaphragm. Because we wish to produce only a signal from the electronic components into the loudspeaker diaphragm (without any additional and negative effects due to the loudspeaker box), this is logical. On the other hand, the loudspeaker box should not exhibit an excessive damping quality, because this would mean too high sound-energy losses.

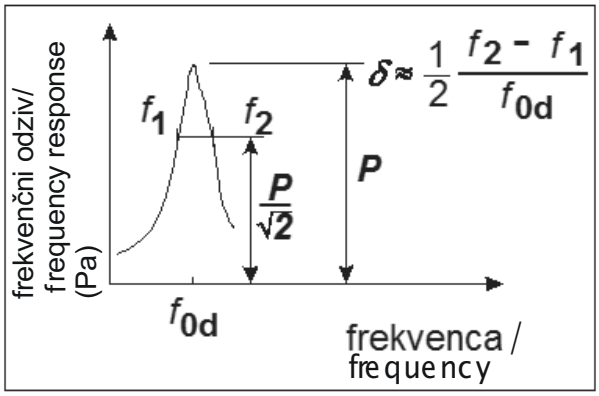

Sl. 2. *Definicija amplitude prvega resonančnega vrha in faktorja viskoznega dušenja δ*
Fig. 2. *Definition of both amplitude of the first resonant peak and factor of viscous damping δ*

energije. To bi se lahko poznalo kot opazno zmanjšanje glasnosti ustvarjenega zvoka, kakor tudi preveliko dušenje vseh ali določenih frekvenčnih pasov. Potemtakem dušenje zvočnega sevanja, ki pravzaprav pomeni zmožnost sevanja zvoka v okolico, pri okrovu zvočnikov ne sme biti preveliko, vsekakor pa mora biti bistveno manjše kakor v primeru zvočnih plošč glasbil. Lahko bi rekli, da manjšanje velike stopnje dušenja zvočnega sevanja, ki je značilna za zvočne plošče glasbil, pomeni izboljševanje zvočnih lastnosti gradiva za okrov zvočnika [8].

Z gotovostjo lahko trdimo, da majhen zvočni upor pomeni majhno zvočno impedanco. To se kaže v razmeroma hitrem odvajanju zvočne energije, torej premajhna zvočna impedanca v primeru zvočnih plošč glasbil pomeni glasne, a kratko trajajoče šume brez glasbenega značaja [9]. V primeru okrova zvočnika bi premajhen zvočni upor torej lahko pomenil interferenco takšnih šumov z vibriranjem membrane zvočnika, kar seveda ni zaželeno. Po drugi strani razmeroma velik zvočni upor pomeni preveliko zvočno impedanco, torej pretirano počasno odvajanje zvočne energije v okrov zvočnika. To bi pomenilo možnost pojava stojnega valovanja in odmevov ustvarjenega zvoka znotraj okrova zvočnika, kar vsekakor ne bi prispevalo h kakovosti zvoka.

Zvočni upor je glede na enačbo (1) proporcionalen zmnožku modula elastičnosti in gostote materiala. Ta dva določata velikost modalne togosti k in mase m. Ob predpostavki, da je zvočni upor nespremenljiv, je višji faktor viskoznega dušenja d posledica večjega koeficienta b (enačbi (1) in (4)). Razmeroma veliko (majhno) dušenje δ pomeni torej razmeroma velike (majhne) izgube zvočne energije znotraj okrova zvočnika [8]. Če torej lahko govorimo o neki idealni vrednosti zvočnega upora gradiva, potem za to vrednost obstaja tudi idealna vrednost faktorja viskoznega dušenja δ, ki ne sme biti ne previsoka, ne prenizka, torej mora biti optimalna. Nadalje, razmeroma velike vrednosti zvočnega upora okrova zvočnika pomenijo ob nespremenljivi vrednosti koeficienta b razmeroma majhne vrednosti faktorja viskoznega dušenja, kar pomeni možnost pojava odmeva in stojnega valovanja [9]. Po drugi strani pomeni razmeroma majhna vrednost zvočnega upora pri nespremenljivem koeficientu b veliko vrednost faktorja δ, s tem pa možnost prevelikih zgub zvočne energije od membrane zvočnika v okrov ([8] in [9]).

Veliko okrovov zvočnikov, med njimi tudi zelo kakovostni sistemi, je narejenih iz materiala MDF. Ta je v osnovi podoben iverni plošči, le da gre pri MDF za bolj drobno mlete lesne delce. Primerjava strukture za MDF in klasično iverno ploščo je prikazana na sliki 3.

Z veliko gotovostjo lahko torej trdimo, da so zvočne lastnosti materiala MDF referenčne

A consequence of this would be a significant decrease in the loudness, as well as too high damping of all, or only certain, frequency ranges. Therefore, the damping of sound radiation, which means the ability to radiate sound energy into the surroundings, must not be too high. In any case, it has to be significantly lower than in the case of the sound boards of musical instruments. One can say that a decrease of the relatively high level of damping of sound radiation, which is typical for musical instruments, indicates an improvement in the acoustic properties of a material for loudspeaker boxes [8].

With great certainty one can say that a low value of sound-wave resistance means low sound impedance. This results in a relatively fast sound-energy drain. Consequently, too low sound impedance of the sound boards results in loud and short-lasting noises without musical character [9]. Therefore, too low sound-wave resistance of a loudspeaker box could cause an interference of these noises with the loudspeaker diaphragm, which of course is not desired. On the other hand, a relatively high sound-wave resistance means too high acoustic impedance, which means that sound-energy drain into the loudspeaker box is too slow. This could result in the appearance of standing waves and echoes of the produced sound inside the loudspeaker box. Of course, this would not contribute to the sound quality in a positive way.

According to expression (1) the sound-wave resistance is proportional to the product of the modulus of elasticity and the material density. These two quantities determine the magnitude of the modal stiffness k and the mass m. Considering that sound-wave resistance is a constant, an increase in the viscous-damping factor δ is a consequence of an increase of coefficient b (see Equations (1) and (4)). A relatively high (low) damping δ therefore means high (low) losses of sound energy inside the loudspeaker box [8]. If we are allowed to speak about an ideal magnitude of sound-wave resistance for a certain material, then for this value there is also an ideal factor of viscous damping δ. This factor should be neither too high nor too low, i.e. it should be optimised. Next, if we assume that coefficient b is a constant, then a relatively high value of sound-wave resistance of the loudspeaker box will result in a relatively low factor of viscous damping. This can lead to the appearance of echoes and standing waves [9]. On the other hand, a relatively low sound-wave resistance, at a constant coefficient b, means a high magnitude of factor δ. This can significantly increase the losses of sound energy from the loudspeaker diaphragm into the box ([8] and [9]).

A lot of loudspeaker boxes, including high-quality systems, are made of MDF (medium-density fibreboard). In comparison to the particle board, MDF consists of smaller wood particles. Figure 3 shows a comparison between the MDF and the particle board structure.

With great certainty we can say that the acoustic properties of MDF are reference in terms of

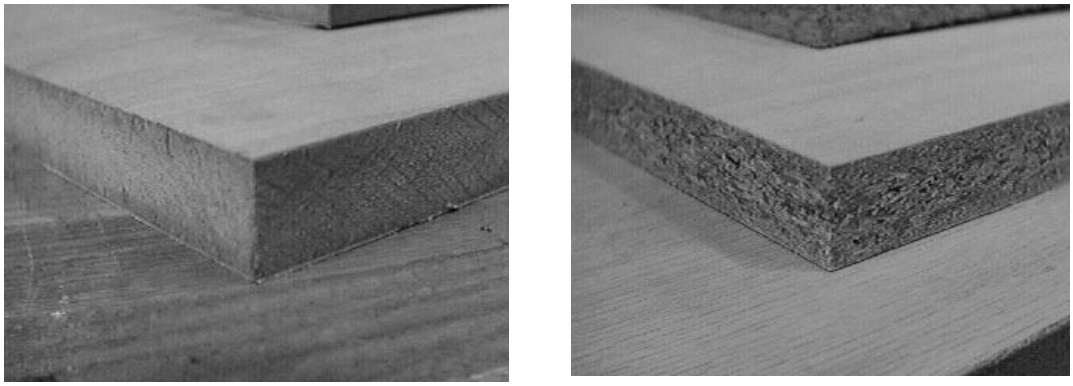

Sl. 3. *Primerjava med MDF (levo) in iverne plošče (desno)*
Fig.3. *Comparison between MDF (left) and particle board (right)*

lastnosti, če imamo v mislih iskanje optimalnega materiala za okrov zvočnikov. V nadaljevanju je predstavljena metoda za merjenje zvočnih lastnosti kvadratastih tankih plošč iz različnih materialov, predvsem kompozitov s plastično osnovo in z vključki iz drobno mletih lesnih delcev. Pri tej metodi smo torej vrednosti veličin (i) dušenje zvočnega sevanja, (ii) zvočni upor in (iii) faktor viskoznega dušenja, ki so značilni za MDF, označili za želene vrednosti. Te so torej merilo za določanje najboljše kombinacije plastične osnove z drobno mletimi lesnimi delci kot polnilom.

1 METODA

1.1 Priprava preizkušancev

Preizkušanci so bili kvadrataste plošče z dimenzijo 150×150 mm. Oznake ter število preizkušancev v vzorcu (n), njihova debelina (d), gostota (ρ) in sestava oziroma vrsta materiala so prikazani v preglednici 1.

Uporabljena sta bila dva tipa drobno mletih lesnih delcev. V primeru preizkušancev z oznako vz4 so bili to razmeroma veliki delci iz mehkega lesa (smreka), v preostalih preizkušancih pa razmeroma majhni delci iz trdega lesa (bukev). Kakor vidimo iz preglednice 1, se preizkušanci vz1 in vz4 ločijo samo po vsebini lesnih delcev. Razlika med preizkušanci vz2 in vz6 je v tipu polipropilena, sicer pa so masni deleži vseh treh sestavnih komponent (pregl. 1) enaki. Enako velja za preizkušance vz3 in vz5. Polistirenski preizkušanci vz9 so bili narejeni z injekcijskim brizganjem zdrobljenega okrova zvočnikov proizvajalca JVC (tip XV THA35). Polistirenski preizkušanci vz10 so bili narejeni za primerjavo s preizkušanci vz9. Postopek izdelave vseh preizkušancev s plastično osnovo je bilo iztiskanje, torej zvezna predelava plastičnih mas, v katerem se polimerna talina potiska skozi orodje specifičnega profilnega prereza. Material MDF je narejen iz drobno mletih lesnih delcev, ki so zlepljeni med seboj. Postopek lepljenja

lastnosti, ki so značilni za MDF, označili za želene vrednosti. Te so torej merilo za določanje najboljše kombinacije plastične osnove z drobno mletimi lesnimi delci kot polnilom.

1 METHOD

1.1 Specimens preparation

The specimens were square-shaped plates with dimensions of 150×150 mm. Denotations and the number of specimens in the group (n), their thickness (d), density (ρ), and composition or material type are presented in Table 1.

In the experiments two types of fine, ground wood particles were applied. For specimens vz4 this pulp consisted of relatively coarse particles of softwood (spruce), whereas for other specimens the fine, ground wood particles consisted of relatively small particles of hardwood (beech). As one can see from Table 1, the only difference between specimens vz1 and vz4 is in the content of wood particles. The difference between specimens vz2 and vz6 is in a type of polypropylene, whereas the mass portions of all three main components (see table 1) are the same. The same is true for specimens vz3 and vz5. Specimens based on polystyrene vz9 were made by injection moulding ground loudspeaker boxes JVC (type XV THA35). Specimens vz10 (also based on polystyrene) were used for a comparison with specimens vz9. All the specimens based on polymer were produced by extrusion, which means the continuous manufacturing of polymers, where a polymer melt is pushed through a die with a specific cross-section. MDF is made of fine, ground wood particles that are glued together. The process of gluing is performed at high

Preglednica 1. *Lastnosti preizkušancev*
Table 1. *Properties of specimens*

Oznaka skupine/ Group denotation	*n*	*d* mm	ρ kg/m^3	sestava preizkušancev/ specimen composition
vz1	4	2	1059	polietilen velike gostote + drobno mleti lesni delci (trdi les)/ high density polyethylene + wood pulp (hardwood)
vz2	4	2	1089	polipropilen (tip A*) + drobno mleti lesni delci (trdi les) + kemično spremenjen polipropilen/ polypropylene (type A*) + wood pulp (hardwood) + chemically modified polypropylene
vz3	4	2	1059,5	polipropilen (tip A*) + drobno mleti lesni delci (trdi les) + termoplastični elastomer/ polypropylene (type A*) + wood pulp (hardwood) + thermoplastic elastic material
vz4	4	2	1089	polietilen velike gostote + drobno mleti lesni delci (mehki les)/ high density polyethylene + wood pulp (softwood)
vz5	4	2	1000	polipropilen (tip B**) + drobno mleti lesni delci (trdi les) + termoplastični elastomer/ polypropylene (type B**) + wood pulp (hardwood) + thermoplastic elastic material
vz6	4	2	1020	polipropilen (tip B**) + drobno mleti lesni delci (trdi les) + kemično spremenjen polipropilen/ polypropylene (type B**) + wood pulp (hardwood) + chemically modified polypropylene
vz7	2	4	1046	ABS (akrilonitril – butadien – stiren)/ ABS (acrylnitril - butadien - styren)
vz8	1	2	2761	aluminij/ aluminium
vz9	3	2	1037	polistiren (zvočniki JVC)/ polystyrene (JVC loudspeakers)
vz10	3	2	1056	polistiren/ polystyrene
vz11	3	2	898	MDF/ MDF (medium density fiberboard)

* kopolimer/copolymer
** homopolimer/homopolymer

poteka pri visoki temperaturi in visokem tlaku. V primerjavi z borovim ali smrekovim lesom ima MDF običajno približno dvakrat manjši modul elastičnosti in približno 70% večjo gostoto.

Preglednica 2 kaže mehanske lastnosti preizkušancev vz1 – vz6. Iz neenakih lastnosti v prečni in vzdolžni smeri (glede na smer iztiskanja) vidimo, da so vsi ti preizkušanci anizotropni.

1.2 Meritve zvočnih lastnosti preizkušancev

Slika 4 kaže mesto meritve in merilno opremo. Vsi preizkušanci so bili vpeti na okoli 2 m dolgi elastični vrvici, debeline okoli 0,3 mm. S tem zagotovimo najmanjši vpliv vpetja na dinamično obnašanje preizkušanca. Vzbujanje je bilo opravljeno s posebej izdelano napravo, katere glavni del je piezoelektrični merilnik vzbujevalnega impulza, ki je prikazan na sliki 5. Tipična oblika vzbujevalnega impulza in odzivnega signala je prav tako prikazana na sliki 5. Kakor vidimo, je amplitudna os vzbujevalnega signala prikazana brezrazsežno, saj prikazani vzbujevalnik ni umerjen v

temperature and pressure. In comparison to a fir or spruce wood, the MDF's modulus of elasticity is approximately 100% smaller and its density is approximately 70% higher.

The mechanical properties of specimens vz1 – vz6 are shown in Table 2. Based on unequal properties in the transversal and longitudinal directions (according to the direction of extrusion) one can see that all the specimens are non-isotropic.

1.2 Measurements of the acoustic properties of the specimens

The measurement arrangement is shown in Figure 4. All the specimens were suspended on approximately 2-m-long (0.3 mm in diameter) nylon line. This ensured a negligible effect of the specimen's support on its dynamic behaviour. A special device with a piezoelectric sensor was used to excite the specimens, as shown in Figure 5. Typical shapes of the excitation and output signals are shown in Figure 5 as well. One can see that the amplitude axis of the input signal is presented on a dimensionless scale. The reason for this is that the excitation device was not calibrated for

Preglednica 2. *Mehanske lastnosti preizkušancev vz1 do vz6*
Table 2. *Mechanical properties of specimens vz1 to vz6*

Preizkušanci/ Specimens	**E-modul vzdolžno/ E-modulus longitudinally (MPa)**	**E-modul prečno/ E-modulus transversally (MPa)**	**upogibna trdnost vzdolžno/ bending stregth longitudinally (MPa)**	**upogibna trdnost prečno/ bending stregth transversally (MPa)**	**MFI* (5kg/190°C)**	**natezna trdnost/ tensile strength (MPa)**
vz1	3112	2275	46,43	37,38	24,5 g/10 min	24,24
vz2	3819	2675	52,32	40,77	3,90 g/10 min	32,90
vz3	3522	2575	40,80	30,43	3,75 g/10 min	28,92
vz4	3564	2786	40,79	33,47	3,70 g/10 min	23,97
vz5	2804	2398	38,71	30,31	10,8 g/10 min	21,07
vz6	3355	2761	58,96	44,09	16,6 g/10 min	37,21

* indeks tečenja/percolation index

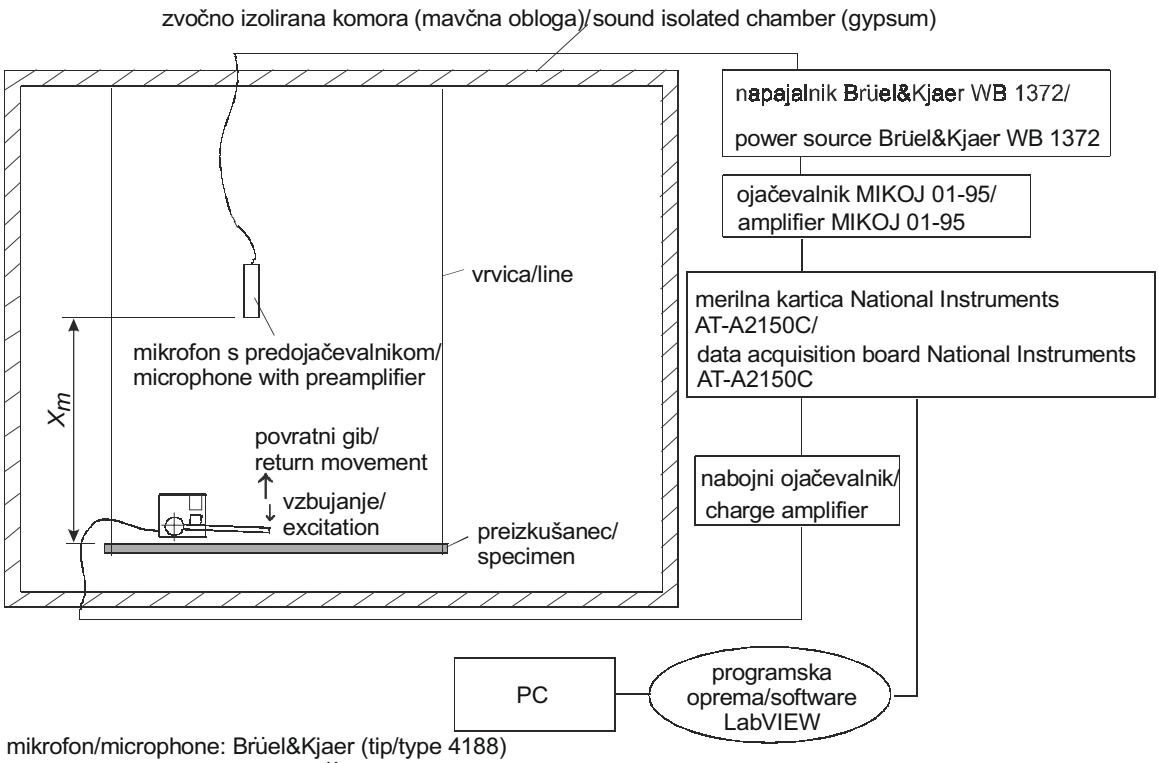

Sl. 4. *Merilno mesto in oprema*
Fig. 4. *Measurement place and arrangement*

fizikalnih enotah. To seveda ne zmanjša njegove uporabnosti, saj je končni cilj meritev t.i. frekvenčni odziv preizkušancev, pri katerem odzivni signal delimo z vzbujevalnim v frekvenčnem področju, torej merimo razmerje med odzivnim signalom ter vzbujevalnim signalom (mehanskim impulzom) [7]. Poleg tega nas niso zanimale absolutne vrednosti frekvenčnih odzivov preizkušancev, temveč le njihova primerjava.

Akustični odziv preizkušanca na mehansko impulzno motnjo (brezrazsežno), merjen s kondenzatorskim mikrofonom, ima enoto Pa, torej je amplituda zveznega frekvenčnega odziva preizkušanca izražena v Pa [7]:

measurements in physical units. This does not affect its applicability because the aim of the measurements is the frequency response of the specimens, which is defined as the ratio of the output to the input signal [7]. In addition, we were interested in a comparison of the different frequency responses of the specimens rather than their absolute values.

The acoustic response of the specimen due to the mechanical impulse (on a dimensionless scale) which is measured with a condenser microphone is defined in Pascal units. Therefore, the amplitude of the continuous frequency-response function of a specimen is defined in Pascal units [7]:

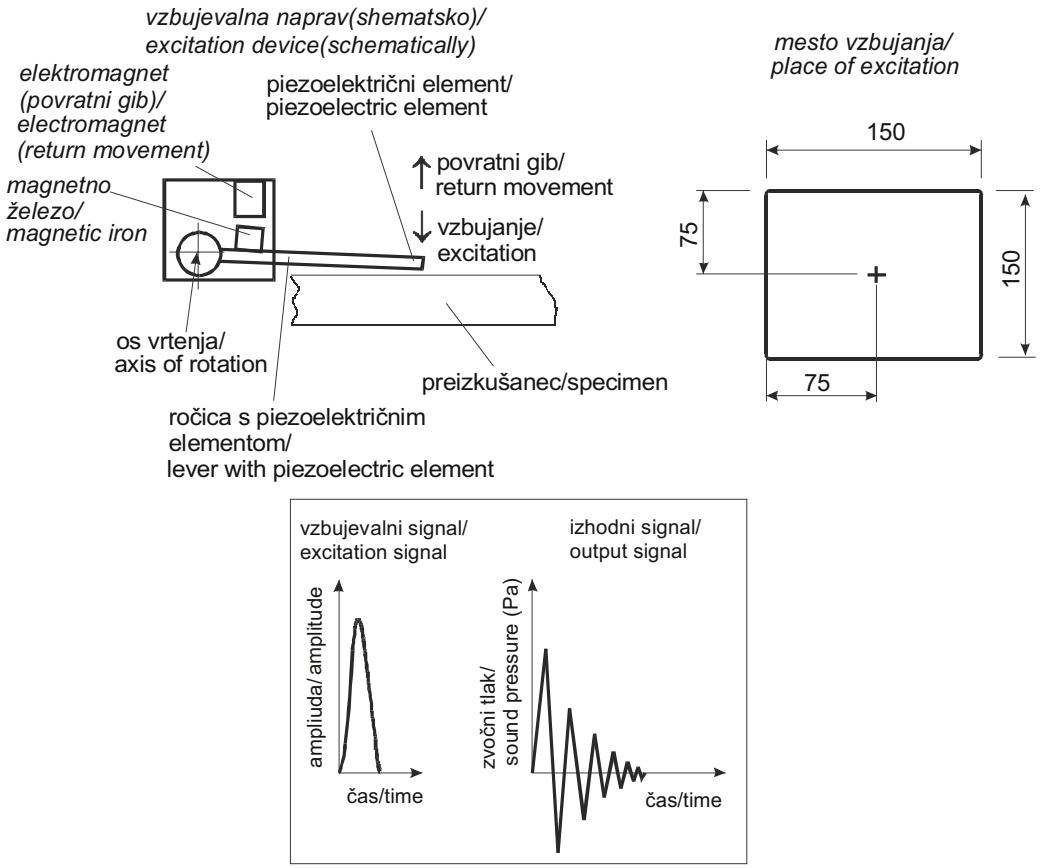

Sl. 5. *Shematski prikaz naprave za vzbujanje preizkušancev, mesto vzbujanja ter oblika vzbujevalnega in odzivnega signala*

Fig. 5. *Schematic representation of excitation device, place of excitation, and both excitation and output signal*

$$H(f) = \left| \frac{\overline{G}_{xy}(f)}{\overline{G}_{xx}(f)} \right| \tag{4},$$

kjer so: $\overline{G}_{xy}(f)$ povprečni križni energijski spekter vhodnega in izhodnega signala, $\overline{G}_{xx}(f)$ povprečni energijski spekter vhodnega signala, f pa frekvenca z izmero Hz. Še nepovprečena spektra izračunamo iz naslednjih enačb [7]:

where $\overline{G}_{xy}(f)$ is an average cross power spectrum of both the input and output signals, $\overline{G}_{xx}(f)$ is an average power spectrum of an input signal, and f is the frequency with dimension Hz. Before the averaging both spectra from expression (4) are [7]:

$$G_{xy}(f) = S_x(f) \cdot S_y^*(f) \tag{5}$$

$$G_{xx}(f) = S_x(f) \cdot S_x^*(f) \tag{6},$$

kjer so: $S_x(f)$ frekvenčna slika vhodnega in $S_y(f)$ izhodnega časovnega signala, $S_x^*(f)$ in $S_y^*(f)$ pa njuni konjugirano kompleksni vrednosti. S tako definiranim frekvenčnim odzivom se izognemo napaki zaradi navzočnosti šuma. Pri meritvah frekvenčnega odziva je pomembna koherenčna funkcija, ki je merilo za moč izhodnega signala zaradi vhodnega signala. Če je koherenca 1, potem je bil ves izhodni signal povzročen zaradi vhodnega, če pa je 0, potem izhodni signal ni posledica vhodnega. Koherenčna funkcija γ^2 je [7]:

where $S_x(f)$and $S_y(f)$are frequency transformations of the input and output signals, respectively, and $S_x^*(f)$ and $S_y^*(f)$ are their complex conjugates. Such an approach ensures that a frequency-response function is not influenced by the presence of noise. A criterion of the quality of the measurements is the coherence function, which indicates the power of the output signal due to the input signal. When this function is 1 then all the power of the output signal is a consequence of the input signal. When the coherence was 0 then the output signal was not caused by the input signal. The coherence function γ^2 is [7]:

$$\gamma^{2}(f)=\frac{\overline{G}_{xy}(f)\cdot\overline{G}_{xy}*(f)}{\overline{G}_{xx}(f)\cdot\overline{G}_{yy}*(f)} \tag{7}$$

kjer je $\overline{G}_{yy}(f)$ povprečni energijski spekter izhodnega signala, * pa označuje kompleksno konjugacijo. Nepovprečeni spekter $G_{yy}(f)$ izračunamo analogno $G_{xx}(f)$ iz enačbe (6), tako da indeks $_x$ nadomestimo z $_y$.

Dejansko so zaradi analogno/digitalne premene z merilno opremo zvezni spektri v izrazih (4) do (7) diskretni. Diskretni amplitudni frekvenčni spekter signala dobimo s hitro Fourierjevo preslikavo signala v časovnem prostoru ([7] in [10]):

where $\overline{G}_{yy}(f)$ is an average power spectrum of the output signal, and * indicates its complex conjugation. A non-averaged spectrum $G_{yy}(f)$ is calculated by analogy to $G_{xx}(f)$ from expression (6), where the index $_x$ is replaced by $_y$.

As a matter of fact, the continuous spectra in expressions (4) to (7) are discrete due to the analogue/digital conversion with the measurement equipment. The discrete amplitude spectrum of a signal is obtained with a fast Fourier transformation of this signal in a time domain ([7] and [10]):

$$FFT(s\cdot\Delta f)=\frac{T}{N}\sum_{n=0}^{N-1}f(n\cdot\Delta t)\cdot e^{-\mathrm{j}2\pi\, sn/N} \tag{8}$$

kjer so: $s = 0, 1, 2 \ldots N/2$, Δf frekvenčna ločljivost, T čas snemanja, N število diskretnih točk, Δt časovni korak med diskretnimi točkami, $f(n\cdot\Delta t)$ diskretna vrednost signala v n-ti točki in $\mathrm{j}=\sqrt{-1}$. Frekvenca vzorčenja f_s je bila 8 kHz pri številu diskretnih točk N=4096. $FFT(s\cdot\Delta f)$ torej pomeni diskretno Fourierjevo preslikavo digitaliziranega diskretnega signala časovne funkcije $f(n\cdot\Delta t)$. Če velja, da je z $f(n\cdot\Delta t)$ opisan vhodni signal v vzbujani predmet, katerega frekvenčni odziv merimo, velja tudi ([7] in [10]):

where $s = 0, 1, 2 \ldots N/2$, Δf is frequency resolution, T is time of signal recording, N is the number of discrete points, Δt is the time interval between these discrete points, $f(n\cdot\Delta t)$ is a discrete value of the signal in the n-th point, and $\mathrm{j}=\sqrt{-1}$. The sampling frequency f_s was 8 kHz and N was 4096. Thus, $FFT(s\cdot\Delta f)$ indicates a discrete Fourier transformation of a digital discrete signal of a time-dependent function $f(n\cdot\Delta t)$. If $f(n\cdot\Delta t)$ describes the input signal into an object whose frequency response is measured, then the following is true ([7] and [10]):

$$S_x(s\cdot\Delta f)\approx FFT(s\cdot\Delta f)=\frac{T}{N}\sum_{n=0}^{N-1}f(n\cdot\Delta t)\cdot e^{-\mathrm{j}2\pi\, sn/N} \tag{9}$$

kjer je $S_x(s\cdot\Delta f)$ frekvenčna slika vhodnega signala v diskretni obliki. Podobno lahko rečemo tudi za izhodni signal. Torej, če je z $f(n\cdot\Delta t)$ opisan izhodni signal iz vzbujanega predmeta, katerega frekvenčni odziv merimo, velja tudi ([7] in [10]):

where $S_x(s\cdot\Delta f)$ is the frequency transformation of the input signal in a discrete form. Similarly, if $f(n\cdot\Delta t)$ describes the output signal from the excited object then the following is true ([7] and [10]):

$$S_y(s\cdot\Delta f)\approx FFT(s\cdot\Delta f)=\frac{T}{N}\sum_{n=0}^{N-1}f(n\cdot\Delta t)\cdot e^{-\mathrm{j}2\pi\, sn/N} \tag{10}$$

kjer je $S_y(s\cdot\Delta f)$ frekvenčna slika izhodnega signala v diskretni obliki.

where $S_y(s\cdot\Delta f)$ is a frequency transformation of the output signal in a discrete form.

Dvostranski amplitudni diskretni frekvenčni spekter je ([7] in [10]):

The two-sided amplitude spectrum in a discrete form is ([7] and [10]):

$$\left|FFT(s\cdot\Delta f)\right|/N \tag{11}$$

N – število diskretnih točk signala mora biti za natančno Fourierjevo preslikavo 2^n, n=1, 2 ... Izraz (11) predstavlja dvostranski spekter, po množenju z 2 pa dobimo amplitudni frekvenčni spekter, ki pomeni amplitude frekvenčnih komponent signala. Frekvenčne komponente so na frekvenčni osi spektra med seboj oddaljene za Δf (Hz). Zveza med frekvenčno ločljivostjo in trajanjem signala je ([7] in [10]):

For a high-quality Fourier transformation the number of discrete points N has to be 2^n, n=1, 2 ... Expression (11) represents a two-sided spectrum, however after multiplying it by a factor at 2 the result is an amplitude spectrum that represents the amplitudes of the frequency components of a signal. The frequency resolution between neighbouring components of this spectrum is Δf (Hz). The relation between the frequency resolution and the time of recording is ([7] and [10]):

$$\Delta f=1/T \tag{12}$$

Zaradi poenostavitve naj za nadaljnjo analizo velja, da je vsak izmerjeni frekvenčni odziv obravnavan kot zvezni odziv $H(f)$ iz enačbe (4), četudi je dejansko nezvezen, torej odvisen od diskretnih vrednosti frekvence f z ločljivostjo Δf.

Kakovosten analogno/digitalni pretvornik na merilni kartici z vgrajenim analognim filtrom za odstranitev visokih frekvenc je zagotovilo, da je bil Nyquistov pogoj (frekvenca vzorčenja vsaj 2-krat višja od najvišje frekvence v signalu) vedno izpolnjen. Čas snemanja vstopnega sunka in akustičnega odziva preizkušancev je bil 0,512 s, torej je bila frekvenčna ločljivost spektrov 1,953 Hz (enačba (12)). Snemanje impulza in rezultirajočega zvočnega tlaka je bilo sočasno. Z obdelavo signala s programsko opremo je bilo poskrbljeno, da sta se oba, izhodni in vhodni signal, začela in končala z amplitudo nič. To prispeva h kakovosti frekvenčne analize, dokaz za to pa je bila vrednost koherenčne funkcije med 0,95 in 1,0 za analizirano frekvenčno območje (prvega resonančnega vrha) za vse materiale. Komponente frekvenčnih spektrov so izražene v vrednostih kpk (korena povprečja kvadratov).

Za meritev morebitnih razlik v akustičnem odzivu kvadratastih plošč iz različnih materialov lahko uporabimo enačbo (13). Ta povezuje frekvenco n-tega modalnega načina f_n in mehanske lastnosti homogene, izotropne in prosto vpete kvadratne plošče [11]:

$$f_n = C_n \cdot t \cdot \sqrt{\frac{E}{\rho \cdot (1-\nu^2) \cdot l^4}} \qquad (13),$$

kjer so C_n konstanta, odvisna od n-tega modalnega načina, t debelina plošče, ν Poissonovo razmerje in l dolžina (širina) plošče. V analizi, ki bo prikazana, je bil analiziran prvi modalni način za vse plošče. Ta modalni način ima največje pomike na sredini vzbujene plošče, proti robovom pa so pomiki postopoma manjši (podobno kakor pri trampolinu) ([11] in [12]). Če torej ploščo vzbudimo v sredini, vzbudimo prvi modalni način v največji možni meri. Veličina f_n je izmerjena, t, l, ν in ρ so točno ali vsaj približno znane. Za prvi modalni način preizkušancev iz enačbe (13) izhaja:

$$E = \frac{1}{C_1} \cdot \frac{f_1 \cdot \rho \cdot (1-\nu^2) \cdot l^4}{t^2} \left[\mathrm{Pa}\right] \qquad (14).$$

Z zelo veliko verjetnostjo lahko rečemo, da je Poissonovo razmerje za aluminij 0,3, za MDF med 0,3 in 0,4, za preostale testirane materiale pa približno 0,4 ([13] in [14]), vsekakor pa med 0,3 in 0,5. V nadaljevanju bosta tako pri analizi vseh materialov, razen aluminija, upoštevani spodnja (0,3) in zgornja meja (0,5) Poissonovega razmerja.

2 REZULTATI IN ANALIZA

Ker gre v nadaljevanju le za relativno primerjavo veličin, lahko konstanto C_1 in izmere

Due to a simplification let us denote that each measured frequency response function is analysed as a continuous response $H(f)$ from expression (4), although in reality all the spectra were discontinuous, thus they were dependent on discrete values of frequency f with frequency resolution Δf.

A high-quality analogue/digital converter on a data-acquisition board with an anti-aliasing filter ensured that the Nyquist criterion (the sampling frequency has to be at least two times higher than the highest frequency of interest in a signal) was fulfilled. The recording time of the input impulse and the specimen's acoustic response was 0.512 sec. Thus, the frequency resolution of all spectra was 1.953 Hz (see expression (12)). The recording of the mechanical impulse and of the resulting sound pressure was performed simultaneously. Additional processing of both input and output signals was performed in order to set the amplitudes at their beginning and end to zero. This improves the quality of the frequency transformation, which was confirmed with a coherence function higher than 0.95 for the analysed frequency range (first resonant peak). The frequency-spectrum components are expressed in rms values.

To measure eventual differences in the acoustic response of square-shaped plates from various materials we can use expression (13). This includes the frequency of n-th mode f_n and the mechanical properties of homogeneous, isotropic and free-supported square-shaped plates [11]:

where C_n is a constant that depends on n-th mode, t is the plate thickness, ν is Poisson's ratio, and l is the length (width) of the plate. In the analysis which follows, only the first mode of all specimens was analysed. The largest displacements for this mode are in the middle of the plate. The amplitudes of the displacements diminish towards the plate's edges (like with trampoline) ([11] and [12]). Thus, when the specimen is excited in its geometrical centre, the first mode is excited as much as possible. The quantity f_n is measured, and t, l, ν and ρ are exactly or approximately known. Based on expression (13) for a first mode it follows:

With great certainty we can say that Poisson's ratio for aluminium is 0.3, for MDF between 0.3 and 0.4, and for other tested materials about 0.4; in any case between 0.3 and 0.5 ([13] and [14]). Therefore, in the following analysis the lower (0.3) and the upper (0.5) limit for Poisson's ratio are considered.

2 RESULTS AND ANALYSIS

Because in the following analysis only a relative comparison of quantities is presented, it is reason-

Preglednica 3. *Rezultati meritev*
Table 3. *Results of measurements*

Preizkušanci Specimens	f_{od} Hz	δ	E_{rel} za / for ν=0,3	E_{rel} za / for ν=0,5
vz1	214,3	0,0258	5,68E9	4,68E9
vz2	228,7	0,0214	6,56E9	5,41E9
vz3	207,6	0,0228	5,26E9	4,33E9
vz4	215,1	0,0144	5,81E9	4,79E9
vz5	209,6	0,0263	5,20E9	4,29E9
vz6	228,0	0,0279	6,16E9	5,08E9
vz7	278,3	0,0084	2,33E9	1,92E9
vz8	535,0	0,0028	91,02E9	/
vz9	158,0	0,0132	2,98E9	2,46E9
vz10	156,3	0,0147	2,97E9	2,45E9
vz11	259,0	0,0142	7,64E9	6,29E9

vseh veličin iz enačbe (14) izvzamemo. Tako namesto veličine E dobimo brezrazsežni modul elastičnosti E_{rel}. Preglednica 3 prikazuje zbrane rezultate meritev za vse testirane plošče. Prikazane so srednje vrednosti frekvenc in faktorjev viskoznega dušenja prvega modalnega načina ter relativnih modulov elastičnosti.

Če v enačbah (1) in (2) namesto veličine E upoštevamo E_{rel}, in če za gostoto ne upoštevamo izmer, dobimo namesto veličine Z t.i. relativni zvočni upor Z_{rel} in namesto veličine ϑ relativno dušenje zvočnega sevanja ϑ_{rel}. Obe relativni veličini in faktor viskoznega dušenja so za vse testirane materiale predstavljeni na slikah 6 oziroma 7. Zaradi zelo velike vrednosti relativnega zvočnega upora za aluminij (vz8) so na sliki 8 še enkrat prikazane vrednosti za vse nekovinske materiale.

able to exclude from Equation (14) the constant C_1 and the dimensions of all quantities. Instead of quantity E we consequently obtain the dimensionless modulus of elasticity E_{rel}. The results of the measurements of all the plates are presented in Table 3. More precisely, the mean values of the frequencies and the factors of viscous damping of the first mode, and the relative moduli of elasticity are presented.

Considering E_{rel} instead of E and ignoring the units for density in Expressions (1) and (2), we obtain a relative sound-wave resistance Z_{rel} instead of Z, and a relative damping of sound radiation ϑ_{rel} instead of ϑ. In addition to the viscous-damping factor, these two quantities are shown in Figures 6 and 7 for all the tested materials. Due to a high value of the relative sound-wave resistance for aluminium (vz8), Figure 8 shows E_{rel}, ϑ_{rel} and δ for all the non-metal materials.

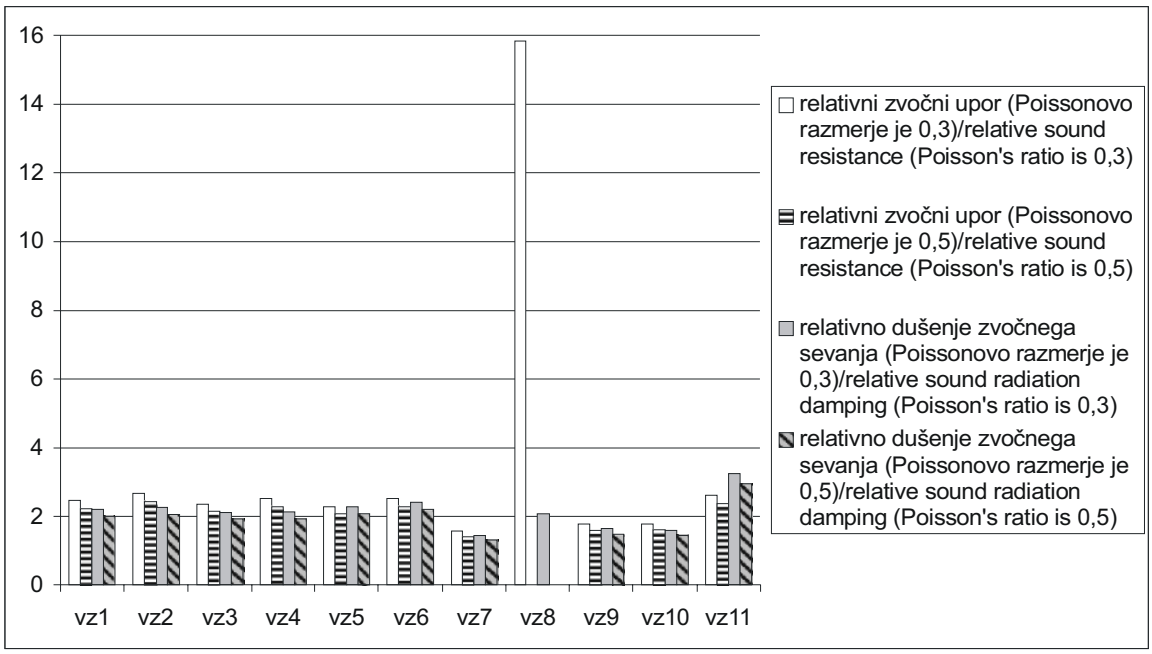

Sl. 6. *Relativni zvočni upor in dušenje zvočnega sevanja (vsi materiali)*
Fig. 6. *Relative sound resistance and sound radiation damping (all materials)*

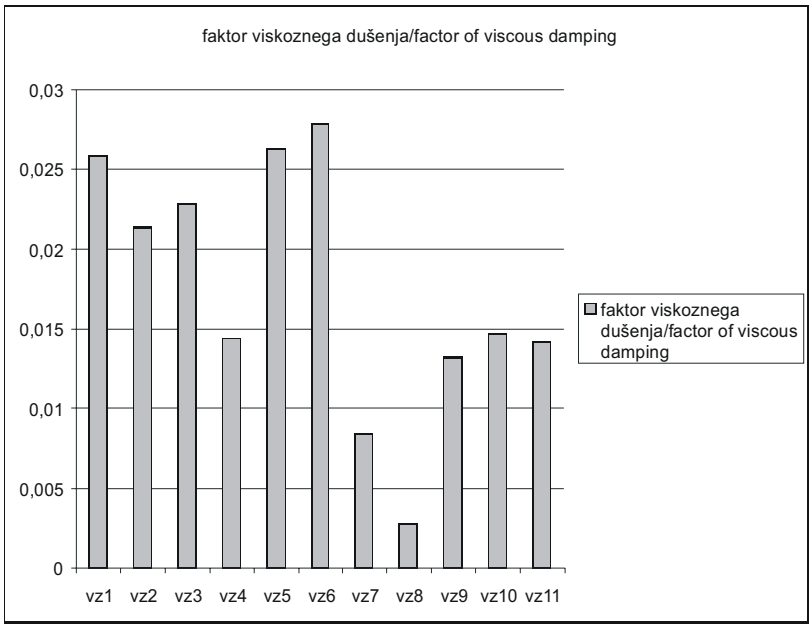

Sl. 7. *Faktor viskoznega dušenja*
Fig. 7. *Factor of viscous damping*

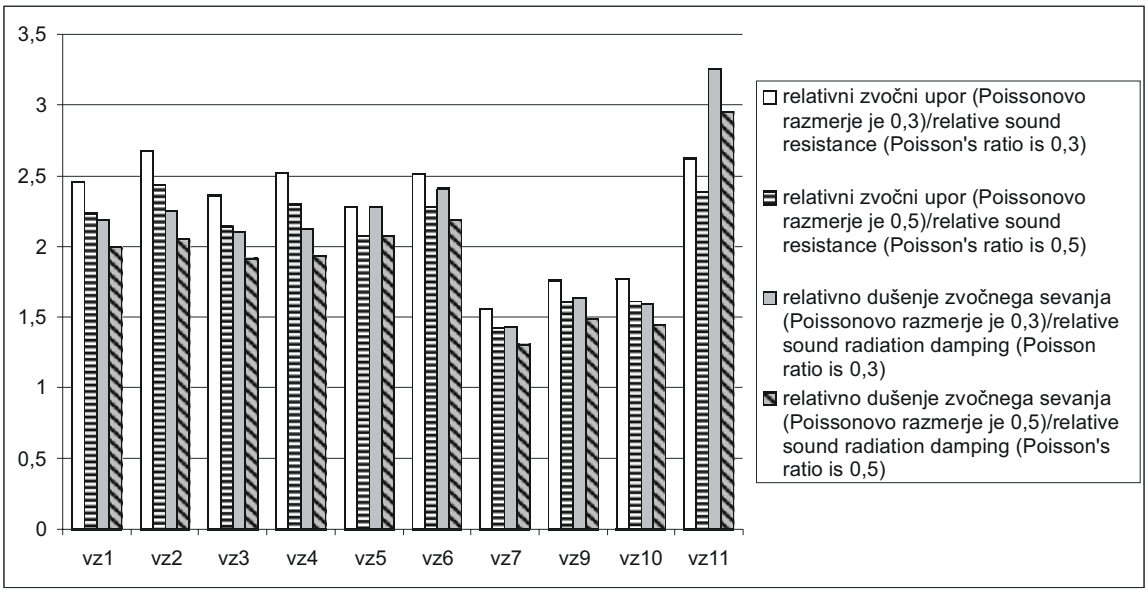

Sl. 8. *Relativni zvočni upor in dušenje zvočnega sevanja (vsi nekovinski materiali)*
Fig. 8. *Relative sound resistance and sound radiation damping (all non-metal materials)*

S slik 6 do 8 je razvidno, da imajo materiali vz4, vz9 in vz10 vse tri analizirane veličine (zvočni upor, dušenje zvočnega sevanja in faktor viskoznega dušenja) podobne tistim za referenčni material MDF. Pri tem velja, da imajo faktor viskoznega dušenja skoraj identičen tistemu za MDF. Med temi tremi materiali je vz4 v splošnem najbliže MDF, saj ima večji zvočni upor in dušenje zvočnega sevanja kakor materiala vz9 in vz10. Iz pregl. 1 je razvidno, da ima samo material vz4 drobno mlete lesne delce iz mehkega lesa. Vpliv drobno mletih lesnih delcev (trdi oziroma mehki les) je razviden iz primerjave materialov vz1 in vz4.

One can see from Figures 6 to 8 that materials vz4, vz9 and vz10 indicate similar acoustic properties (sound-wave resistance, damping of sound radiation and viscous-damping factor) to the reference material MDF. In addition, their factor of viscous damping is almost identical to that of MDF. Among all three materials the closest to MDF is vz4, because it has a higher sound-wave resistance and a higher damping of sound radiation than materials vz9 and vz10. It is evident from Table 1 that only fine, ground wood particles in vz4 are made of softwood. The influence of fine, ground wood particles (hardwood, softwood) is evident from a comparison between materials vz1 and vz4. It seems that

Kakor kaže je ta vpliv precej značilen, saj je faktor viskoznega dušenja za material vz1 za približno 80% večji od tistega za vz4, medtem ko sta za oba materiala zvočni upor in dušenje zvočnega sevanja primerljiva.

3 SKLEP

Eden najbolj razširjenih materialov za tudi najbolj kakovostne okrove zvočnikov je t.i. MDF. Zato smo zvočne lastnosti, ki jih ima ta material, definirali za referenčne. Zvočne lastnosti gradiva so definirane z (i) zvočnim uporom, (ii) dušenjem zvočnega sevanja in (iii) faktorjem viskoznega dušenja. V primerjavi z zvočnimi ploščami glasbil, ki morajo čim več vibracijske energije sevati v okolico (pri čim manjših notranjih izgubah), je funkcija okrova zvočnikov drugačna. Podrobneje, dušenje zvočnega sevanja mora biti za zvočne plošče glasbil razmeroma veliko, zvočni upor pa majhen. Energija tresenja membrane zvočnika se mora pravilno absorbirati, pri tem pa stopnja absorpcije ne sme biti prevelika ali premajhna. Rečemo lahko torej, da mora biti zvočni upor materiala za okrov zvočnikov razmeroma velik, da se ne ojačujejo resonančne frekvence zvočnika kot celote. Dušenje zvočnega sevanja, torej sevanje zvoka v okolico, pa mora biti razmeroma majhno. Vendar bi previsok zvočni upor pomenil slabo prehajanje zvočne energije v okrov zvočnika, kar pomeni veliko možnost pojava odmevov in stojnega valovanja. Lep primer tega je velika vrednost zvočnega upora za aluminij (sl. 6). Ni si težko predstavljati, da bi se aluminijski okrov zvočnika kazal v nezaželenih stranskih pojavih, na primer stojno valovanje in posledično resonančna nihanja membrane zvočnika. Logično je namreč, da namen okrova zvočnika ni poudarjati določenih frekvenc, temveč prav nasprotno, takšne pojave mora preprečiti. Po drugi strani je majhen zvočni upor materiala povezan z razmeroma majhno zvočno impedanco in hitrim odvajanjem zvočne energije v okrov zvočnika, kar se lahko kaže v kratko trajajočih, a izrazitih resonančnih frekvencah okrova zvočnika. To lahko pomeni velike izgube zvočne energije, sploh če se razmeroma majhen zvočni upor pojavi v kombinaciji z razmeroma visokim faktorjem viskoznega dušenja (velike izgube zaradi notranjega trenja).

Smiselno je skleniti, da so zvočne lastnosti, ki smo jih izmerili na materialu MDF, optimalne. Tako lahko rečemo, da je material vz4 med vsemi testiranimi materiali najbolj primeren za okrove zvočnikov. Ker sta oba, dušenje zvočnega sevanja in zvočni upor za ta material nekoliko manjša v primerjavi z MDF, se pojavi vprašanje, kako obe veličini povečati, ne da bi bistveno spremenili faktor viskoznega dušenja, ki se zelo dobro ujema s tistim za MDF.

this influence is quite significant because the viscous-damping factor for material vz1 is approximately 80% higher than that one for vz4, whereas both the sound-wave resistance and the damping of sound radiation for these two materials are comparable.

3 CONCLUSION

One of the most common materials for loudspeaker boxes, including high-quality products, is MDF (medium-density fibreboard). Therefore, we denoted the acoustic properties that are significant for this material as the reference properties. The acoustic properties of a material are defined by (i) the sound-wave resistance, (ii) the damping of sound radiation, and (iii) the viscous damping factor. In comparison to the sound boards of musical instruments, which should radiate their vibration energy into the surroundings as much as possible (in addition to minimal internal losses), the function of loudspeaker boxes is different. More precisely, the damping of sound radiation for the sound boards of musical instruments has to be relatively high, and the sound-wave resistance should be low. The energy contained in the vibrations of a loudspeaker diaphragm has to be absorbed in a proper way, which means that the intensity of the absorption should be neither too high nor too low. We can say that the sound-wave resistance of a material for loudspeaker boxes has to be relatively high in order not to amplify the resonant frequencies of a whole loudspeaker. The damping of the sound radiation, and thus the radiating of sound into the surroundings, has to be relatively low. However, too high sound-wave resistance means an insufficient transition of acoustic energy into the loudspeaker box, which can result in phenomena like echoes and standing waves. A nice example of this is the high value of sound-wave resistance for aluminium (see Figure 6). It is not hard to understand that an aluminium loudspeaker box would result in undesired effects like standing waves and, consequently, resonant vibrations of the loudspeaker diaphragm. It is logical that the purpose of a loudspeaker box is not to emphasize certain frequencies, but on the contrary, to prevent this phenomenon. On the other hand, too low sound-wave resistance correlates with a relatively low sound impedance and fast sound-energy drain into the loudspeaker box. This can result in short-lasting but distinctive resonant frequencies of the loudspeaker box. Finally, this can lead to high sound-energy losses, especially if relatively low sound-wave resistance appears together with a relatively high factor of viscous damping (high losses due to internal friction).

It is reasonable to conclude that the acoustic properties measured for MDF are the best ones. Thus, one can say that the most suitable material for loudspeaker boxes among the tested materials is vz4. Because both the damping of sound radiation and the sound-wave resistance for this material are slightly lower in comparison to MDF, the question is how to increase these two parameters and not significantly affect the viscous-damping factor that corresponds to that for MDF.

Zahvala

Prispevek je bil pripravljen s sodelovanjem projekta Eureka 2819: "Razvoj in označba okolju prijazne termoplastike" ter podjetja ECOPLAST iz Slovenije.

Aknowlegment

This paper was prepared with the cooperation with Eureka project 2819: "Development and characterisation of eco-friendly thermoplastics", and the ECOPLAST factory in Slovenia.

4 LITERATURA
4 REFERENCES

[1] Petzing, J.N., J.R. Tyrer (1996) The effect of metallographic structure on clamped plate vibration characteristics, *Experimental mechanics*, Vol. 36, No. 2, 127-134.
[2] Elbeyli, O., G. Anlas (2000) The nonlinear response of a simply supported rectangular metallic plate to transverse harmonic excitation, *Journal of Applied Mechanics*, Vol. 67, Issue 3, 621-626.
[3] Durán, R. G., L. Hervella-Nieto, E. Liberman, L. Hervella-Nieto, J. Solomin (1999) Approximation of the vibration modes of a plate by Reissner-Mindlin equations, *Mathematics of Computation 68*, 1447-1463.
[4] Ma, C.-C., C.-H. Huang (2001) Experimental and numerical analysis of vibrating cracked plates at resonant frequencies, *Experimental Mechanics*, Vol.41, No. 1, 8-18.
[5] Kopač, J., S. Šali (1999) The frequency response of differently machined wooden boards, *Journal of Sound and Vibration*, Vol. 227, No. 2, 259-269.
[6] Kollmann, F., A. Côté (1968) Principles of wood science and technology, Part 1: Solid wood. Berlin, *Springer Verlag*.
[7] Ewins, D.J. (1984) Modal testing; Theory and practice. Letchworth, *Research Studies Press Ltd.*
[8] T. ONO (1989) Concise encyclopedia of wood & wood-based materials. Oxford, *Pergamon Press*.
[9] Hall, D.E. (1980) Musical acoustics. Pacific Grove: *Brooks/Cole Publishing Company*.
[10] The fundamentals of signal analysis, Application note 243. *Hewlett-Packard.*
[11] Harris, C.M. (1988) Shock vibration handbook, 3rd edition. New York, *McGraw-Hill Book Company.*
[12] Olson, H.F. (1967) Music, physics and engineering. New York, *Dover Publications, Inc.*
[13] Bodig, J., B. Jayne (1982) Mechanics of wood and wood composites. New York, *Van Nostrand Reinhold Company.*
[14] http://composite.about.com/library/data/bldata.htm

Naslova avtorjev: mag. Samo Šali
prof.dr. Janez Kopač
Univerza v Ljubljani
Fakulteta za strojništvo
1000 Ljubljana

Uroš Žnidarič
ISOKON. d.o.o.
Mestni trg 5a
3210 Slovenske Konjice

Authors' Addresses: Mag. Samo Šali
Prof.Dr. Janez Kopač
University of Ljubljana
Facaulty of Mechanical Eng.
Aškerčeva 6
1000 Ljubljana, Slovenia

Uroš Žnidarič
ISOKON. d.o.o.
Mestni trg 5a
3210 Slovenske Konjice, Slovenia

Prejeto: 22.9.2004
Received:
Sprejeto: 2.12.2004
Accepted:
Odprto za diskusijo: 1 leto
Open for discussion: 1 year

© Strojniški vestnik 50(2004)12,594-597
ISSN 0039-2480
UDK 621.914
Pregledni znanstveni članek (1.02)

© Journal of Mechanical Engineering 50(2004)12,594-597
ISSN 0039-2480
UDC 621.914
Review scientific paper (1.02)

Nov pristop k preračunu aritmetičnega srednjega odstopanja profila pri kopirnem frezanju

A New Approach to Calculating the Arithmetical Mean Deviation of a Profile during Copy Milling

Jozef Peterka

Hrapavost površine, kot posledica frezanja s krogelnim frezalom, je v strokovni literaturi in univerzitetnih učbenikih le redko opisana. Problem je pogosto poenostavljen. Kar pomeni, da so uporabljena poenostavljena razmerja za teoretične izračune hrapavosti površine pri kopirnem frezanju s krogelnim frezalom: računski parameter Rz in največja višina valovitosti profila. V tem prispevku je predstavljen izpopolnjen izračun, ne samo parametra Rz, ampak tudi parametra Ra, aritmetičnega srednjega odstopanja profila. V prispevku so predstavljene nove enačbe za neposredni izračun aritmetičnega srednjega ostopanja prečnih in vzdolžnih profilov pri kopirnem frezanju ravne površine in poševne površine.

(Ključne besede: frezanje kopirno, finiširanje, hrapavost površin, oblike proste)

Surface roughness as a result of milling with a cylindrical ball-end cutter is determined in the technical literature, as it is in university textbooks, relatively infrequently. The problem is usually simplified, which means simplified relations for the calculations of theoretical surface roughness during copy milling with cylindrical ball-end cutters are introduced: the calculation of parameter Rz, and the maximum height of the undulation profile. In this contribution an improved calculation, not only for parameter Rz , but also for parameter Ra, the arithmetical mean deviation of the profile, is presented. The paper presents new equations for the direct calculation of the arithmetical mean deviation of the transverse and longitudinal profiles during copy milling on a plane (face) surface and an oblique surface.

(Keywords: copy milling, finishing, surface roughness, free form surfaces)

0 PREFACE

Reference [1] describes various possibilities for calculating theoretical surfaces roughness. The surface roughness can be evaluated using different parameters. Theoretically, it is best to calculate ten points for the height of the irregularities, *Rz*. But this parameter is not mentioned in a drawing. This function fulfils the arithmetical mean deviation of the profile *Ra*. An alternative is an empirically determined equation between *Ra* and *Rz*, but this equation is assigned in the large enough interval [2] (see Equation (3), it depends on other parameters too, mainly on the cutting conditions) and its sum arithmetic value does not need to match the actual relation between Ra and Rz during the copy milling using copy tools. The copy-milling tools are mainly use in the CAD/CAM systems branch [3], in order to manufacture oblique surfaces and free-form surfaces [4].

1 ROUGHNESS ON THE PLANE SURFACE

This section will show the calculation of roughness for two cases: for parameter *Rz* [5] and *Ra*, and for the transverse and longitudinal roughness.

1.1 The parameter *Rz* on the plane surface

Fig. 1. shows the situation for the origin of theoretical transverse roughness during copy milling on a plane surface. Equation (1) is valid from Fig. 1:

$$Rz = R - \frac{1}{2}\sqrt{4R^2 - a_e^2} \cong \frac{a_e^2}{8R} \qquad (1),$$

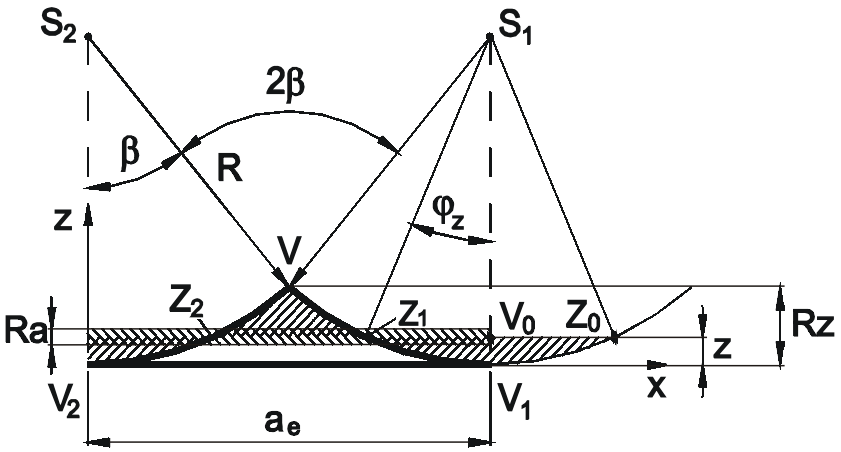

Fig. 1. *The origin of the transverse roughness during copy milling on a plane surface*

where
R is the tool radius
a_e is the stepover (path interval),
or the same equation for parameter R_t is published in [6]:

$$R_t = \frac{D_C}{2} - \sqrt{\frac{D_C^2 - a_e^2}{4}} \qquad (2),$$

where
D_c is the tool diameter
a_e is the stepover (path interval).

Next, we can calculate the *Ra* parameter from its dependence on *Rz* parameter using different empirical equations. The reference example, according to [2], is shown in the following empirical equation (3) for conventional machining (turning, milling, drilling):

$$Ra \cong \frac{Rz}{(3-5)} \qquad (3).$$

The selection of the denominator value from the interval (3 to 5) depends on the methods of cutting and on the other experimental cutting parameters. The question is can we calculate directly the arithmetical mean deviation of the profile *Ra* using the tool radius R and the stepover (path interval) a_e (or feed per tooth f_z)? The answer is yes.

1.2 The direct calculation of *Ra* on the plane surface

In this section we will show the derivation for the direct calculation of the arithmetical mean deviation of the profile during copy milling on a plane surface. From Fig.1 the angle β is:

$$\beta = \arcsin\frac{a_e}{2R} \qquad (4).$$

The area of profile A_r (butted and bounded with points V_2VV_1) between two surfaces of the ball-shaped miller above stepover a_e will be the area of the rectangle $V_1V_2S_2S_1$ reduced to the area of the triangle S_1S_2V and to the area of the circular segments VV_2S_2 a V_1S_1V, Equation (5):

$$A_r = a_e \cdot R - R^2 \sin\beta\cos\beta - R^2 arc\beta \qquad (5).$$

Next, it is possible to express from Fig.1. the area of the profile valley A_p that is bounded by the points $Z_1V_1Z_0$. The calculation of this area requires Equation (6):

$$A_p = \frac{1}{2}R^2\left(arc2\varphi_z - \sin 2\varphi_z\right) \qquad (6).$$

In the next step we need to present the area of the profile peak A_v that is butted and bounded by the points Z_2VZ_1. This area we can calculate using the following Equation (7):

$$A_v = A_r - \left[a_e \cdot z - \frac{1}{2}R^2\left(arc2\varphi_z - \sin 2\varphi_z\right)\right] \qquad (7).$$

The definition of the mean line of the profile needs to compare the area of the profile valley and the profile peak, $A_v = A_r$. After the substitution and editing we obtain Equation (8):

$$a_e \cdot z = a_e \cdot R - \frac{1}{2}a_e \cdot R\cos\beta - R^2 arc\beta \qquad (8)$$

and from equation (8) we can find the position of the mean line of the profile (see the Fig.1) of surface roughness:

$$z = R - \frac{1}{2}R\cos\beta - \frac{R^2}{a_e}arc\beta \qquad (9)$$

or:

$$z = R\left(1 - \frac{1}{2}\cos\beta - \frac{R}{a_e}arc\beta\right) \qquad (10).$$

From the definition of the arithmetical mean deviation of the profile *Ra* we can calculate this deviation as the width of the strip (of length a_e) on which it is possible to transform the double area of the profile valley (or the double area of the profile

peak, or the area sum of the profile valley and the profile, depending on which is the better to calculate). For the area of the profile valley we need the angle φ_z, which from Fig.1. is:

$$\cos\varphi_z = \frac{R-z}{R} = \frac{1}{2}\cos\beta + \frac{R}{a_e} arc\beta \qquad (11)$$

from Equation (11) we can obtain the angle φ_z:

$$\varphi_z = \arccos\left(\frac{1}{2}\cos\beta + \frac{R}{a_e} arc\beta\right) \qquad (12)$$

and the parameter R_a we designate from the following condition (13):

$$Ra \cdot a_e = 2A_p \qquad (13),$$

after the substitution and editing we obtain the equation:

$$Ra = \frac{R^2}{a_e}\left(arc2\varphi_z - \sin 2\varphi_z\right) \qquad (14),$$

where:
Ra is the arithmetical mean deviation of the profile,
R is the radius of the copy milling tool,
a_e is the stepover (path interval),
φ_z is the angle,
and the total equation for the calculation of the transverse roughness on the plane surface by milling with a ball-end cutter will be:

$$Ra = \frac{R^2}{a_e}\left\{arc2\left[\arccos\left(\frac{1}{2}\cos\arcsin\frac{a_e}{2R} + \frac{R}{a_e} arc\arcsin\frac{a_e}{2R}\right)\right] - \right.$$
$$\left. -\sin 2\left[\arccos\left(\frac{1}{2}\cos\arcsin\frac{a_e}{2R} + \frac{R}{a_e} arc\arcsin\frac{a_e}{2R}\right)\right]\right\}\cdot 1000 \qquad (15).$$

Equation (15) is exactly the final relation. Now we can calculate directly the arithmetical mean deviation of the transverse profile *Ra* from the radius of the copy milling tool and from the technological parameter a_e, the milling width, which the technology recommends in the CAM system.

For the arithmetical mean deviation of the longitudinal profile we substitute the stepover, a_e, with feed per cutter tooth, f_z, and the new equation is (16):

$$Ra = \frac{R^2}{f_z}\left(arc2\varphi_z - \sin 2\varphi_z\right) \qquad (16),$$

where:
Ra is the arithmetical mean deviation of the profile,
R is the radius of the copy milling tool,
f_z is the feed per tooth,
φ_z is the angle,
and the total equation for the calculation of the longitudinal roughness on the plane surface when milling with a ball-end cutter can also be used if we change the parameter a_e in Equation (15) to parameter f_z.

2 ROUGHNES ON THE OBLIQUE SURFACE

The described situation in the previous section is for calculating *Ra* on a plane surface. A similar sequence is possible for calculating *Ra* on an oblique surface.

2.1 The direct calculation of *Ra* on the oblique surface

We have here the new parameter α - the ramp of the milling oblique surface Fig.2.

In this case, instead of the stepover a_e for the transverse profile or the feed per cutter tooth f_z for the longitudinal profile, we need to use the new parameter a'_e:

$$a'_e = \frac{a_e}{\cos\alpha} \qquad (17),$$

where
a'_e is the stepover on the oblique surface,
a_e is the stepover on the plane surface,
α is the ramp angle of the oblique surface.

After substituting, Equation (17) into (14) we obtain the following Equation (18) for the transverse profile:

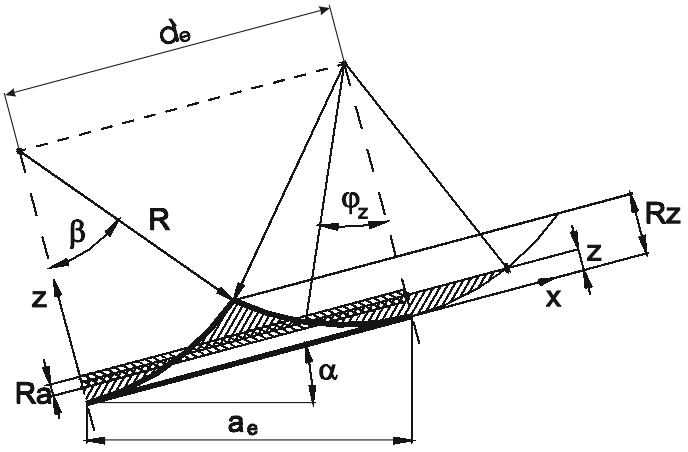

Fig. 2. *The origin of the transverse roughness during copy milling on an oblique surface*

$$Ra = \frac{R^2 \cos\alpha}{a_e}\left(arc2\varphi_z - \sin 2\varphi_z\right) \qquad (18)$$

and the total equation for the calculation of the transverse roughness on the oblique surface during milling with a ball-end cutter will be:

$$Ra = \frac{R^2\cos\alpha}{a_e}\left\{arc2\left[\arccos\left(\frac{1}{2}\cos\arcsin\frac{a_e}{2R\cos\alpha} + \frac{R\cos\alpha}{a_e}arc\sin\frac{a_e}{2R\cos\alpha}\right)\right] - \right.$$
$$\left. - \sin\ 2\left[\arccos\left(\frac{1}{2}\cos\arcsin\frac{a_e}{2R\cos\alpha} + \frac{R\cos\alpha}{a_e}arc\sin\frac{a_e}{2R\cos\alpha}\right)\right]\right\}\cdot 1000 \qquad (19).$$

For the longitudinal profile of roughness the equation (20):

$$Ra = \frac{R^2 \cos\alpha}{f_z}\left(arc2\varphi_z - \sin 2\varphi_z\right) \qquad (20)$$

and the total equation for the calculation of the longitudinal roughness on the oblique surface by milling with a ball-end cutter can also be used if we change the parameter a_e in Equation (19) to parameter f_z.

Equations (15) and (19) are the new equations for the direct calculation of roughness *Ra* with the technological parameters *R*, a_e (or f_z) and α during milling with a ball-end cutter.

3 CONCLUSION

The relations for the calculation of parameter *Ra* (3) presented in the scientific literature are inexact for milling, because they are only valid with a selected accuracy, depending on the type of machining (turning, milling, drilling, etc. Through relations (15) and (19) it is possible to directly calculate the surface roughness (parameter *Ra*) during copy milling. These relations will be added to the computer support of technology parameters' optimisation. This article aims to contribute to the possibilities of theoretical surface roughness' determination during milling with a cylindrical ball-end cutter, because the specialized literature has paid only a little attention to this problem.

This paper was supported under Slovak national grant VEGA 1/0302/03.

4 REFERENCES

[1] Bekes, J., J. Kicko, Z. Lipa (1999) Theory of machining. *DTP STU*, Bratislava.
[2] Lipa, Z., A. Janáč (2000) The finishing methods of machining. *DTP STU*, Bratislava.
[3] Peterka, J. (1996) 3D frézovanie kopírovacími frézami – rezný proces (3D milling by copy tools - cutting process). *Proceedings of International Conference on Computer-Materials-Technology (CO-MAT-TECH)*, Trnava, 24.-26. october 1996.
[4] Kuric, I. et al. (2002) Počítačom podporované systémy v strojárstve (The computer aided systems in manufacturing). *EDIS*, Žilina.
[5] Peterka, J. (1997) The analyse of the geometery and kinematics of copy milling. *J Scientific Works,* 5(1997) Trnava, 53-58.
[6] Miko, E. (2001) Investigation into the surface finish in milling using a ball nose end mill. *J. Advances in Manufacturing Science and Technology*, 25(2001)3 Warszawa, 71-86.
[7] Standard ISO 4287.

Autors Address: Prof. Dr. Ing. Jozef Peterka
Faculty of Materials' Science and Technology in Trnava,
Slovak University of Technology in Bratislava
J. Bottu 24
917 24 Trnava, Slovakia
peterka@mtf.stuba.sk

Prejeto: Received: 6.5.2003
Sprejeto: Accepted: 2.12.2004
Odprto za diskusijo: 1 leto
Open for discussion: 1 year

© Strojniški vestnik 50(2004)12,598-612
ISSN 0039-2480
UDK 621.833.3:621.824
Kratki znanstveni prispevek (1.03)

© Journal of Mechanical Engineering 50(2004)12,598-612
ISSN 0039-2480
UDC 621.833.3:621.824
Short scientific paper (1.03)

Dinamični model rotorskega sistema z gibkim členom in dvema nesoosnima gredema

A Dynamic Model of a Rotor System Consisting of a Flexible Link with Misaligned Shafts

Marijonas Bogdevičius - Bronislovas Spruogis - Vytautas Turla

Zanesljivost in trajnost strojno gnanih sistemov, ki jih uporabljamo v prenosih, sta odvisni od izbire povezovalnih elementov v gonilih. Pomembno je, da pri takšnih sistemih pravilno ocenimo in izravnamo pojav nesoosnosti. V pričujočem prispevku predstavljamo dinamični model rotorskega sistema, ki sestoji iz motorja in delovnega stroja z gredema, ki sta povezani z elastično izravnalno gredno vezjo.

Enačbe gibanja polovičnih grednih vezi in rotorskih sistemov smo izpeljali na način, ki omogoča določitev kinetične in potencialne energije, kinetičnih in dinamičnih parametrov deformiranega sistema ter lege in oblike gibkega člena, ki povezuje sistem. Izračunali smo tudi krivuljo pospeškov elastičnih sil gibkega člena (gredne vezi).

(Ključne besede: gonila kompleksna, vezi gredne, nesoosnost, modeli dinamični, metode končnih elementov)

The reliability and durability of the machine-drive systems used in transport depend on the selection of the connecting elements used in the drives. In such systems the evaluation and compensation of incoaxiality is an important task. In this paper we discuss the dynamic model of a rotary system consisting of an engine and a working machine with the shafts connected by an elastic compensation coupling.

The equations of motion of the half-couplings and the rotary systems are derived in such a way that the kinetic and potential energies, the kinetic and dynamic parameters of the deformed system, and the location and shape of the flexible link joining the system can be determined. We have also calculated the hodograph of the elastic forces of the flexible link (coupling).

(Keywords: complex drive, couplings, misalignment, dynamic models, finite element methods)

0 UVOD

Rotorski sistem sestoji iz mnogih, sočasno vrtečih se, členov. Zaradi nesoosnosti grednih vezi, neuravnoteženosti posameznih delov, zunanjih in drugih motenj ter zaradi sprememb v dovedeni energiji se členi vrtijo nepravilno. Ti dejavniki povzročijo povečanje dinamične obremenitve v strojih in mehanizmih, kar poveča vrtilno vibriranje. V pričujoči študiji smo raziskovali, kako lahko zmanjšamo vrtilno vibriranje in sile, ki ga povzročajo. Ugotovili smo, da je eden najbolj učinkovitih načinov zmanjšanja vibracij izboljšanje konstrukcije strojnih sestavnih delov in zamenjava teh elementov z deli, ki so odporni proti vibriranju. Za ta namen lahko uporabimo učinkovite naprave za prenos kroženja in za stabilizacijo, npr.: različne sklopke in dušilnike vibriranja.

0 INTRODUCTION

A rotor system consists of many synchronously rotating links. Because of the misalignment of the coupling-link shafts, the non-balanced parts, the external and other disturbances, and the variations in the supplied energy, the links rotate irregularly. These factors result in an increased dynamic load in machines and mechanisms that gives rise to rotary vibration. In this study we have investigated how to reduce these rotary vibrations and the forces that cause them. We found that one of the most effective ways of decreasing vibrations is to improve the construction of the machine's assembly elements and substitute these elements with parts that are resistant to vibration. For this we can use effective rotary-motion transmission and stabilization devices in the form of various clutches and vibration dampers.

Tu predstavljamo dinamično analizo nelinearne, torzijske, gibke gredne vezi z elastičnimi členi [1]. Z rezultati analize ravnovesnega stanja in prehodnega osciliranja smo določili optimalna razmerja grednih vezi. Mohiuddin in Khulief [2] sta prikazala splošni dinamični model velikega sistema rotorskih ležajev z razpokano gredjo. Model predvideva gredi s klinastimi deli, več diskov in anizotropne ležaje. Upoštevali smo tudi vpliv togosti gibke gredne vezi na amplitudo torzijskega vrtilnega momenta [3].

Trdnost in zanesljivost zobnikov v stroju sta močno odvisni od izbire pravih elementov gredne vezi. V primeru takšnih strojev je zelo pomembno, da pravilno ocenimo izravnavo nesoosnosti gredi. V pričujoči študiji predstavljamo dinamični model rotorskega sistema, ki sestoji iz asinhronega motorja in delovnega stroja, čigar gredi sta povezani s izravnalno sklopko. Sklopka, ki rabi kot gibek člen med motorjem in gredema delovnega stroja, ima lahko različne prostostne stopnje. Glede nesoosnosti pa smo dinamiko povezanih gredi rešili z uporabo metode končnih elementov.

Za prikaz geometrijske oblike gredne vezi in člena med polovičnima grednima vezema v primeru nesoosnih gredi uporabimo zapletene elemente. Izpeljemo matematične odvisnosti med globalnimi točkami sklopk v začetnih in deformiranih legah in določimo njihove soodnose. Ugotovimo matematičen odnos med silami, ki delujejo na zapletene elemente sklopke; prav tako izračunamo sile in momente, ki delujejo v polovični gredni vezi in se prenašajo na pripadajoči gredi ter na podporne dele. Razvijemo enačbe gibanja za sistem polovične gredne vezi in rotorja ter jih združimo v matematični model. Dobljena rešitev omogoči, da izračunamo kinetično in potencialno energijo, kinematične in dinamične parametre deformiranih sistemov ter ugotovimo lego in obliko gibke gredne vezi.

1 DINAMIČNI MODEL ROTORSKEGA SISTEMA

Analizirali bomo sistem, ki je sestavljen iz motorja in delovnega stroja, čigar gredi sta povezani z gibko gredno vezjo (gibko sklopko – GS). Motor in delovni stroj sta pritrjena na gibke opornike, ki dušijo vibriranje. Predpostavljamo, da so okvir delovnega stroja in diski rotorjev popolnoma togi, kar pomeni, da ima sistem zgoščene parametre. Dinamiko povezanih gredi bomo raziskali z metodo končnih elementov (MKE).

Zunanje vzbujanje sistema je posledica radialne in kotne nesoosnosti povezanih gredi motorja in delovnega stroja. Naredili smo naslednje predpostavke: deformacije so majhne, gredi rotorjev sta gibki telesi in bočne sile so zanemarljive.

We present a dynamic analysis of a nonlinear torsional flexible coupling with elastic links [1]. The results of analyses of the steady-state and transient-oscillation performances are applied to determine optimum proportions for the couplings. Mohiuddin and Khulief [2] presented a general dynamic model for a large-scale rotor-bearing system with a cracked shaft. The model accommodates shafts with tapered portions, multiple disks and anisotropic bearings. The influence of the stiffness of a flexible coupling on the amplitude of the torsional torque is considered [3].

The strength and the reliability of the gears in machines very much depend on choosing the right coupling elements. For such machines it is very important to evaluate the compensation of the shafts' misalignment. In this study we present a dynamic model of a rotor system consisting of an asynchronous engine and a working machine, the shafts of which are connected by a compensating clutch. The clutch, which serves as a flexible link between the engine and the shafts of the working machine, can have many degrees of freedom. For the case of misalignment, the dynamics of the connected shafts is solved using the finite-element method.

We present the geometry of the coupling as well as the link between its half-couplings using complex elements for the case when the shafts are misaligned. We derive mathematical dependencies between the global points of the clutches in the initial and deformed positions and determine their interrelations. We establish a mathematical relation between the forces influencing the complex elements of the clutch; and the forces and moments acting in the half-coupling, which are transferred to the corresponding shafts and the support parts, are calculated. We develop the equations of motion for the half-coupling and the rotor system and join them in a mathematical model. The solution allows us to calculate the kinetic and potential energies, the kinematics and dynamics parameters of the deformed systems, as well as establish the location and the shape of the flexible coupling.

1 DYNAMIC MODEL OF A ROTOR SYSTEM

We will analyse a system composed of an engine and a working machine, whose shafts are connected by a flexible coupling (a flexible clutch – FC). The engine and the working machine are attached to flexible supports that suppress the vibration. We assume that the frame of the working machine and the disks of the rotors are absolutely stiff, i.e., the system possesses concentrated parameters. The dynamics of the connected shafts will be investigated using the finite-element method (FEM).

The external excitation of the system is caused by the radial and angular misalignment of the connected engine and working-machine shafts. We have made the following assumptions: the deformations are small, the shafts of the rotors are flexible bodies, and the lateral forces are negligible.

Slika 1 prikazuje dinamični model rotorskega sistema, čigar globalni sistem koordinat je *OXYZ*. Za sistem prve polovične gredne vezi smo izbrali koordinatni sistem $O_1X_1Y_1Z_1$, za sistem druge polovične gredne vezi pa smo izbrali koordinatni sistem $O_2X_2Y_2Z_2$. Vsaka polovična gredna vez ima lahko šest prostostnih stopenj. Poleg tega ima lahko gibka gredna vez (GS) še precej več notranjih prostostnih stopenj (v odvisnosti od strukture povezovalne gredne vezi). Dinamiko modela smo razrešili z uporabo MKE. Vrednosti začetnih deformacij gredi so znane. Analizirali bomo, kako nastane deformacija rotorskega sistema, prav tako bomo ugotovili premike, kote deformacije in njihove odvode ([4] do [10]).

Fig. 1 shows the dynamic model of the rotor system, whose global system of coordinates is *OXYZ*. For the system of the first half-coupling we selected the $O_1X_1Y_1Z_1$ coordinate system, while for the system of the second half-coupling we selected the $O_2X_2Y_2Z_2$, coordinate system. Every half-coupling can have six degrees of freedom. Furthermore, a flexible coupling (FC) can have many more internal degrees of freedom (depending on the structure of the connecting coupling). The dynamics is solved using the FEM. The values of the initial deformations of a shaft are known. We will analyse how the deformation of the rotor system occurs, and we will also find the displacements, the angles of deformation and their derivatives ([4] to [10]).

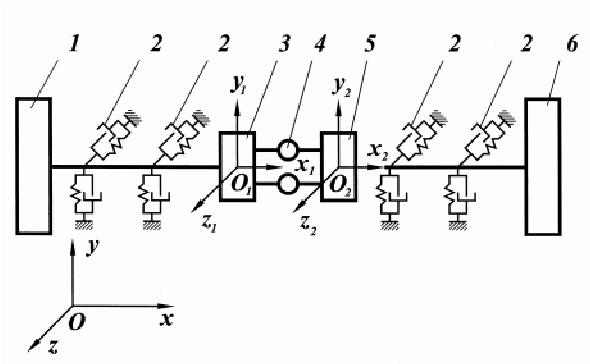

Sl. 1. *Dinamični model rotorskega sistema: 1 – rotor motorja; 2 – gibki oporniki; 3 – prva polovična gredna vez; 4 – gibki povezovalni elementi polovične gredne vezi; 5 – druga polovična gredna vez; 6 – rotor delovnega stroja; I – gonilna gred; II – gnana gred*

Fig. 1. *Dynamic model of the rotor system: 1 – engine rotor; 2 – flexible supports; 3 – first half-coupling; 4 – half-coupling's flexible connecting elements; 5 – second half-coupling; 6 – rotor of the working machine; I – driving shaft; II – driven shaft*

1.1 Geometrijska oblika sklopke

Analizirali bomo splošen primer sklopke: gonilna gred I in gnana gred II rotorskega sistema sta povezani s polovično gredno vezjo. Števili prve in druge polovične gredne vezi sta $i = 1$ in $i = 2$. Števila zapletenih elementov (KE) v gibki gredni vezi so $j = 1, 2, \ldots NZ$, pri čemer je NZ skupno število zapletenih

1.1 Geometry of the Clutch

We will analyse a general case for the clutch: the driving shaft I and the driven shaft II of the rotor system are connected by a half-coupling. The numbers of the first and second half-couplings are $i = 1$ and $i = 2$. The numbers of the complex elements (CE) in the flexible coupling are $j = 1, 2, \ldots NZ$, where

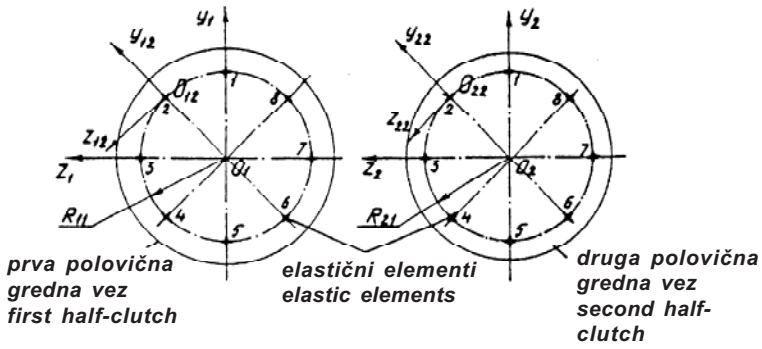

Sl. 2. *Shematični prikaz geometrije gredne vezi, če je NZ = 8*

Fig. 2. Schematic view of the coupling geometry when NZ = 8

elementov v gibki gredni vezi (sl. 2). Zahtevni elementi so razvrščeni v krogih s premeroma R_{11} in R_{21} (sl. 2).

Točke so določene s koordinatnim sistemom $O_{ij}X_{ij}Y_{ij}Z_{ij}$. Polovični gredni vezi sta povezani z zapletenimi elementi, od katerih vsak sestoji iz treh elementov (sl. 3).

NZ is the total number of complex elements in the flexible coupling (Fig.2). The complex elements are arranged in circles with radii R_{11} and R_{21} (Fig. 2).

The points are defined in the coordinate system $O_{ij}X_{ij}Y_{ij}Z_{ij}$. The half-couplings are interlinked by complex elements, with each of them consisting of three elements (Fig. 3).

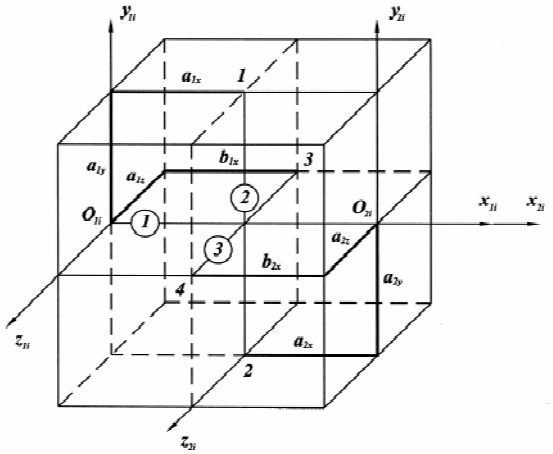

Sl. 3. *Zahtevni element: 1 – prvi element deluje v vzdolžni smeri; 2 – drugi element deluje v prečni smeri ; 3 – tretji element deluje pravokotno na prečno in vzdolžno smer*

Fig. 3. Complex element: 1 – the first element acts in the axial direction; 2 – the second element acts in the radial direction; 3 – the third element acts perpendicular to the radial and axial directions

1.2 Sile in momenti sil, ki delujejo na zapletene elemente

Koordinate točk O_1 in O_2 v koordinatnem sistemu *OXYZ* (sl. 1) so naslednje:

1.2 Forces and moments of the forces acting on the complex elements

The coordinates of points O_1 and O_2 in the coordinate system *OXYZ* (Fig. 1) are as follows:

$$\{X\}_{O1} = \{X_0\}_{O1} + \{U(t)\}_{O1} \quad (1)$$

$$\{X\}_{O2} = \{X_0\}_{O2} + \{U(t)\}_{O2} \quad (2),$$

kjer so $\{X_0\}_{O1}$, $\{X_0\}_{O2}$ začetne koordinate točk O_1 in O_2, in sta $\{U(t)\}_{O1}$, $\{U(t)\}_{O2}$ premika točk O_1 in O_2.

Razmerje med koordinatnima sistemoma $O_1X_1Y_1Z_1$ in $O_{1i}X_{1i}Y_{1i}Z_{1i}$ lahko izrazimo takole:

where $\{X_0\}_{O1}$, $\{X_0\}_{O2}$ are the initial coordinates of the points O_1 and O_2, and $\{U(t)\}_{O1}$, $\{U(t)\}_{O2}$ are the displacements of the points O_1 and O_2.

The relationship between the coordinate systems$O_1X_1Y_1Z_1$ and $O_{1i}X_{1i}Y_{1i}Z_{1i}$ can be expressed as follows:

$$\{X_1\} = \{X_1\}_{1i} + [G_{1i}]\{X_{1i}\} \quad (3),$$

kjer so $\{X_1\}_{1i}$ koordinate točke O_{1i} v koordinatnem sistemu $O_1X_1Y_1Z_1$, $[G_{1i}]$ matrika koordinatne premene in $\{X_{1i}\}$ koordinate zapletenega elementa *i* polovične gredne vezi 1.

Razmerje med koordinatnima sistemoma $O_2X_2Y_2Z_2$ in $O_{2i}X_{2i}Y_{2i}Z_{2i}$ lahko izrazimo na naslednji način:

where $\{X_1\}_{1i}$ are the coordinates of the point O_{1i} in the $O_1X_1Y_1Z_1$ coordinate system, $[G_{1i}]$ is the matrix of coordinates transformation, and $\{X_{1i}\}$ are the coordinates of the complex element *i*of the half-coupling 1.

The relationship between the coordinate systems $O_2X_2Y_2Z_2$ and $O_{2i}X_{2i}Y_{2i}Z_{2i}$ can be expressed as follows:

$$\{X_2\} = \{X_2\}_{2i} + [G_{2i}]\{X_{2i}\} \quad (4),$$

kjer so $\{X_2\}_{2i}$ koordinate točke O_{2i} v koordinatnem sistemu $O_2X_2Y_2Z_2$, $[G_{2i}]$ matrika koordinatne premene in $\{X_{2i}\}$ koordinate zahtevnega elementa *i* polovične gredne vezi 2.

Razdalja med točkama O_{1i} in O_{2i} je naslednja:

where $\{X_2\}_{2i}$ are the coordinates of point O_{2i} in the $O_2X_2Y_2Z_2$ coordinate system, $[G_{2i}]$ is the matrix of coordinates transformation, and $\{X_{2i}\}$ are the coordinates of the complex element *i* of the half-coupling 2.

The distance between the points O_{1i} and O_{2i} is as follows:

$$\{L_{i,1}(t)\} = \{X\}_{2i} - \{X\}_{1i} = \{X_0\}_{O2} + \{U(t)\}_{O2} + [A_2]\{X_2\}_{2i} - \{X_0\}_{O1} - \{U(t)\}_{O1} - [A_1]\{X_1\}_{1i} \quad (5)$$

in časovni odvod vektorja $\{L_{i,1}(t)\}$ je:

and the derivative of vector $\{L_{i,1}(t)\}$ with respect to time is equal to:

$$\frac{d}{dt}\{L_{i,1}(t)\} = \{\dot{U}(t)\}_{O2} + [\dot{A}_2]\{X_2\}_{2i} - \{\dot{U}(t)\}_{O1} - [\dot{A}_1]\{X_1\}_{1i} \quad (6),$$

kjer sta $[A_1]$, $[A_2]$ matriki koordinatne premene;

where $[A_1]$, $[A_2]$ are the matrices of coordinates transformation;

$$\frac{d}{dt}[A_i] = [\dot{A}_i], \quad \text{in/and } \frac{d}{dt}\{U(t)\} = \{\dot{U}(t)\} \qquad i = 1,2$$

Premik med točkama O_{1i} in O_{2i} je:

The displacement between the points O_{1i} and O_{2i} is:

$$\Delta L_{i,1}(t) = \left|\{L_{i,1}(t)\}\right| - \left|\{L_{i,1}(t=0)\}\right| \quad (7).$$

Premik prvega elementa v *i*-tem zahtevnem elementu je:

The displacement of the first element in the *i*-th complex element is:

$$\Delta U_{i,1}(t) = \begin{cases} \Delta L_{i,1}(t), & \Delta L_{i1}(t) < 0 \\ 0, & \Delta L_{i1}(t) \geq 0 \end{cases} \quad (8).$$

Hitrost premika prvega elementa v *i*-tem zahtevnem elementu izrazimo takole:

The velocity at which the displacement of the first element in the *i*-th complex element takes place is expressed as:

$$\Delta\dot{U}_{i,1}(t) = \frac{d}{dt}\left(\Delta L_{i,1}(t)\right) = \frac{d}{dt}\left|\{L_{i,1}(t)\}\right| - \frac{d}{dt}\left|\{L_{1,i}(t=0)\}\right| = \frac{d}{dt}\left|\{L_{1,i}(t)\}\right| = \frac{\{\dot{L}_{1,i}(t)\}^T\{L_{1,i}(t)\}}{\left|\{L_{1,i}(t)\}\right|} \quad (9).$$

Razdalja med točko 1 in točko 2 v *i*-tem zahtevnem elementu prve polovične gredne vezi in druge polovične gredne vezi je naslednja:

The distance between point 1 and point 2 in the i-th complex element of the first half-coupling and the second half-coupling is equal to:

$$\{L_{i,2}(t)\} = \{X\}_{2i,2} - \{X\}_{1i,1} = \{X_0\}_{O2} + \{U(t)\}_{O2} + [A_2]\left(\{X_2\}_{2i} + [G_{2i}]\{X_{2i,2}\}\right) - \{X_0\}_{O1} - \{U(t)\}_{O1} - [A_1]\left(\{X_1\}_{1i} + [G_{1i}]\{X_{1i,1}\}\right) \quad (10),$$

kjer je $\{X_{1i,1}\}^T = [a_{1x}, a_{1y}, 0]$; $\{X_{2i,2}\}^T = [-a_{2x}, -a_{2y}, 0]$ (glej sl. 3).

where $\{X_{1i,1}\}^T = [a_{1x}, a_{1y}, 0]$; $\{X_{2i,2}\}^T = [-a_{2x}, -a_{2y}, 0]$ (see Fig.3).

Časovni odvod je:

The derivative with respect to time is as follows:

$$\frac{d}{dt}\{L_{i,2}(t)\} = \{\dot{U}(t)\}_{O2} + [\dot{A}_2]\left(\{X_2\}_{2i} + [G_{2i}]\{X_{2i,2}\}\right) - \{\dot{U}(t)\}_{O1} - [\dot{A}_1]\left(\{X_1\}_{1i} + [G_{1i}]\{X_{1i,1}\}\right) \quad (11).$$

Premik med točkama 2 in 1 v drugem elementu *i*-tega zahtevnega elementa je:

The displacement between points 2 and 1 in the second element of the *i*-th complex element is equal to:

$$\Delta L_{i,2}(t) = \left|\{L_{1,2}(t)\}\right| - \left|\{L_{1,2}(t=0)\}\right| \quad (12).$$

$$\Delta U_{i,2}(t) = \begin{cases} 0, & \Delta L_{i,2}(t) \geq 0 \\ \Delta L_{i,2}, & \Delta L_{i,2}(t) < 0 \end{cases} \quad (13).$$

Hitrost premika v drugem elementu zahtevnega *i*-tega elementa lahko izrazimo takole:

The velocity of the displacement in the second element of the *i*-th complex element can be expressed as:

$$\Delta\dot{U}_{1,2}(t)=\frac{d}{dt}\left(\Delta L_{i,2}(t)\right)=\frac{\left\{\dot{L}_{i,2}(t)\right\}^{T}\left\{L_{i,2}(t)\right\}}{\left|\left\{L_{i,2}\right\}\right|} \tag{14}$$

Razdalja med točko 3 in točko 4 v *i*-tem zahtevnem elementu prve in druge polovične gredne vezi je:

The distance between point 3 and point 4 in the i-th complex element of the first and the second half-coupling is equal to:

$$\begin{aligned}\left\{L_{i,3}(t)\right\}=\left\{X\right\}_{2i,4}-\left\{X\right\}_{1i,3}=\left\{X_0\right\}_{O2}+\left\{U(t)\right\}_{O2}+\left[A_2\right]\left(\left\{X_2\right\}_{2i}+\left[G_{2i}\right]\left\{X_{2i}\right\}_4\right)-\\ \left\{X_0\right\}_{O1}-\left\{U(t)\right\}_{O1}-\left[A_1\right]\left(\left\{X_1\right\}_{1i}+\left[G_{1i}\right]\left\{X_{1i,3}\right\}\right)\end{aligned} \tag{15}$$

kjer je $\{X_{1i,3}\}^T=[b_{1x}, 0, -a_{1z}]$; $\{X_{2i,4}\}^T=[-b_{2x}, 0, -a_{2z}]$ (glej sl. 3).

where $\{X_{1i,3}\}^T=[b_{1x}, 0, -a_{1z}]$; $\{X_{2i,4}\}^T=[-b_{2x}, 0, -a_{2z}]$ (see Fig.3).

Časovni odvod vektorja je:

The derivative of the vector with respect to time is as follows:

$$\frac{d}{dt}\left\{L_{i,3}(t)\right\}=\left\{\dot{U}(t)\right\}_{O2}+\left[\dot{A}_2\right]\left(\left\{X_2\right\}_{2i}+\left[G_{2i}\right]\left\{X_{2i,4}\right\}\right)-\left\{\dot{U}(t)\right\}_{O1}-\left[\dot{A}_1\right]\left(\left\{X_1\right\}_{1i}+\left[G_{1i}\right]\left\{X_{1i,3}\right\}\right). \tag{16}$$

Premik tretjega elementa *i*-tega zahtevnega elementa je naslednji:

The displacement of the 3rd element of the *i*-th complex element is as follows:

$$\Delta U_{i,3}(t)=\Delta L_{i,3}(t)=\left|\left\{L_{i,3}(t)\right\}\right|-\left|\left\{L_{i,3}(t=0)\right\}\right| \tag{17}$$

Hitrost premika v tretjem elementu *i*-tega zahtevnega elementa lahko izrazimo takole:

The velocity of displacement in the third element of the *i*-th complex element can be expressed as:

$$\Delta\dot{U}_{i,3}(t)=\frac{d}{dt}\left(\left|\left\{L_{i,3}(t)\right\}\right|-\left|\left\{L_{i,3}(t=0)\right\}\right|\right)=\frac{\left\{\dot{L}_{i,3}(t)\right\}^{T}\left\{L_{i,3}(t)\right\}}{\left|\left\{L_{i,3}(t)\right\}\right|} \tag{18}$$

Sila, ki deluje na prvi element *i*-tega zahtevnega elementa, je:

The force acting on the first element of the *i*-th complex element is as follows:

$$\left\{F_{i,1}(t)\right\}=F_{i,1}\left(\Delta U_{i,1}(t),\Delta\dot{U}_{i,1}(t)\right)\frac{\left\{L_{i,1}(t)\right\}}{\left|\left\{L_{i,1}(t)\right\}\right|} \tag{19}$$

kjer je

where

$$F_{i,1}\left(\Delta U_{i,1}(t),\Delta\dot{U}_{i,1}(t)\right)=\left(F_{T,i,1}+f_{T,i,2}F_{i,2}^{N}+f_{T,i,3}F_{i,3}^{N}\right)sign\left(\Delta\dot{U}_{i,2}(t)\right)+\sum_{k=1}^{n_1}\left(k_{1i,2i,k}\cdot\Delta U_{i,1}^{k}(t)+h_{1i,2i,k}\cdot\Delta\dot{U}_{i,1}^{k}(t)\right) \tag{20}$$

kjer je $F_{T,i,1}$ sila trenja; $F_{i,2}^{N}, F_{i,3}^{N}$ sta normalni sili, ki sta iz drugega in tretjega elemeta preneseni na prvi element; $f_{T,i,2}, f_{T,i,3}$ sta koeficienta trenja; $k_{1i,2i,k}$, $h_{1i,2i,k}$ sta koeficienta togosti oziroma dušenja; n_1 je število elementov.

where $F_{T,i,1}$ is the frictional force; $F_{i,2}^{N}, F_{i,3}^{N}$ are the normal forces transferred to the first element from the second and third elements; $f_{T,i,2}, f_{T,i,3}$ are the frictional coefficients; $k_{1i,2i,k}$, $h_{1i,2i,k}$ are the stiffness and damping coefficients, respectively; and n_1 is the number of elements.

Sila, ki deluje na drugi element *i*-tega zahtevnega elementa, je enaka:

The force acting on the second element of the *i*-th complex element is equal to:

$$\left\{F_{i,2}(t)\right\}=F_{i,2}\left(\Delta U_{i,2}(t),\Delta\dot{U}_{i,2}(t)\right)\frac{\left\{L_{i,2}(t)\right\}}{\left|\left\{L_{i,2}(t)\right\}\right|} \tag{21}$$

kjer je

where

$$F_{i,2}\left(\Delta U_{i,2}(t),\Delta\dot{U}_{i,2}(t)\right)=\left(F_{T,i,2}+f_{T,i,1}F_{i,1}^{N}+f_{T,i,3}F_{i,3}^{N}\right)sign\left(\Delta\dot{U}_{i,2}(t)\right)+\sum_{k=1}^{n_2}\left(k_{12,k}\cdot\Delta U_{1,2}^{k}(t)+h_{12,k}\cdot\Delta\dot{U}_{1,2}(t)\right) \tag{22}$$

kjer je $F_{T,i,2}$ sila trenja; $F_{i,2}^{N}, F_{i,3}^{N}$ sta normalni sili, ki sta iz prvega in tretjega elementa preneseni na drugi strukturni element; $f_{T,i,2}, f_{T,i,3}$ sta koeficienta trenja; $k_{12,k}$, $h_{12,k}$ sta koeficienta togosti oziroma dušenja; n_2 je število elementov.

where $F_{T,i,2}$ is the frictional force; $F_{i,2}^{N}, F_{i,3}^{N}$ are the normal forces transferred to the second structural element from the first and third elements; $f_{T,i,2}, f_{T,i,3}$ are the frictional coefficients; $k_{12,k}$, $h_{12,k}$ are the stiffness and damping coefficients, respectively; n_2 is the number of elements.

Sila, ki deluje na tretji sestavni element, je enaka:

The force acting on the third structural element is equal to:

$$\{F_{i,3}(t)\} = F_{i,3}\left(\Delta U_{i,3}(t), \Delta \dot{U}_{i,3}(t)\right) \frac{\{L_{i,3}(t)\}}{|\{L_{i,3}(t)\}|} \tag{23}$$

$$F_{i,3}\left(\Delta U_{i,3}(t), \Delta \dot{U}_{i,3}(t)\right) = \sum_{k=1}^{n_3} k_{34,k} \cdot \Delta U_{i,3}^{k}(t) + h_{34,k} \cdot \Delta \dot{U}_{i,3}^{k}(t) \tag{24},$$

kjer sta $k_{34,k}$, $h_{34,k}$ koeficienta togosti oziroma dušenja. Moment sile lahko izrazimo takole:

where $k_{34,k}$, $h_{34,k}$ are the stiffness and damping coefficients, respectively.
The moment of force can be expressed as follows:

$$\{M\} = \{r\} \times \{F\} = [B]\{F\} \tag{25},$$

kjer je [B] antisimetrična matrika:

where [B] is the skew-symmetric matrix:

$$[B] = \begin{bmatrix} 0 & -r_z & r_y \\ r_z & 0 & -r_x \\ -r_y & r_x & 0 \end{bmatrix}$$

in so r_x, r_y, r_z projekcije razdalje.

Vektor vsote sil, ki delujejo na prvi, drugi in tretji element v vsakem zahtevnem elementu prve polovične gredne vezi glede na točko O_1, je:

and r_x, r_y, r_z are the projections of radius.

The vector of the total force relative to the point O_1 of the forces acting on the first, second and third elements in each complex element of the first half-coupling is:

$$\{F_{O1}\} = \sum_{i=1}^{NZ} \sum_{j=1}^{3} \{F_{i,j}\} \tag{26}.$$

Vektor celotnega momenta sil, ki delujejo na prvi, drugi in tretji element v vsakem zahtevnem elementu prve polovične gredne vezi glede na točko O_1, je:

The vector of the total moment relative to the point O_1 of the forces acting on the first, second and third elements in each complex element of the first half-coupling is:

$$\{M_{O1}\} = \sum_{i=1}^{NZ} \sum_{j=1}^{3} \{r_{O1}\}_{i,j} \times \{F_{i,j}\} = \sum_{i=1}^{NZ} \sum_{j=1}^{3} [B_{O1}]_{i,j} \{F_{i,j}\} \tag{27},$$

kjer so $\{r_{O2}\}_{i,j}$ koordinate točke, v kateri deluje sila $\{F_{i,j}\}$; $[B_{O1}]_{i,j}$ je antisimetrična matrika, ki je dobljena iz vektorja $\{r_{O1}\}_{i,j}$.

Vektor vsote sil, ki delujejo na prvi, drugi in tretji element v vsakem zahtevnem elementu druge polovične gredne vezi glede na točko O_2, je:

where $\{r_{O2}\}_{i,j}$ are the coordinates of the point in which the force $\{F_{i,j}\}$ acts; $[B_{O1}]_{i,j}$ is the skew-symmetric matrix that is generated from the vector $\{r_{O1}\}_{i,j}$.

The vector of the total force relative to the point O_2 of the forces acting on the first, second and third elements in each complex element of the second half-coupling is:

$$\{F_{O2}\} = -\sum_{i=1}^{NZ} \sum_{j=1}^{3} \{F_{i,j}\} \tag{28}.$$

Vektor celotnega momenta sil, ki delujejo na prvi, drugi in tretji element v vsakem zahtevnem elementu druge polovične gredne vezi glede na točko O_2, je:

The vector of the total moment relative to the point O_2 of the forces acting on the first, second and third elements in each complex element of the second half-coupling is:

$$\{M_{O2}\} = -\sum_{i=1}^{NZ} \sum_{j=1}^{3} \{r_{O2}\}_{i,j} \times \{F_{i,j}\} = -\sum_{i=1}^{NZ} \sum_{j=1}^{3} [B_{O2}]_{i,j} \{F_{i,j}\} \tag{29},$$

kjer so $\{r_{O2}\}_{i,j}$ koordinate točke, v kateri deluje sila -$\{F_{i,j}\}$; -$[B_{O2}]_{i,j}$ je antisimetrična matrika, ki je dobljena iz vektorja $\{r_{O2}\}_{i,j}$.

where $\{r_{O2}\}_{i,j}$ are the coordinates of the point in which the force $\{F_{i,j}\}$ acts; -$[B_{O2}]_{i,j}$ is the skew-symmetric matrix generated from vector $\{r_{O2}\}_{i,j}$.

1.3 Enačbe gibanja rotorja

Osnovna shema splošnega rotorskega sistema je prikazana v diagramu 1. Rotorski sistem sestoji iz dveh gredi, na katerih sta pritrjeni dve

1.3 Equations of Rotor Motion

The principal scheme of a general rotor system is presented in Fig.1. The rotor system consists of shafts, on which half-couplings are

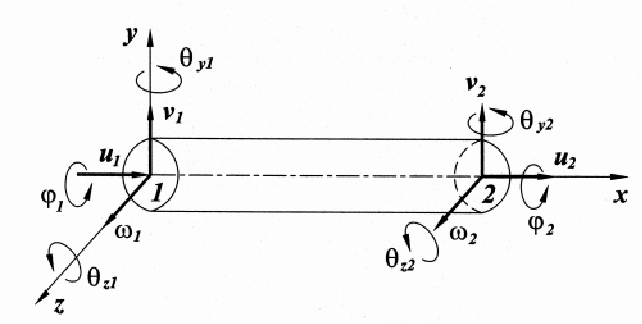

Sl. 4. *Palični končni element*
Fig. 4 *The beam finite element*

polovični gredni vezi; gredi sta podprti z dvema ali več gibkimi oporniki (dušeni ali nedušeni). Vsaka gred je razdeljena v palične končne elemente z naslednjimi lastnostmi: material elementov je homogen z gostoto ρ, Youngov modul je E in strižni modul je G; intervalno dušenje gredi zanemarimo; prerez je krožen, uporabljena je Bernoulli-Eulerjeva teorija togega (konzolnega) vpetja. Število prostostnih stopenj v vozliščni točki je šest (sl. 4).

Posplošene koordinate paličnih končnih elementov so:

mounted, supported by two or more flexible supports (damped or undamped). The shaft is divided into beam finite elements with the following properties: the material of the element is homogeneous, with density ρ, Young's modulus E and shear modulus G; the interval damping of the shaft is neglected; the cross-section is circular; the theory of Bernoulli-Euler clam is applied. The number of degrees of freedom at a nodal point is six (Fig. 4).

The generalized coordinates in the beam finite elements are:

$$\{q\}^T = \left[u_1, v_1, w_1, \varphi_1, \theta_{y_1}, \theta_{z_1}, u_2, v_2, w_2, \varphi_2, \theta_{y_2}, \theta_{z_2}\right] \tag{30},$$

kjer sta q_y, q_z kotna premika rotorja:

where, q_y, q_z are angular rotor displacements,

$$\theta_y = -\frac{dw}{dx}; \quad \theta_z = \frac{dv}{dx}$$

Geometrične značilnosti paličnega končnega elementa so naslednje: L je dolžina elementa; A je prerez; J_x je polarni vztrajnostni moment glede na os X; J_y, J_z sta prečna vztrajnostna momenta glede na osi Y, Z; J_p je polarni vztrajnostni moment; J_D je prečni vztrajnostni moment.

Kinetično energijo paličnega končnega elementa lahko izrazimo takole:

The geometrical properties of the beam finite element are as follows: L is the length of the element; A is the cross-sectional area; J_x is the polar moment of inertia with respect to the X axis; J_y, J_z are the transverse moments of inertia with respect to the Y, Z axes; J_p is the polar moment of inertia; J_D is the transverse moment of inertia.

The kinetic energy of the beam finite element can be expressed as:

$$T^{(e)} = \frac{1}{2}\int_0^L \rho A \begin{Bmatrix} \dot{u} \\ \dot{v} \\ \dot{w} \end{Bmatrix}^T \begin{Bmatrix} \dot{u} \\ \dot{v} \\ \dot{w} \end{Bmatrix} dx \tag{31},$$

kjer so $\dot{u}, \dot{v}, \dot{w}$ premiki glede na osi X, Y in Z.
Kinetična energija diska je:

where $\dot{u}, \dot{v}, \dot{w}$ are displacements with respect to the X, Y and Z axes.
The kinetic energy of the disk is:

$$T_{disk} = \frac{1}{2}\int_0^{L_{disk}} \begin{Bmatrix} \dot{\varphi} \\ \dot{\theta}_y \\ \dot{\theta}_z \end{Bmatrix}^T \left[T_{disk}\right] \begin{Bmatrix} \dot{\varphi} \\ \dot{\theta}_y \\ \dot{\theta}_z \end{Bmatrix} dx \tag{32},$$

kjer je L_{disk}- dolžina diska; $[T_{disk}]$ je matrika

where L_{disk}- is the length of the disk; $[T_{disk}]$ is the matrix

$$\left[T_{disk}\right] = \rho \begin{bmatrix} J_p & 0 & -J_p\theta_y \\ 0 & J_D & 0 \\ -J_p\theta_y & 0 & J_D \end{bmatrix}$$

Deformacijsko energijo paličnega elementa lahko izrazimo:

The strain energy of the beam element can be expressed as:

$$\Pi^{(e)} = \frac{1}{2}\int_0^L \left(EA\left(\frac{du}{dx}\right)^2 + EJ_z\left(\frac{dv}{dx^2}\right)^2 + EJ_y\left(\frac{d^2w}{dx^2}\right)^2 + GJ_p\left(\frac{d\varphi}{dx}\right)^2 + P\left[\left(\frac{d^2v}{dx^2}\right)^2 + \left(\frac{d^2w}{dx^2}\right)^2\right]\right)dx \qquad (33),$$

kjer je P vzdolžna obremenitev.

where P is the axial load.

Premiki in kotni premiki rotorja so v približku naslednji:

The displacements and the angular rotor displacements are approximated as follows:

$$\begin{Bmatrix} u \\ v \\ w \end{Bmatrix} = [N_1]\{q\}, \quad \begin{Bmatrix} \varphi \\ \theta_y \\ \theta_z \end{Bmatrix} = [N_2]\{q\} \qquad (34).$$

$$[N_1] = \begin{bmatrix} N_5 & 0 & 0 & 0 & 0 & 0 & N_6 & 0 & 0 & 0 & 0 & 0 \\ 0 & N_1 & 0 & 0 & 0 & N_2 & 0 & N_3 & 0 & 0 & 0 & N_4 \\ 0 & 0 & N_1 & 0 & -N_2 & 0 & 0 & 0 & N_3 & 0 & -N_4 & 0 \end{bmatrix}$$

$$[N_2] = \begin{bmatrix} 0 & 0 & 0 & N_5 & 0 & 0 & 0 & 0 & 0 & N_6 & 0 & 0 \\ 0 & 0 & -\frac{dN_2}{dx} & 0 & \frac{dN_2}{dx} & 0 & 0 & 0 & \frac{dN_3}{dx} & 0 & \frac{dN_4}{dx} & 0 \\ 0 & \frac{dN_1}{dx} & 0 & 0 & 0 & \frac{dN_2}{dx} & 0 & \frac{dN_3}{dx} & 0 & 0 & 0 & \frac{dN_4}{dx} \end{bmatrix}$$

kjer so $N_i = N_i(x)$ ($i = 1, 2, ..., 6$) oblikovne funkcije; $N_1(x)$, ..., $N_4(x)$ polinomi tretjega reda; in $N_5(x)$, $N_6(x)$ polinoma prvega reda.

where $N_i = N_i(x)$ ($i = 1, 2, ..., 6$) are the shape functions; $N_1(x)$, ..., $N_4(x)$ are the third-order polynomials; and $N_5(x)$, $N_6(x)$ are the first-order polynomials.

Če v obrazcih za energijo (31) in (32), upoštevamo obrazca (34), dobimo naslednja obrazca za kinetično in deformacijsko energijo paličnega končnega elementa z diskom:

Substituting expressions (34) into the energy expressions (31) and (32) gives us the following kinetic and strain-energy expressions for a beam finite element with a disk:

$$T^{(e)} = \frac{1}{2}\{\dot{q}\}^T \left(\left[M_1^{(e)}\right] + \left[M_2^{(e)}(q)\right] \right)\{\dot{q}\} \qquad (35)$$

$$\Pi^{(e)} = \frac{1}{2}\{q\}^T \left[K^{(e)}\right]\{q\} \qquad (36),$$

kjer je

where

$$\left[M_1^{(e)}\right] = \int_0^L \rho A [N_1]^T [N_1] dx \qquad (37)$$

$$\left[M_2^{(e)}(q)\right] = \int_0^L [N_2]^T [T_{disk}][N_2] dx \qquad (38)$$

$$\left[K^{(e)}\right] = \int_0^L \left([N_3]^T [D][N_3] dx \right. \qquad (39).$$

$$[N_3] = \begin{bmatrix} \frac{dN_5}{dx} & 0 & 0 & 0 & 0 & 0 & \frac{dN_6}{dx} & 0 & 0 & 0 & 0 & 0 \\ 0 & \frac{d^2N_1}{dx^2} & 0 & 0 & 0 & \frac{d^2N_2}{dx^2} & 0 & \frac{d^2N_3}{dx^2} & 0 & 0 & 0 & \frac{d^2N_4}{dx^2} \\ 0 & 0 & \frac{d^2N_1}{dx^2} & 0 & -\frac{d^2N_2}{dx^2} & 0 & 0 & 0 & \frac{d^2N_3}{dx^2} & 0 & -\frac{d^2N_4}{dx^2} & 0 \\ 0 & 0 & 0 & \frac{dN_5}{dx} & 0 & 0 & 0 & 0 & 0 & \frac{dN_6}{dx} & 0 & 0 \end{bmatrix}$$

$$[D] = diag\left(EA, (EJ_z + P), (EJ_y + P), GJ_p\right) \qquad (40).$$

Enačbe gibanja končnega elementa rotorja dobimo z uporabo Lagrangeve enačbe drugega reda in jih lahko prikažemo z matrično enačbo:

The equations of motion of the finite element of the rotor are obtained by using the second-order Lagrange equation, and can be represented by the matrix equation:

$$\left(\left[M_1^{(e)}\right]+\left[M_2^{(e)}(q)\right]\right)\{\ddot{q}\}+\left[\dot{M}_2^{(e)}(q)\right]\{\dot{q}\}+\left[K^{(e)}\right]\{q\}=\left\{F^{(e)}(t,q,\dot{q})\right\} \quad (41).$$

1.4 Enačbe gibanja sklopke

Učinke vrteče se polovične gredne vezi lahko izpeljemo iz enačb gibanja togega diska. Enačbo kinetične energije sklopke lahko izrazimo:

$$T=\frac{1}{2}\begin{Bmatrix}\dot{q}_1\\ \dot{q}_2\\ \dot{q}_3\end{Bmatrix}^T[T_1]\begin{Bmatrix}\dot{q}_1\\ \dot{q}_2\\ \dot{q}_3\end{Bmatrix}+\frac{1}{2}\begin{Bmatrix}\dot{q}_7\\ \dot{q}_8\\ \dot{q}_9\end{Bmatrix}^T[T_2]\begin{Bmatrix}\dot{q}_7\\ \dot{q}_8\\ \dot{q}_9\end{Bmatrix}+\frac{1}{2}\begin{Bmatrix}\dot{q}_4\\ \dot{q}_5\\ \dot{q}_6\end{Bmatrix}^T[D_1]^T[T_3][D_1]\begin{Bmatrix}\dot{q}_4\\ \dot{q}_5\\ \dot{q}_6\end{Bmatrix}+$$
$$+\frac{1}{2}\begin{Bmatrix}\dot{q}_{10}\\ \dot{q}_{11}\\ \dot{q}_{12}\end{Bmatrix}^T[D_2]^T[T_4][D_2]\begin{Bmatrix}\dot{q}_{10}\\ \dot{q}_{11}\\ \dot{q}_{12}\end{Bmatrix}=\frac{1}{2}\{\dot{q}\}^T\left(\left[M_3\right]+\left[M_4(q)\right]\right)\{\dot{q}\} \quad (42),$$

kjer so

$$[T_1]=diag(m_1,m_1,m_1)$$
$$[T_3]=diag(J_{p_1},J_{D_1},J_{D_1})$$
$$[D_1]=\begin{bmatrix}1&0&-\theta_{y_1}\\ 0&1&\varphi_1\\ 0&-\varphi_1&1\end{bmatrix}$$

m_1, m_2 sta masi prve oziroma druge polovične gredne vezi; J_{pi}, J_{Di} sta masni polarni vztrajnostni moment in masni prečni vztrajnostni moment polovične gredne vezi ($i = 1, 2$).

Enačbe gibanja sklopk dobimo z uporabo Lagrangejeve enačbe drugega reda in jih lahko prikažemo z matrično enačbo:

$$\left(\left[M_3^{clutch}\right]+\left[M_4^{clutch}(q)\right]\right)\{\ddot{q}\}+\left[\dot{M}_4^{clutch}(q)\right]\{\dot{q}\}=\left\{F^{clutch}(q,\dot{q})\right\} \quad (43),$$

kjer je $\left\{F^{clutch}(q,\dot{q})\right\}$ nelinearni vektor obremenitve.

1.5 Sistem enačb asinhronega motorja

Sistem enačb asinhronega motorja lahko zapišemo kot ([11], [12] in [14]):

$$\left\{\dot{Z}\right\}=\left[A_{asyn}\right]\{Z\}+\left\{B_{asyn}(Z,\dot{\varphi}_1)\right\} \quad (44),$$

kjer sta $[A_{asyn}]$ in $\left\{B_{asyn}(Z,\dot{\varphi}_1)\right\}$ matrični oziroma vektorski element, ki sta odvisna od rotorske in statorske induktivnosti ter od števila polarnih dvojic; $\dot{\varphi}_1$ je kotna hitrost rotorja asinhronega motorja.

Vrtilni moment asinhronega motorja je nelinearna funkcija elementov vektorja $\{Z\}$, $M_{asyn}(Z)$.

1.6 Sistem enačb rotorskega sistema

Splošni matematični model rotorskega sistema lahko oblikujemo po enačbah (44), (41) in (42): sistemov enačb gibanja asinhronega motorja, rotorjev in sklopk. Splošni sistem enačb lahko

1.4 Equations of Motion of the Clutch

The effects of a rotating half-coupling can be derived from the equations of motion for a rigid disk. The kinetic-energy expression of the clutch can be presented as:

where

$$[T_2]=diag(m_2,m_2,m_2)$$
$$[T_4]=diag(J_{p_2},J_{D_2},J_{D_2})$$
$$[D_2]=\begin{bmatrix}1&0&-\theta_{y_2}\\ 0&1&\varphi_2\\ 0&-\varphi_2&1\end{bmatrix}$$

m_1, m_2 are the mass of the first and the second half-couplings, respectively; J_{pi}, J_{Di} are mass polar inertia moment and transverse inertia moment of half-coupling ($i = 1, 2$).

The equations of motion of the clutches are obtained by using the second-order Lagrange equation and can be represented by the matrix equation:

where $\left\{F^{clutch}(q,\dot{q})\right\}$ is the non-linear load vector.

1.5 System of Equations of the Asynchronous Engine

The system of equations of the asynchronous engine can be written as ([11], [12] and [14]):

where $[A_{asyn}]$ and $\left\{B_{asyn}(Z,\dot{\varphi}_1)\right\}$ are the matrix and vector elements that depend on rotor and stator inductivities, and the number of pole pairs; $\dot{\varphi}_1$ is the angular velocity of the rotor of an asynchronous engine.

The torque of an asynchronous engine is a non-linear function of the elements of the vector $\{Z\}$, $M_{asyn}(Z)$.

1.6 System of Equations of the Rotor System

A general mathematical model of the rotor system can be constructed from (44), (41) and (42): the systems of equations of motion of an asynchronous engine, the rotors and the clutch,

prikažemo takole:

$$\left[M(Y)\right]\left\{\ddot{Y}\right\}+\left[C(Y)\right]+\left[K\right]\left\{Y\right\}=\left\{F\left(t,Y,\dot{Y}\right)\right\} \quad (45),$$

kjer so

$$\left[M(Y)\right]=\begin{array}{|c|c|}\hline [0] & [0] \\ \hline [0] & \left[M_q(q)\right] \\ \hline \end{array}$$

$$\left[K\right]=\begin{array}{|c|c|}\hline -\left[A_{asyn}\right] & [0] \\ \hline [0] & \left[K_q\right] \\ \hline \end{array}$$

$$\left[C(Y)\right]=\begin{array}{|c|c|}\hline [E] & [0] \\ \hline [0] & \left[C_q(q)\right] \\ \hline \end{array}$$

$$\left\{F\left(t,Y,\dot{Y}\right)\right\}=\begin{Bmatrix}\{B(Z,\dot{q})\} \\ \{F(Z,q,\dot{q})\}\end{Bmatrix}$$

[*E*] je enotna matrika 4 × 4.

Poznamo mnogo metod, ki jih lahko uporabimo za numerično časovno integracijo sistema enačb (45). Na splošno lahko te metode klasificiramo kot izrecne ali posredne sheme ([15] in [16]). Izrecne sheme so preproste z računskega vidika, a dolžina njihovega časovnega intervala je odvisna od stabilnosti sistema. Posredne sheme zahtevajo več preračunavanja za posamezni časovni korak, a njihove omejitve dolžine časovnega koraka niso tako stroge. Uporabljali smo posredno shemo, osnovano na trapeznem pravilu. Ob predpostavki, da so vse spremenljivke v enačbi (45) znane za čas t_k, smo trapezno pravilo za ta primer razvili takole:

respectively. A general system of equations can be represented as follows:

where

[*E*] is the 4 × 4 identity matrix.

There are many methods that can be used for the numerical time integration of a system of equations (45). Generally speaking, these methods can be classified as either explicit or implicit schemes ([15] and [16]). Explicit schemes are computationally simple but the time-step size is limited by stability considerations. Implicit schemes require more computation per time step, but time-step size limitations are much less stringent. We have used an implicit scheme based on the trapezoidal rule. Assuming all the variables in equation (45) are known at time t_k, the trapezoidal rule for this problem is:

$$\{Y\}_{k+1}=\{Y\}_k+\frac{\Delta t}{2}\left(\{\dot{Y}\}_k+\{\dot{Y}\}_{k+1}\right),\quad \{\dot{Y}\}_{k+1}=\{\dot{Y}\}_k+\frac{\Delta t}{2}\left(\{\ddot{Y}\}_k+\{\ddot{Y}\}_{k+1}\right) \quad (46)$$

in če združimo obrazca (46), dobimo vektor pospeška za čas t_{k+1}:

and combining expressions (46), we obtain the vector of acceleration at time t_{k+1}:

$$\{\ddot{Y}\}_{k+1}=\frac{4}{\Delta t^2}\left(\{Y\}_{k+1}-\{Y\}_k\right)-\frac{4}{\Delta t}\{\dot{Y}\}_k-\{\ddot{Y}\}_k \quad (47).$$

Z upoštevanjem formul (46) in (47) v sistemu enačb (45) dobimo sistem nelinearnih algebrskih enačb:

Substituting expressions (46) and (47) into the system of equations (45) we obtain a non-linear algebraic system of equations:

$$\left[\Phi\left(\{Y\}_{k+1}\right)\right]=0 \quad (48).$$

Dobljeni sistem nelinearnih algebrskih enačb (48) smo rešili z uporabo Newtonove metode ([11] do [14]).

The obtained system of nonlinear algebraic equations (48) was solved using Newton's method ([11] to [14]).

2 NUMERIČNI REZULTATI

Preučili smo rotorski sistem z gibko sklopko in neporavnanima grednima osema. Sklopka sestoji iz prosto nameščenih obročev (zahtevni element), čigar osi ležijo pravokotno na os sklopke (sl. 5).

Izračunali smo prečne togosti sklopke in izdelali krivulje pospeškov sil za različne vrednosti neporavnanosti grednih osi (*e*) ter različna števila obročev (*NZ*) (sl. 6).

2 NUMERICAL RESULTS

A rotor system with a flexible clutch and the misalignment of the shaft axes was investigated. The clutch consists of freely located rings (complex element), the axes of which are perpendicular to the axis of the clutch (Fig.5).

The radial rigidities of the clutch were calculated and hodographs of the forces for various values of misalignment of the shaft axes (*e*) and different numbers of rings (*NZ*) (Fig. 6) were constructed.

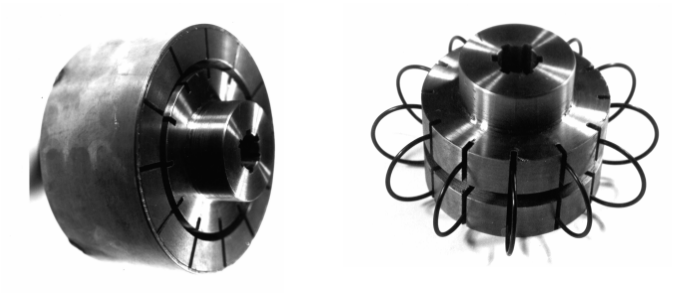

a) *b)*

Sl. 5. *Gonilna polovična gredna vez z obroči, nameščenimi v režah*
a – celovit prikaz, b – gonilna polovična sklopka z obroči, nameščenimi v režah
Fig.5 *Driving half-coupling with rings located in slits*
a – general view, b – driving half-clutch with rings located in slits

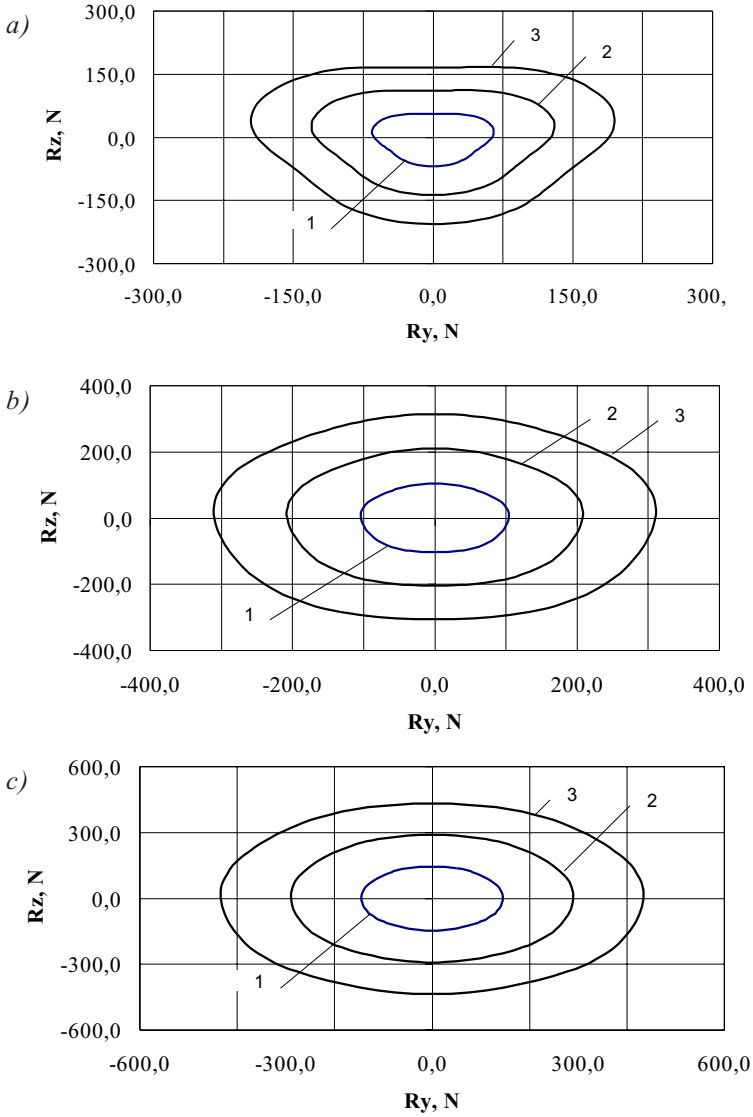

Sl. 6. *Krivulje pospeškov togosti prečnih sil: sklopka s spremenljivim številom obročev (NZ) in neporavnanostjo grednih osi(e):*
Fig. 6. Stiffness hodographs of the radial forces: the clutch with a variable number of rings (NZ) and misalignment of the shaft axes(e):
a - NZ = 3; b - NZ = 5; c - NZ = 7; 1 - e = 0,5 mm; 2 - e = 1,0 mm; 3 - e = 1,5 mm; r_{21} = 0,09m;
$a_{1x} = a_{1y}$ = 0,025 m; a_{1z} = 0,01 m; $b_{1x} = b_{2x}$ = 0,025 m; $a_{2x} = a_{1x}$; $a_{2y} = a_{1y}$; $a_{2z} = a_{1z}$;
$k_{1,i,2i} = k_{1,2,i} = k_{3,4,i} = 10^5$ N/m; i = 1 ... NZ

Slika 6 kaže, da so radialne sile večje pri večji neporavnanosti grednih osi, kadar imajo povezovalni obroči enake prečne togosti. Poleg tega se sile prečnih togosti povečajo in se oblika krivulje pospeškov togosti prečnih sil približa obliki kroga, kadar se poveča tudi število obročev (*NZ*), ki povezujejo gonilno in gnano polovično gredno vez.

Prečna togost sklopke se periodično spremeni glede na število zahtevnih elementov (obročev) (*NZ*) in frekvenco vrtenja gredi (ω). Frekvenca prečne togosti (Ω) je enaka:

Fig. 6 shows that when the connecting rings are of the same radial rigidities, the radial forces are larger for larger misalignments of the shaft axes. In addition, the forces of the radial rigidities increase and the shape of the stiffness hodograph of the radial forces approaches that of a circle when the number (*NZ*) of rings connecting the driving and the driven half-couplings is increased.

The radial stiffness of the clutch changes periodically according to the number of complex elements (rings) (*NZ*) and the frequency of the shaft rotation (ω). The frequency of radial stiffness (Ω) is equal to:

$$\Omega = \frac{NZ \cdot \omega}{2\pi} \qquad (49).$$

Kadar se sistem vrti, se lahko pojavijo parametrične vibracije. Da bi zmanjšali pojav parametričnih vibracij, moramo povečati frekvenco prečne togosti sklopke tako, da le-ta ni v fazi s frekvenco vrtenja gredi. Frekvenca prečne togosti sklopke se poveča s povečanim številom elastičnih elementov (*NZ*), vendar mora biti povečanje *NZ* zmerno, sicer bo sklopka toga, kar pa ni zaželeno. Lahko povečamo tudi število zahtevnih elementov (*NZ*), s čimer zmanjšamo njihovo prečno togost. V tem primeru se približamo bandažni sklopki z izboljšanimi značilnostmi vrtilnega gibanja. Ker so takšne sklopke bolj zanesljive, so njihove obratovalne značilnosti primerljive z značilnostmi gumenih (bandažnih) sklopk. [9].

Naš model vključuje rotorski sistem, ki sestoji iz asinhronega motorja (4A100/4SY3), dveh gredi in gredne vezi, narejene iz dveh polovičnih grednih vezi in sedmih zahtevnih elementov (obročev) – sl. 7.

Premera in dolžini obeh gredi so $d_1 = d_2 =$ 0,040 m in $L_1 = L_2 = 1{,}0$ m; vztrajnostna momenta mas polovičnih grednih vezi sta $I_{p1} = I_{p2} = 0{,}624$ kgm^2; $I_{D1} = I_{D2} = 0{,}312$ kgm^2; $k_i = 10^6$ N/m; $h_i = 10^3$ Ns/m; ($i = 1$, 2, ..., 8). Obremenitveni moment je $M_{load} = 10$ Nm. Časovna odvisnost premika prve polovične gredne vezi v smeri osi *Y* je prikazana na sliki 8, odvisnost amplitude premika od frekvence pa je podana na sliki 9.

When the system rotates, parametric vibrations can occur. To reduce the occurrence of parametric vibrations, it is necessary to increase the frequency of the clutch radial stiffness in such a way that it is not in phase with the frequency of shaft rotation. But the frequency of the clutch radial stiffness increases with an increasing number of elastic elements (*NZ*). However, the increase in *NZ* must be moderate, because, otherwise, we will have a stiff clutch, which is undesirable. One can also increase the number of complex elements (*NZ*), simultaneously decreasing their radial stiffness. In such a case, we approach a tyre-type clutch with improved characteristics of rotational motion. As such clutches are much more reliable, their operational characteristics are better compared with rubber (tyre-type) clutches [9].

A rotor system consisting of an asynchronous engine (4A100/4SY3), two shafts and a coupling made of two half-couplings and seven complex elements (rings) (Fig.7) is considered.

The diameters and the lengths of both shafts are equal to$d_1 = d_2 = 0.040$ m and $L_1 = L_2 = 1.0$ m, the inertia moments of the half-couplings' masses are $I_{p1} = I_{p2} = 0.624$ kgm^2; $I_{D1} = I_{D2} = 0.312$ kgm^2; $k_i = 10^6$ N/m; $h_i = 10^3$ Ns/m; ($i = 1, 2, ..., 8$). The load moment $M_{load} =$ 10 Nm. The dependence of the displacement of the first half-coupling in the direction of the *Y* axis on time is shown in Fig. 8, while the dependence of the displacement amplitude on frequency is given in Fig.9.

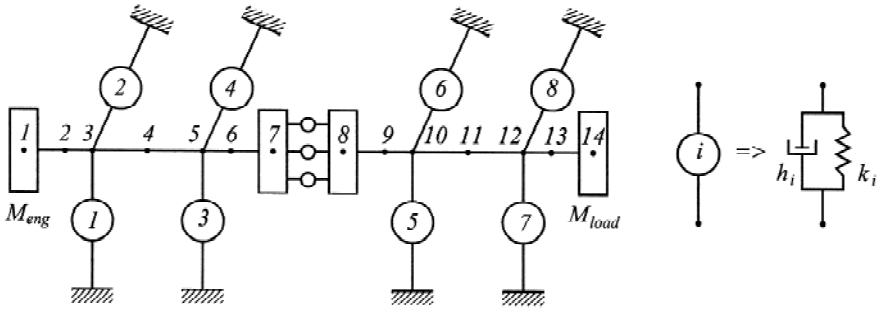

Sl. 7. *Shema rotorskega sistema*
Fig. 7. *A scheme of the rotor system*

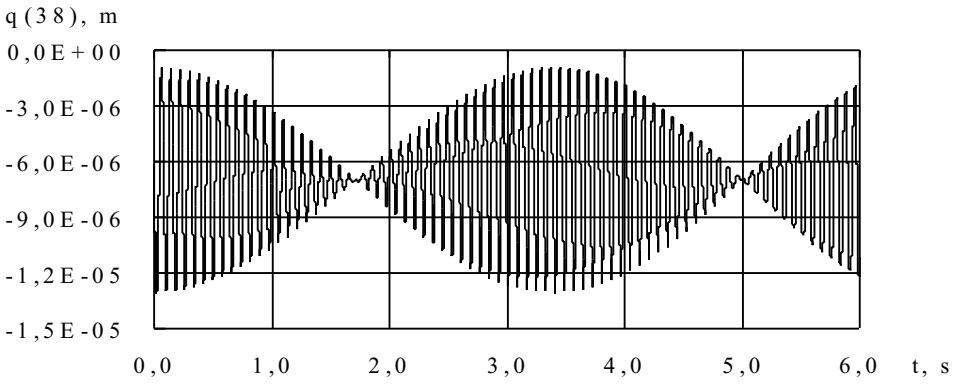

Sl. 8. *Časovna odvisnost premika q_{38} prve polovične gredne vezi v smeri osi Y*
Fig. 8. *The dependence of the displacement q_{38} of the first half-coupling in the direction of the* Y *axis on time*

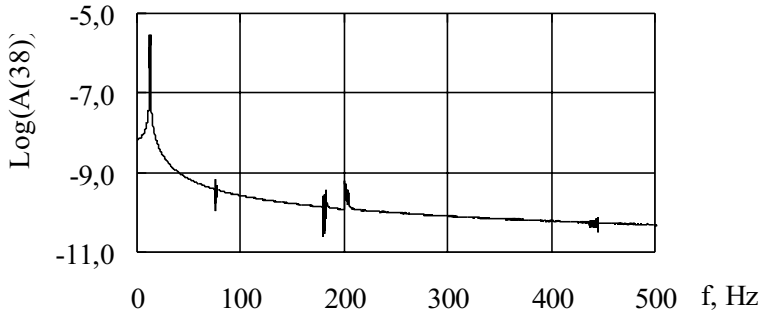

Sl. 9. *Odvisnost amplitude premika q_{38} od frekvence*
Fig. 9 *The dependence of the displacement q_{38} amplitude on frequency*

3 SKLEPI

1. Naš dinamični model rotorskega sistema z gibko, centrifugalno gredno vezjo opiše prostorska, geometrična, tehnološka in konstrukcijska odstopanja pa tudi dinamične posebnosti.
2. Z modelom lahko ovrednotimo sistem z želenim številom prostostnih stopenj na naslednje načine:
   - s povezovanjem koordinat začetnega sistema z ustreznimi koordinatami deformiranega sistema, pri čemer uporabljamo matematične odvisnosti;
   - s prikazom medsebojnih odnosov med začetnimi in deformiranimi točkami v različnih koordinatnih smereh;
   - s prikazom matematičnega odnosa med silami sestavljenih elementov rotorskega sistema in momenti, pa tudi njihov vpliv na gredi in oporne dele;
   - z določitvijo kinetične in potencialne energije kinematičnih in dinamičnih parametrov deformiranega sistema, lege in oblike elastičnih grednih vezi, ki povezujeta sistem.

3 CONCLUSIONS

1. Our dynamic model of a rotor system with a flexible, centrifugal coupling describes the spatial, the geometrical, the technological and the constructional deviations as well as the dynamic peculiarities.
2. The model can evaluate the system with a desired number of degrees of freedom in the following ways:
   - Connecting the initial system's coordinates with the corresponding coordinates of the deformed system using mathematical dependences;
   - Showing the interrelations of the initial and deformed points in various directions of the coordinates;
   - Showing a mathematical relation between the forces of the rotor system's composite elements and the moments, as well as their influence on the shafts and the supporting parts;
   - Finding the kinetic and potential energies of the deformed system's kinematic and dynamic parameters, and the position and the shape of the elastic couplings connecting the system.

4 LITERATURA
4 REFERENCES

[1] Bert, C.W., S. Wu (2003) Dynamic analysis of a nonlinear torsional flexible coupling with elastic links. *Journal of Mechanical Design*. Vol.125, Issue 3, 509-517.

[2] Mohiuddin, M.A., Y.A. Khulief (2002) Dynamic response analysis of rotor-bearing systems with cracked shaft. *Journal of Mechanical Design*. Vol.124, Issue 4, 690-696.
[3] Domachowski, Z., W. Prochnicki, Z. Puhaczewski, M. Dzida (2003) Influence of control loop on torsional vibrations of rotating machinery. *The 2nd International Symposium on Stability Control of Rotating Machinery.* Gdansk-Poland, 4-8 August 2003, 122-129.
[4] Spruogis, B. (1997) The devices of transmission and stabilization of rotary motion. *V.: Technika*, 476 p. (v ruskem jeziku).
[5] Bogdevičius, M., B. Spruogis (1996) Theoretical investigations into rotary systems with elastic link caused by the deflection of the shafts. *Transportas (Transport Engineering). V.: Technika,* No2(13), 70-81 (v ruskem jeziku).
[6] Spruogis, B. (1994) The counting of elements of rotary motion transmission and their parameters optimisation. *Taikomoji mechanika (Applied Mechanics*). *Kaunas: Technologija*, No2. 99-105 (v litovskem jeziku).
[7] Bogdevičius, M., B. Spruogis (1997) Dynamic and mathematical models of rotor system with elastic link in the presence of shafts misalignment. 2nd International Conference of Mechanical Engineering "Mechanics'97". *Proceedings. Part 1. V.: Technika*, 78-84.
[8] Ragulskis, K., B. Spruogis, M. Ragulskis (1999) Transformation of rotational motion by inertia couplings. *Vilnius: Technika*, 236 p.
[9] Spruogis, B. (1998) Rotary systems motion stabilization devices. Science and Arts of Lithuania. Vibroengineering. *Vilnius: Lithuania*, 452-465.
[10] Adiletta, G. and A.R. Guido (2000) Dynamical behaviour of a torsional system with parametric and external excitations. *Journal of Mechanical Engineering Science. Proceedings part C.* Vol. 214 NoC7. 955-973.
[11] Bogdevičius, M. (2000) Simulation of dynamic processes in hydraulic, pneumatic and mechanical drivers and their elements. *Vilnius: Technika*, 96 p.
[12] Aladjev, V., M. Bogdevičius (2001) Maple 6: Solution of the mathematical, statistical and engineering – physical problems. *Moscow: Laboratory of Basic Knowledges*, 824 (v ruskem jeziku).
[13] Áladjev, V., M. Bogdevicius, O. Prentkovskis (2002) New software for mathematical package maple of releases 6, 7 and 8. *Vilnius: Technika*, 404 p.
[14] Bogdevicius, M. (2002) Simulation of dynamic processes in mechanical drive with coupling gas. *Proceedings of the Six International Conference on Motion and Vibration Control,* August 19-23, Saitama, Japan, 543-546.
[15] Goudreau, G.L., R.L. Taylor (1973) Evaluation of numerical integration methods in elastodynamics. *Computer Methods in Appied Mechanics and Engineering*. Vol. 2, 69-97
[16] Fellipa, C.A., K.C. Park (1979) Direct time integration methods in nonlinear structural dynamics. *Computer Methods in Appied Mechanics and Engineering.* Vol. 17, 277-313.

Naslova avtorjev: prof. dr. Marijonas Bogdevičius
prof. dr. Bronislovas Spruogis
Fakulteta za transportno tehniko
Tehnična univ. Vilnius Gediminas
Sauletekio al. 11
LT-2040 Vilnus, Litva
marius@ti.vtu.lt

doc. dr. Vytautas Turla
Fakulteta za mehaniko
Tehnična univ. Vilnius Gediminas
J. Basanavicius str. 28
LT-2006 Vilnus, Litva
pgkatedra@me.vtu.lt

Authors' Addresses: Prof.Dr. Marijonas Bogdevičius
Prof.Dr. Bronislovas Spruogis
Faculty of Transport Eng.
Vilnius Gediminas Tech. Univ.
Sauletekio al. 11
LT-2040 Vilnus, Lithuania
marius@ti.vtu.lt

doc. dr. Vytautas Turla
Mechanical Faculty
Vilnius Gediminas Tech. Univ.
J. Basanavicius str. 28
LT-2006 Vilnus, Lithuania
pgkatedra@me.vtu.lt

Prejeto: 28.7.2003
Received:
Sprejeto: 30.9.2004
Accepted:
Odprto za diskusijo: 1 leto
Open for discussion: 1 year

© Strojniški vestnik 50(2004)12,613-622
ISSN 0039-2480
UDK 621.9.048:621.753.5.001.41
Kratki znanstveni prispevek (1.03)

© Journal of Mechanical Engineering 50(2004)12,613-622
ISSN 0039-2480
UDC 621.9.048:621.753.5.001.41
Short scientific paper (1.03)

Uporaba vodnega curka za postopno preoblikovanje pločevine

The Application of Water-Jet Technology for Incremental Sheet-Metal Forming

Mihael Junkar - Kurt C. Heiniger - Boštjan Jurišević

V zadnjih desetletjih je tehnologija obdelave s curki z velikimi hitrostnmi doživela velik razvoj. Od prvih primerov uporabe v zgodnjih sedemdesetih letih prejšnjega stoletja se je uporaba močno povečala. Med vsemi postopki, ki temeljijo na uporabi curkov z velikimi hitrostmi, ima vodilno vlogo rezanje z abrazivnim vodnim curkom (AVC), pri katerem vodni curek z velikimi hitrostmi (VC) pospešuje trde abrazivne delce, ki razjedajo material obdelovanca. Po drugi strani se VC uporablja za rezanje mehkejših materialov, čiščenje, površinsko obdelavo ter za uporabo v medicini in živilski industriji. V zadnjem času se VC uporablja tudi pri preoblikovanju, predvsem za utrjevanje površine izdelka, nekaj raziskav pa je pokazalo, da ima VC velike možnosti kot orodje za postopno preoblikovanje pločevine (PPP).

V tej raziskavi smo preučili možnosti uporabe vodnega curka z velikimi hitrostmi kot orodja za PPP. Prikazana je vplivnost postopkovnih parametrov kakor sta tlak in pretok vode, prav tako je definirana najbolj primerna geometrijska oblika vodne šobe za tvorbo curka. Predstavljen je tudi primer postopnega preoblikovanja 0,5 mm debele pločevine iz aluminijeve zlitine v preprosto obliko z VC.

Med primerjavo PPP z orodjem z določeno obliko se izkaže, da je predlagana tehnologija ekološko bolj sprejemljiva, saj ni potrebe po uporabi mazalnih sredstev. Prve raziskave nakazujejo, da se izboljša preoblikovalnost pri uporabi VC kot orodja za PPP.

(Ključne besede: preoblikovanje pločevine, postopki nekonvencionalni, izdelava prototipov hitra, curek vodni)

High-speed jetting technology has developed quickly over the past few decades. Since its first introduction in the early 1970s the number of applications has rapidly increased. Of the high-speed jet-based processes, cutting with an abrasive water jet (AWJ) is the most common. In this process, hard abrasive particles, which are accelerated by a high-speed water jet (WJ), can erode practically any known material. On the other hand, a plain WJ is used mostly for cutting softer materials, cleaning, surface preparation, applications in medicine and food processing. Recently, WJs have been used in forming, mostly as a tool for surface peening, but some research has shown great potential for a WJ as a tool for incremental sheet-metal forming (ISMF).

In this study we analyzed the possibility to apply a high-speed WJ as a tool for ISMF. The importance of process parameters such as water pressure and volume flow were determined, and the most appropriate water-nozzle geometry was defined as well. A case study is included, where a simple geometry was incrementally formed by a WJ in 0.5-mm-thick aluminum-alloy plate.

Compared to ISMF with a rigid tool, the proposed technology is more environmentally friendly, since no lubrication is required, and from our first investigation it seems that the formability is increased as well.

(Keywords: sheet-metal forming, nonconventional processes, fast prototyping, high speed water jet)

0 UVOD

V sodobni proizvodnji, pri kateri so serije izdelkov vedno manjše, je navzočnost neobičajnih postopkov zelo močna. Med razvojem novega izdelka ali optimizaciji že znanega obstoja zelo velika potreba po postopkih za hitro prototipno proizvodnjo.

0 INTRODUCTION

The presence of advanced, non-conventional processes is very strong in modern production, where production series are becoming smaller. During the development phase of a new product or the optimization of an existing one, fast-

Pomanjkljivost postopkov prototipne izdelave je, da v velikem številu primerov izdelki nimajo vseh lastnosti, ki so zahtevane pri končnem izdelku. V primeru, ko je treba izdelati večje število prototipnih izdelkov ali manjše serije, so ti postopki stroškovno in časovno neprimerni. Rešitev bi bila v tehnologiji, ki bi omogočala izdelavo prototipov in majhnih serij ustreznih izdelkov v razumnem času in stroškovno ugodno, kar bi pripomoglo k večji konkurenčnosti teh izdelkov na trgu. Na področju preoblikovanja pločevine je eden od takih postopkov, ki vsebuje zgoraj naštete zahteve, postopno preoblikovanje pločevine z vodnim curkom (PPPVC).

Pri postopnem preoblikovanju pločevine (PPP) se orodje preproste oblike giblje po definirani poti vzdolž trdno vpete pločevine. Pri tem se postopno preoblikuje pločevino v končno obliko z nadzorovanim vnosom plastičnih deformacij na lokalno omejeno področje. Na področju PPP z orodjem z določeno obliko je bilo opravljenih več študij ([1] do [4]). Ta tehnologija je že bila uspešno uporabljena v avtomobilski in letalski industriji [5]. V primerjavi z običajnim preoblikovanjem pločevine, pri katerem orodje deloma ali v celoti vsebuje obliko izdelka, so pri PPP stroški orodja bistveno nižji, obenem pa je izboljšana preoblikovalnost postopka. Po drugi strani je čas izdelave posameznega izdelka z PPP daljši, kar nakazuje, da je postopek bolj primeren za prototipno izdelavo in majhne serije izdelkov.

Številni argumenti nakazujejo primernost uporabe VC namesto orodja z določeno obliko za PPP. Predštudija, narejena pri sodelovanju Univerze v Ljubljani, Slovenija in Univerzo uporabnih znanosti Aargau, Windisch, Švica [6], je pokazala, da se lahko preoblikovalnost izboljša, ko se kot orodje za PPP uporabi VC. Torne razmere med VC in pločevino so bolj ugodne, med prehodom curka deluje na površino pločevine enakomerno porazdeljen tlak. Zelo verjetno ima tudi nihanje sile VC, ki jo povzroči periodično nihanje tlaka vode, pozitiven vpliv na tok materiala med preoblikovanjem. Poleg tega je rezanje z abrazivnim vodnim curkom (AVC) zelo razširjen postopek, ki se je v zgodnjih 80. letih prejšnjega stoletja razvil iz rezanja z VC, ki omogoča rezanje praktično kateregakoli materiala, ne da bi pri tem nastalo omembe vredno toplotno prizadeto področje. Standardni stroj za rezanje z AVC se lahko razmeroma preprosto dogradi v napravo za PPPVC. Ker so v slednjem primeru zahtevani nižji tlaki in večji pretoki vode kakor pri rezanju z AVC, je potrebna dodatna črpalka. Za pridobivanje primernega VC za PPP pa je potrebna posebna preoblikovalna glava, katero se pritrdi na vodila stroja poleg glave za rezanje z AVC. Za dogradnjo stroja za rezanje z AVC v stroj za PPPVC potrebujemo še vpenjalo za pločevino, ki ga namestimo na obdelovalno mizo. S temi spremembami bi bil na voljo stroj, na katerem bi bilo mogoče rezanje in

prototyping techniques are required. However, a common disadvantage of fast-prototyping techniques is that in many occasions they cannot produce a prototype that incorporates all the demanded characteristics of the final product. In the case where more prototypes or a small batch is required, those techniques fail due to unacceptable production costs or time. The solution would be a technology that would allow the production of prototypes or a small batch series of functional products in a reasonable time and for acceptable costs in order to make such a product competitive on the market. In the field of sheet-metal forming, water-jet incremental sheet-metal forming (WJISMF) seems to be a technology with all the above attributes.

In incremental sheet-metal forming (ISMF) the procedure involves a tool of simple geometry moving along an arbitrary geometry over a fixed metal sheet. It incrementally forms the workpiece to the final shape by introducing plastic deformations over a small controlled region. Many studies were made on ISMF with a rigid tool ([1] to [4]). This process was also successfully applied in the automotive and aerospace industries [5]. Compared to conventional sheet-metal forming processes, where the tool has to fully or partially reflect the product geometry, in ISMF the tooling costs are substantially reduced and the formability is increased. On the other hand, more time is required to produce a single part, which makes ISMF more suitable for prototyping and small batch production.

There are many arguments in favour of using a high-speed WJ instead of a rigid tool in ISMF. A feasibility study made in a collaboration between the University of Ljubljana, Slovenia and the University of Applied Sciences of Aargau, Windisch, Switzerland [6] showed that the formability might be further increased when a WJ is used as a tool. Friction conditions at the interface between the WJ and the workpiece are better, and the hydrostatic pressure is evenly distributed during the passage of the WJ over the sheet-metal surface. It is also very likely that the WJ force oscillation due to the oscillation of water pressure has a positive influence on the flow of workpiece material. Furthermore, abrasive water-jet (AWJ) machining is already a well-established cutting process developed from WJ cutting in the early 1980s, able to cut virtually any material, and no relevant heat-affected zone is produced. A standard AWJ cutting machine can be relatively easily upgraded to a WJISMF platform. Since lower water pressures and higher volume flows of water compared to AWJ cutting are required for WJISMF an additional water pump is needed. To produce a WJ that is able to incrementally form a sheet of metal, a special forming head has to be mounted on the AWJ's machine steering system. The last thing needed to upgrade an AWJ cutting system to a WJISMF machine is a sheet-metal holder that can be placed on the working table. The result is a machine where cutting and sheet-metal forming can be carried

preoblikovanje pločevine. Takšen stroj bi bil zelo uporaben za izdelavo prototipov in majhnih serij pločevinastih izdelkov.

Pred uporabo predlagane tehnologije je treba preučiti številne dejavnike. Najprej je treba definirati optimalne vrednosti pomembnih postopkovnih parametrov, iz česar bosta izhajali oblikovanje primerne šobe in izbira ustrezne črpalke, kar bo prikazano v nadaljevanju. V predstavljenem primeru je opisano PPPVC, pri katerem je bila izdelana preprosta oblika iz 0,5 mm debele pločevine iz aluminijeve zlitine. V sklepu so predstavljene načrtovane dejavnosti na področju PPPVC.

1 NAČELA PPPVC

V primerjavi z rezanjem z AVC, pri katerem VC z velikimi hitrostmi pospešuje trde abrazivne delce, mora pri PPP, VC izpolnjevati drugačne zahteve. Površinski tlak med VC in pločevino mora biti dovolj majhen, da ne pride do erozije obdelovanca. Hkrati pa naj bo sila VC dovolj velika, da povzroči plastično deformacijo pločevine.

Pri rezanju AVC nastaja v rezalni glavi, ki jo sestavljajo šoba, mešalna komora, dovod za abraziv in fokusirna šoba. Rezalna glava je pritrjena na kolimacijsko cev, ki stabilizira tok tekočine pod visokim tlakom. Na začetku rezalne glave nastaja vodni curek že v šobi, pri čemer se potencialna energija vode pod visokim tlakom spremeni v kinetično energijo vodnega curka z velikimi hitrostmi. VC z velikimi hitrostmi vstopi v mešalno

out. Such a machine could be very useful for prototyping and the small batch production of sheet-metal products.

In order to apply the proposed technology, several issues have to be addressed. First, the optimal values of relevant process parameters have to be defined, from which an appropriate nozzle can be designed and a suitable water pump selected. This is presented in what follows. Then a case study on WJISMF is described, where a simple geometry was incrementally formed using a WJ and 0.5-mm-thick aluminum alloy. In the conclusions we describe our activities planned for the future.

1 PRINCIPLES OF WJISMF

Compared to AWJ cutting, where hard abrasive particles are accelerated by a high-speed jet of water, a WJ for ISMF must meet different requirements. The resulting pressure of the WJ on the workpiece metal sheet surface has to be much smaller in order to not initiate the erosion process. At the same time, the jet force has to be high enough to enable plastic deformations of the plate.

In AWJ cutting, the jet is continuously generated in the cutting head, which is composed of a nozzle, a mixing chamber, an abrasive inlet and a focusing tube. The cutting head is connected to the collimating tube, which has the function of stabilizing the water flow. The nozzle at the beginning of the cutting head converts the potential energy of the water under high pressure to the kinetic energy of a high-speed water jet. Such a high-speed WJ enters the mixing chamber and

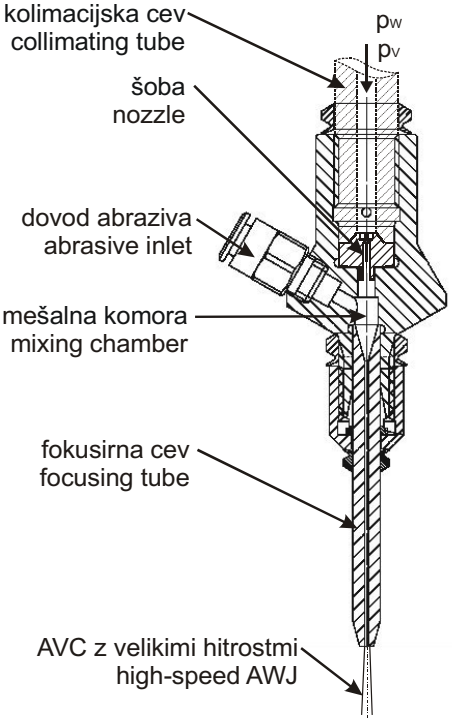

Sl. 1. *Rezalna glava za obdelavo z AVC*
Fig. 1. *Cutting head for AWJ machining*

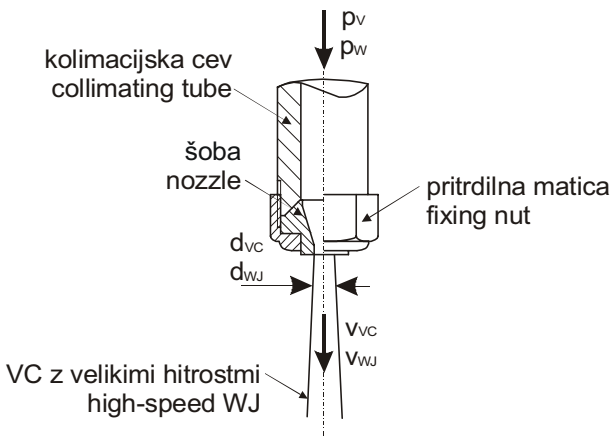

Sl. 2. *Preoblikovalna glava za PPPVC*
Fig. 2. *Forming head for WJISMF*

komoro, v kateri sesa abrazivne delce in zrak skozi dovod za abraziv, ki je nameščen na steno mešalne komore. Abrazivni delci pospešujejo v fokusirni šobi, ki je pritrjena pod mešalno komoro. Rezultirajoči curek je sestavljen iz vode, abrazivnih delcev in zraka. Ko AVC zadene površino obdelovanca, abrazivni delci razjedajo material. Na sliki 1 je prikazana rezalna glava z vsemi glavnimi sestavinami.

Preoblikovalna glava za PPPVC se nekoliko razlikuje od glave za rezanje z AVC. Načeloma ne potrebuje mešalne komore, dovoda za abraziv in fokusirne šobe. Najpomembnejša komponenta je šoba, v kateri nastaja VC . Zamisel take preoblikovalne glave je predstavljena na sliki 2.

Prvi vtis bi bil, da je preoblikovalna glava v bistvu glava za rezanje z AVC brez mešalne komore, dovoda za abraziv in fokusirne šobe. Naše izkušnje [6] so pokazale, da je za PPPVC bolj primeren drugačen tip šobe kakor pri rezanju z AVC. V slednjem primeru se največ uporabljajo šobe z ostrim robom, medtem ko so za PPPVC bolj primerne zvezne šobe. Obe zasnovi šob sta prikazani na sliki 3.

Postopkovni parametri za PPPVC se prav tako razlikujejo od tistih, uporabljenih za obdelavo z AVC. Da ne pride do erozije obdelovanca pri PPPVC, mora biti površinski tlak med curkom in pločevino znižan, kar se doseže z nižjim tlakom vode. Trenutno so za rezanje z AVC uporabljeni tlaki vode do 400 MPa, v prihodnosti, ko bodo na voljo novi tipi črpalk, pa se bodo delovni tlaki zvišali do 1000 MPa. Pri uporabi VC v preoblikovanju, tlak vode ne presega 25 MPa.

Poleg površinskega pritiska je zelo pomembna lastnost sila VC, ki mora biti dovolj velika da plastično deformira obdelovanec. Ker je tlak vode definiran z največjim dopustnim površinskim tlakom, se lahko silo curka poveča z večanjem premera šobe. Pri obdelavi z AVC je premer šobe med 0,1 in 0,3 mm ter premer fokusirne šobe med 0,3 in 0,8 mm. Pri PPPVC pa mora biti premer šobe vsaj 2 mm, da je mogoče

sucks abrasive particles and air through the abrasive inlet placed on the side of the mixing chamber. Once the abrasive has been inserted it accelerates inside the focusing tube placed downstream of the mixing chamber. The resulting jet is therefore composed of a stream of abrasive particles, water and air. When such a high-speed AWJ hits the workpiece, the abrasive particles remove the material by eroding it. Figure 1 shows an AWJ cutting head with all its main components.

A forming head for WJISMF differs slightly from an AWJ cutting head. The main difference is that it does not need a mixing chamber, an abrasive inlet and a focusing tube. The most important component is the nozzle, where a high-speed WJ is generated. A schematic of such a forming head is presented in Figure 2.

At this point the first impression would be that a forming head is actually an AWJ cutting head, where the abrasive inlet is closed and the focusing tube is removed. Nevertheless, our experiences [6] showed that a different type of nozzle is more appropriate for generating a WJ for ISMF. In AWJ cutting, sharp-edge nozzles are commonly used, while in WJISMF a continuous nozzle gives much better results. Both types of nozzles are shown in Figure 3.

The process parameters in WJISMF are different from those used in AWJ machining. In order to prevent any erosion of the workpiece material in WJISMF, the surface pressure at the interface between the WJ and the metal sheet has to be reduced by reducing the water pressure. Currently, in AWJ cutting the water pressure is up to 400 MPa, and it seems that in the near future this operating pressure will be raised to 1000 MPa, as new pumps will soon be available. In WJ forming applications, the water pressure does not need to exceed 25 MPa.

Another crucial attribute of the WJ is the jet force, which has to be high enough to allow plastic deformation of the workpiece. Because the water pressure is defined by the highest allowed surface pressure, the jet force can be increased by increasing the nozzle diameter. In AWJ machining the nozzle diameter is between 0.1 and 0.3 mm and the focusing tube diameter between 0.3 and 0.8 mm. In WJISMF

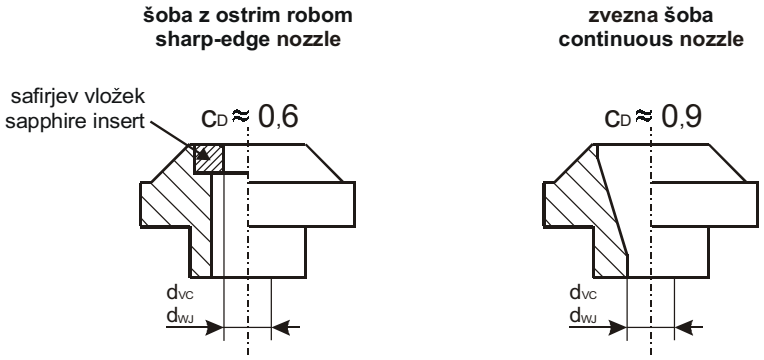

Sl. 3. *Šoba z ostrim robom in zvezna šoba za obdelavo s curki z velikimi hitrostmi*
Fig. 3. *Sharp-edge and continuous nozzles in high-speed jet technology*

preoblikovati pločevino iz aluminijeve zlitine z debelino 1 mm.

Za zvezno šobo, prikazano na sliki 3, se površinski tlak p_P in silo VC F_{VC} lahko dovolj natančno popiše z enačbo (1) oz. enačbo (2):

the nozzle diameter has to be at least 2 mm in order to form an aluminum alloy plate of thickness up to 1 mm.

In the case of a continuous nozzle, which is shown in Figure 3, Equation 1 and 2 can approximate accurately enough for the proposed application the surface pressure, $p_{S,}$ and the WJ force, F_{WJ}.

$$p_P = 2 \cdot c_D^2 \cdot p_V \tag{1}$$

$$F_{VC} = 2 \cdot c_D^2 \cdot A_{VC} \cdot p_V \tag{2},$$

kjer je p_V tlak vode, A_{VJ} prečni prerez curka in c_D razbremenilni koeficient šobe. Za zvezno šobo je vrednost razbremenilnega koeficienta okoli 0,9. Iz zgoraj navedenih enačb se lahko opazi, da je površinski tlak odvisen od tlaka vode, medtem ko je sila VC odvisna od tlaka vode in premera curka za določen tip šobe.

Zaradi uporabe večje šobe mora črpalka dovajati precej večji prostorninski tok vode v primeru uporabe VC v preoblikovanju. V primeru obdelave z AVC prostorniski tok vode ne presega 5 l/min, za PPPVC pa mora biti prostorninski tok vsaj 50 l/min, po navadi celo več, ko se preoblikuje pločevino večje debeline.

Zgoraj opisane značilnosti in zahteve obdelave z VC/AVC na eni strani in uporab VC v preoblikovanju na drugi strani so povzete v preglednici 1.

where p_W is the water pressure, A_{WJ} the jet's cross-sectional area and c_D the nozzle discharge coefficient. For a continuous nozzle the discharge coefficient is around 0.9. It can be observed from the above equations that the surface pressure is a function of the water pressure, while the WJ force is a function of the water pressure and the jet dimension for a given type of nozzle.

As a direct consequence of a larger nozzle diameter, the pump has to generate a much higher volume flow of water in the case of WJ forming applications. While the required volume flow for AWJ cutting usually does not exceed 5 l/min, for WJISMF the volume flow has to be at least 50 l/min, but usually even more, especially when thicker plate has to be incrementally formed.

The above described characteristics and requirements for WJ/AWJ cutting and WJ forming are summarised in Table 1.

2 PRIMER UPORABE

Pred kratkim smo opravili poskusno raziskavo na področju PPPVC [6]. Zaradi pomanjkanja izkušenj na

2 CASE STUDY

We have recently made an experimental investigation of WJISMF [6]. As we had no

Preglednica 1. *Primerjava med rezanjem z CV/AVC in preoblikovanjem z CV*
Table 1. *Comparison of WJ/AWJ cutting and WJ forming*

Zahteva / značilnost Requirements / characteristic	Rezanje z VC/AVC WJ/AWJ cutting	Preoblikovanje z VC WJ forming
tlak vode water pressure	čim višji trenutno 400 MPa, v prihodnosti do 1000 MPa as high as possible currently 400 MPa, in future up to 1000 MPa	do 25 MPa, da ne pride do erozije obdelovanca up to 25 MPa in order to prevent erosion of the workpiece
vrsta črpalke type of water pump	hidravlično ojačevalo (nespremenljiv tlak) hydraulic intensifier (constant pressure)	batna črpalka (nespremenljiv volumski tok) plunger pump (constant volume flow)
premer šobe nozzle diameter	0,3 mm ali manj 0.3 mm or less	1 mm ali več 1 mm or more
vrsta šobe nozzle type	z ostrim robom ($c_D \approx 0,6$) sharp-edge ($c_D \approx 0.6$)	zvezna ($c_D \approx 0,9$) continuous ($c_D \approx 0.9$)
prostorninski tok vode volume flow of water	nekaj l/min up to a few l/min	do 50 l/min in več up to 50 l/min or more
sila curka jet force	čim manjša as small as possible	čim večja as high as possible

tem področju smo kot izhodišče predstavljene raziskave uporabili rezultate, ki jih je dobil Iseki [7] na Tokijskem tehnološkem inštitutu na Japonskem. Glede na razpoložljivo literaturo je njegovo delo prvo na področju PPPVC. V našem preizkusu smo preoblikovali stopničasto stožčasto obliko iz 0,5 mm debele pločevine iz aluminijeve zlitine AlMgSi1. Končno obliko pločevine smo dosegli z večkratnim izvajanjem sosrednjih krogov, kar je prikazano na sliki 5. Kinematika VC vzdolž pločevine je podana v preglednici 2.

experience in this field we used, as a starting point, the results of Iseki [7] from the Tokyo Institute of Technology, Japan. According to the available literature he made pioneering work in the field of WJISMF. In our trial we formed a stepped conical shape in 0.5-mm-thick AlMgSi1 aluminum alloy by passing several times along concentric circles as showed in Figure 4. The kinematics parameters are listed in Table 2.

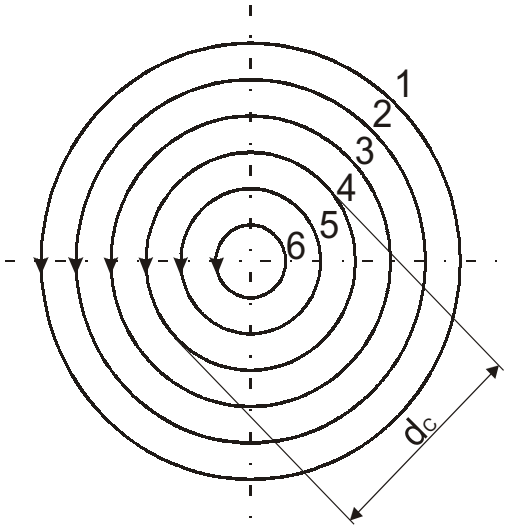

Sl. 4. *Kinematika VC vzdolž obdelovanca [6]*
Fig. 4. *Kinematics of the WJ over the workpiece [6]*

Preglednica 2. *Kinematika VC [6]*
Table 2. *WJ kinematics parameters [6]*

Krog Circle	d_C mm	n_P 1	t_O / t_M s	E_{VC} / E_{WJ} kJ
1	60	2	377	1943
2	50	3	471	2428
3	40	4	503	2590
4	30	5	471	2428
5	20	6	377	1943
6	10	7	220	1133
		skupaj total	2419	12465

Razdalja med šobo in obdelovancem je bila nastavljena na 30 mm, podajalna hitrost VC vzdolž obdelovanca pa je bila 1 mm/s. Preizkus je bil opravljen na predelanem sistemu za rezanje z AVC tipa PERENDORFER WSS 1010 z delovno površino 1×1 m, dvema RNK vodenima osema in ročno vodeno navpično osjo. Za dvigovanje tlaka vode in dovajanje ustreznega prostorninskega toka je bila uporabljena batna črpalka tipa WOMA 180 Z P18, ki omogoča prostorninski tok vode 21 l/min pri največjem tlaku 200 MPa in moči 78 kW. Obdelovanec je bil vpet v posebej razvitem pridržalu, prikazanem na sliki 5, in položen na obdelovalno mizo kakor prikazuje slika 6.

The stand-off distance between the nozzle and the workpiece was set to 30 mm and the traverse rate of the jet over the workpiece was 1 mm/s. This experiment was performed on a modified PERNDORFER AWJ cutting system WSS 1010 with a working area of 1×1 m, two CNC driven axis and a manually driven vertical axis. To generate high-pressure water with the required volume flow we used a WOMA plunger pump type 180 Z P18 with a water volume flow of 21 l/min at a maximum pressure of 200 MPa and a power of 78 kW. The workpiece was fixed in a specially designed holder shown in Figure 5 and placed on the working table as shown in Figure 6.

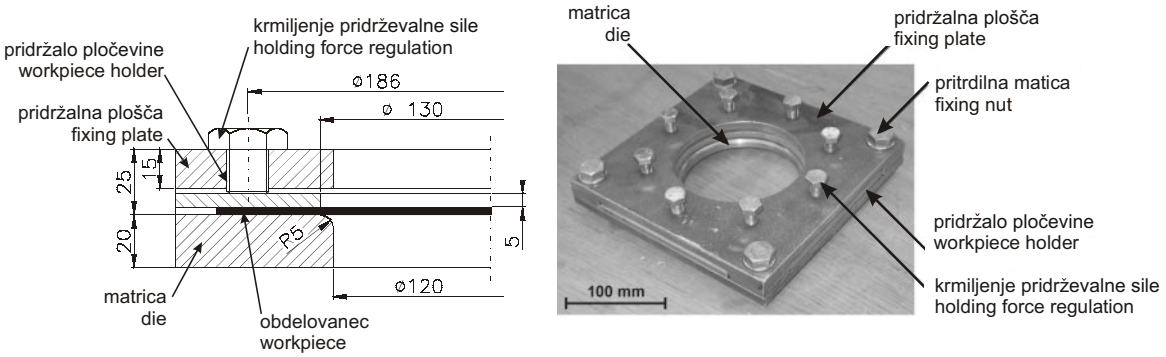

Sl. 5. *Posebej razvito pridržalo pločevine za PPPVC [6]*
Fig. 5. *Specially developed workpiece holder for WJISMF [6]*

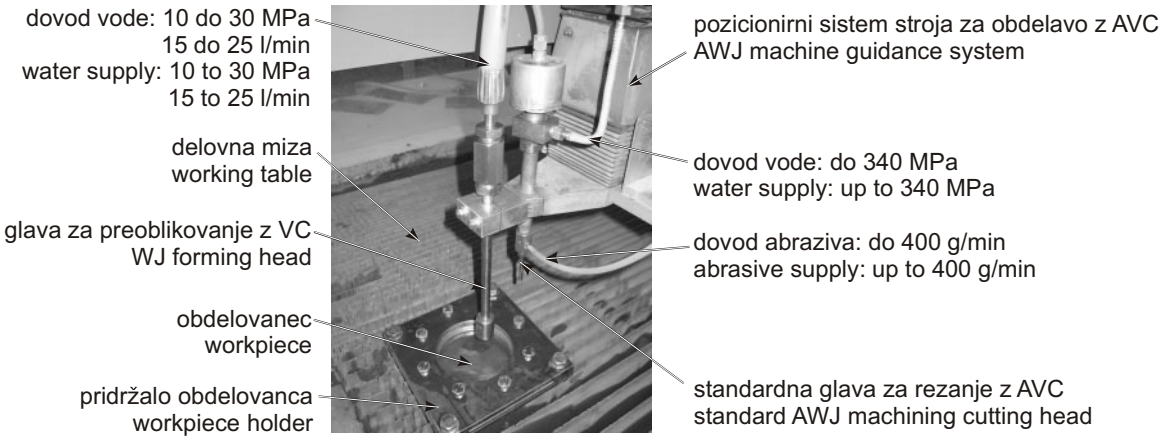

Sl. 6. *Namestitev obdelovanca na obdelovalno mizo [6]*
Fig. 6. *Positioning of the workpiece on the working table [6]*

Preglednica 3. *Glavne lastnosti VC pri različnih tlakih vode*
Table 3. *Relevant WJ attributes for different water-pressure levels*

Značilnosti šobe: Nozzle characteristics:	p_V / p_W MPa	V_V / V_W l/min	F_{VC} / F_{WJ} N	P_{VC} / P_{WJ} kW	p_P / p_S MPa
$d_Š$=1,5 mm d_O=1.5 mm vrsta: zvezna type: continuous c_D=0,9	10	13,5	28,6	1,82	16,2
	20	**19,1**	**57,3**	**5,15**	**32,4**
	30	23,4	85,9	9,47	48,6

Ob upoštevanju tipa šobe se lahko izračuna glavne lastnosti VC za PPPVC, ter določi ustrezen tlak vode. V preglednici 3 so navedene pomembnejše lastnosti VC pri treh različnih tlakih vode za uporabljeno šobo.

V svojem delu [7] je Iseki uporabil tlak vode 19,5 MPa in zvezno šobo premera 1,34 mm, kar se je kazalo v prostorninskem toku vode 15 l/min. V njegovem primeru je preoblikoval pločevino iz aluminijeve zlitine debeline 0,3 mm. Glede na te parametre smo se odločili uporabiti tlak vode 20 MPa, pri čemer so drugi postopkovni parametri in lastnosti VC ustrezali vrednostim, navedenim v preglednici 3. Rezultirajoča geometrijska oblika izdelka po PPPVC je prikazana na sliki 7.

By taking into account the type of nozzle it is possible to calculate the WJ attributes that are relevant in WJISMF and set the appropriate water pressure accordingly. Table 3 lists the relevant WJ attributes at three values of water pressure for the applied nozzle.

In his work Iseki [7] used a water pressure of 19.5 MPa and a continuous nozzle of diameter 1.34 mm, which resulted in a volume flow of 15 l/min. In this case the workpiece was a 0.3 mm annealed aluminum sheet. Taking this into account, we chose a water pressure of 20 MPa with the corresponding process parameters and WJ attributes listed in Table 3. The resulting geometry is shown in Figure 7.

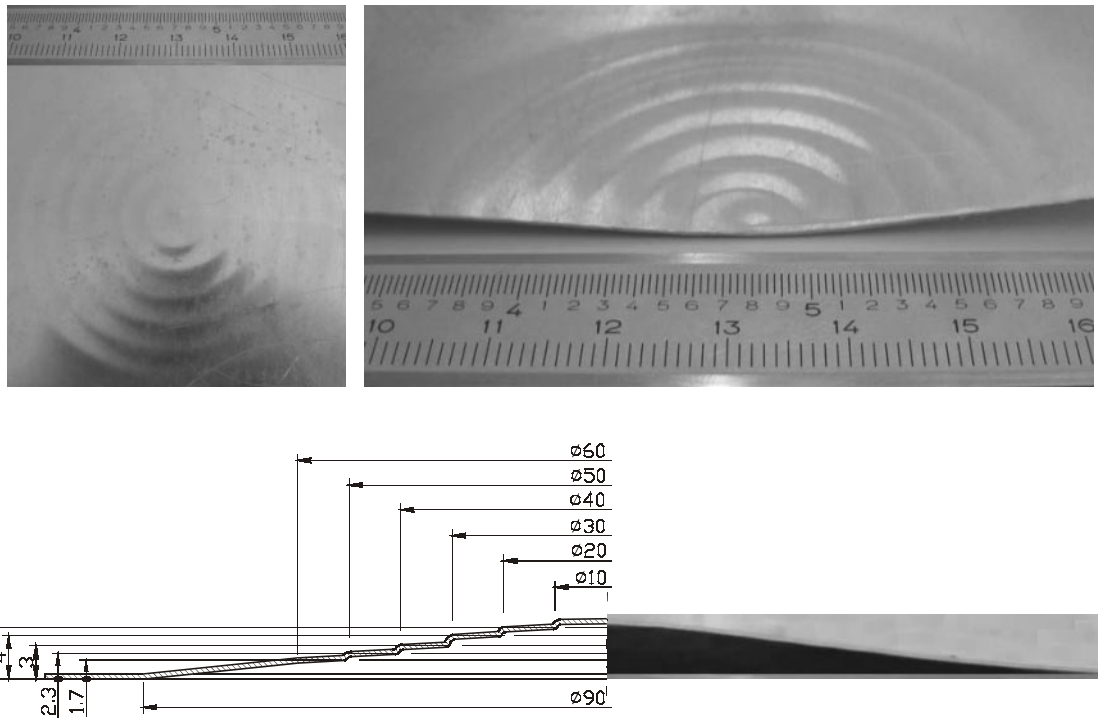

Sl. 7. *Stopničasta stožčasta geometrijska oblika preoblikovana z PPPVC [6]*
Fig. 7. *Stepped conical geometry formed by WJISMF [6]*

Rezultati predstavljene raziskave so zelo spodbudni. Uspelo nam je definirati ustrezne postopkovne parametre za postopno preoblikovanje 0,5 mm debele pločevine iz aluminijeve zlitine AlMgSi1 brez kakršnekoli poškodbe površine. V tem primeru ni bilo uporabljeno nikakršno podporno orodje ali matrica, geometrijska oblika je bila enakomerno preoblikovana, kar nakazuje visoko stopnjo stabilnosti postopka.

3 SKLEPI IN NADALJNJE DELO

Podobno kakor na številnih področjih se je tehnologija obdelave s curki z velikimi hitrostmi izkazala tudi pri preoblikovanju, kjer se lahko VC uporabi kot orodje za PPP. Dejstvo, da se lahko običajni sistem za obdelavo z AVC preprosto dogradi v stroj za PPPVC, odpira veliko možnosti predstavljene tehnologije na področju hitre izdelave prototipov in maloserijske proizvodnje izdelkov iz pločevine.

V primerjavi z rezanjem s VC/AVC je treba pri preoblikovanju s VC tlak znižati na 25 MPa in manj, da se prepreči erozija obdelovanca. Hkrati je treba povečati silo curka, kar se doseže s povečanjem premera šobe. S tem je potreben večji prostorninski tok vode v primerjavi z rezanjem z VC/AVC, iz česar izhaja, da je batna črpalka bolj primerna od hidravličnega ojačevala za preoblikovanje s VC.

V predstavljenem primeru je bila oblikovana preprosta geometrijska oblika iz 0,5 mm debele pločevine iz aluminijeve zlitine AlMgSi1. V prihodnosti bodo dejavnosti na področju PPPVC

The results of the presented feasibility study are extremely encouraging. We were able to predict the appropriate process parameters to incrementally form a 0.5-mm-thick AlMgSi1 aluminum alloy with a damage-free surface. In this case no special tool or die was used, while the final geometry was evenly formed, indicating a high degree of process stability.

3 CONCLUSIONS AND FUTURE WORK

High-speed jet technology has proved itself in forming, where a high-speed WJ can be applied as a tool for ISMF. The fact that a conventional AWJ cutting machine can be relatively easily upgraded to a WJISMF platform makes the proposed technology very attractive in the field of rapid prototyping and the small batch production of sheet-metal parts.

Compared to WJ/AWJ cutting, in forming applications the water pressure has to be reduced down to 25 MPa, or even less, in order to prevent the erosion of the workpiece. At the same time the jet force has to be increased, which is achieved by increasing the nozzle diameter. This means that the required water volume flow is higher than with WJ/AWJ cutting applications, which makes a plunger pump more appropriate than a hydraulic intensifier for WJ forming.

In a case study a simple geometry was formed in 0.5-mm-thick AlMgSi1 aluminum alloy. Our future activities in the field of WJISMF will consist of building an experimental installation at the University

obsegale gradnjo preizkuševališča na Univerzi v Ljubljani. V ta namen bo uporabljena batna črpalka s prostorninskim tokom vode 50 l/min in tlakom do 25 MPa.

Prav tako so načrtovane raziskave na področju PPPVC na krojenih prirezih, zvarjenih s tornim gnetenjem, kar bo v primeru uporabnih rezultatov vodilo v neposredno uvajanje predlagane tehnologije v industrijo.

Vpliv tlaka vode (prostorninskega toka vode) in karakteristik šobe na PPPVC je definiran. Trenutno lahko določimo primerne postopkovne parametre ter izberemo ustrezno šobo. Vseeno pa je treba raziskati še številne vidike, med katerimi je najbolj pomemben razvoj geometrijske oblike preoblikovalne glave. Prav tako bo treba raziskati še številne postopkovne parametre, npr. razdalja med šobo in obdelovancem ter kinematiko VC vzdolž obdelovanca.

of Ljubljana. A plunger pump is anticipated, which will allow a water flow of 50 l/min and a pressure up to 25 MPa.

We also plan to apply the presented technology for ISMF of tailor blanks welded by friction stir welding (FSW), which if succesful would lead to a direct implementation of the proposed technology in industry.

The influence of the water pressure (volume flow) and nozzle characteristics on WJISMF is understood. We are now able to define appropriate process parameters and select a suitable nozzle. Nevertheless, many issues remain to be addressed, among which the most important seems to be a development of an advanced forming head with better performance. Also, the influence of process parameters, such as stand-off distance and WJ kinematics, over the workpiece have to be further investigated.

4 ZAHVALA

Avtorji se zahvaljujejo Univerzi aplikativnih znanosti Aargau v Švici za podporo med eksperimentalnim delom.

4 ACKNOWLEDGMENT

The authors wish to express their gratitude to the University of Applied Sciences, Aargau, Switzerland for support during the experimental work.

5 OZNAKE
5 NOMENCLATURE

abrazivni vodni curek	AVC/AWJ		Abrasive Water Jet
postopno preoblikovanje pločevine	PPP/ISMF		Incremental Sheet-Metal Forming
postopno preoblikovaanje pločevine z vodnim curkom	PPPVC/WJISMF		Water-Jet Incremental Sheet-Metal Forming
vodni curek	VC/WJ		Water Jet
prečni prerez vodnega curka	A_{VC}/A_{WJ}	mm^2	water-jet cross-sectional area
razbremenilni koeficient šobe	c_D	-	nozzle discharge coefficient
premer krogov	d_C	mm	circles diameter
premer vodnega curka	d_{VC}/d_{WJ}	mm	water-jet diameter
energija vodnega curka	E_{VC}/E_{WJ}	J	water-jet energy
sila vodnega curka	F_{VC}/F_{WJ}	N	water-jet force
število prehodov	n_P	-	number of passes
površinski tlak	p_P/p_S	MPa	surface pressure
tlak vode	p_V/p_W	MPa	water pressure
moč vodnega curka	P_{VC}/P_{WJ}	W	water-jet power
čas obdelave	t_O/t_M	s	machining time
prostorninski tok vode	V_V/V_W	l/min	water volume flow
hitrost vodnega curka	v_{VC}/v_{WJ}	m/s	water jet velocity

6 LITERATURA
6 REFERENCES

[1] Hirt, G., S. Junk and N. Witulski (2002) Incremental sheet metal forming: Quality evaluation and process simulation. *Proceedings of the 7th International Conference on Technology of Plasticity, ICTP 2002, The Japan Society for Technology of Plasticity,* vol. 2, 925-930, Yokohama, Yapan, 28-31 October 2002.

[2] Hirt, G., J. Ames and M. Bambach (2003) Economical and ecological benefits of CNC incremental sheet forming (ISF). In *Proceedings of the 9th International Workshop on Ecology and Economy in Manufacturing, ICEM 2003*.

[3] Kim, T. J. and D.Y. Yang (2000) Improvement of formability for the incremental sheet metal forming process. *International Journal of Mechanical Sciences*, Vol. 42, 1271-1286.
[4] Iseki, H. (2001) Flexible and incremental bulging of sheet metal using high-speed waterjet. *JMSE International Journal*, Series C, Vol. 44, 2, 486-493.
[5] Jeswiet, J., D. Young and A. Szekeres (2003) Forming limit diagram for CNC RPIF of sheet metal. In Bley H., editor, *Proceedings of the 36th CIRP-International Seminar on Manufacturing Systems: Progress in Virtual Manufacturing Systems*, 551-553, Saarbruecken, Germany, 03-05 June 2003.
[6] Jurišević, B., K.C. Heiniger, K. Kuzman and M. Junkar (2003) Incremental sheet metal forming with a high-speed water jet. In Kuzman K., Janssen E., Col A., Kerge R., Kessler L., Lenze F.-J., editors, *Proceedings of the International Deep Drawing Research Group Conference*, IDDRG 2003, 139-148, Bled, Slovenia, 11-15 May 2003.
[7] Iseki, H. (2001) Flexible and incremental bulging of sheet metal using high-speed waterjet. *JMSE International Journal*, Series C, Vol. 44, 2, 486-493.

Naslova avtorjev: prof.dr. Mihael Junkar
Boštjan Jurišević
Fakulteta za strojništvo
Univerza v Ljubljani
Aškerčeva 6
1000 Ljubljana

prof.dr. Kurt C. Heiniger
Švicarski kompetenčni center za
tehnologijo vodnih curkov
Univerza uporabnih znanosti Aargau
Windisch, Švica

Authors' Addresses: Prof.Dr. Mihael Junkar
Boštjan Jurišević
Faculty of Mechanical Eng.
University of Ljubljana
Aškerčeva 6
1000 Ljubljana, Slovenia

Prof.Dr. Kurt C. Heiniger
Swiss Competence Centre for
Water Jet Technology
University of Applied Sciences
Aargau, Windisch Switzerland

Prejeto: 21.4.2004
Received:
Sprejeto: 2.12.2004
Accepted:
Odprto za diskusijo: 1 leto
Open for discussion: 1 year

© Strojniški vestnik 50(2004)12,623-630
ISSN 0039-2480
UDK 621.182:519.61/.64
Strokovni članek (1.04)

© Journal of Mechanical Engineering 50(2004)12,623-630
ISSN 0039-2480
UDC 621.182:519.61/.64
Speciality paper (1.04)

Numerična simulacija toka delovne tekočine v razpoki stene cevi uparjalnikove membrane parnega kotla

Numerical Simulation of Working-Fluid Flow Cut in a Tube of a Steam-Boiler Membrane-Wall Evaporator

Namir Neimarlija - Nagib Neimarlija

Prispevek prikazuje problem neustaljenega prenosa toplote in napetosti v cevi stene uparjalnikove membrane parnega kotla s predpostavko nenadne zaustavitve toka delovne tekočine skozi eno od njegovih cevi. Gre za skrajen primer, v katerem je konvektiven prenos toplote s stene cevi na delovno tekočino nenadno ustavljen. Opravljena je dvorazsežna analiza z metodo končnih prostornin ob predpostavki, da je material termoelastično zvezno telo. Analiza je pokazala razmeroma hitro dosego kritične vrednosti napetosti.

(Ključne besede: kotli parni, uparjalniki, prenos toplote, metode numerične)

This paper presents the problem of transient heat transfer and the stress in the tube of a steam-boiler membrane-wall evaporator, assuming a sudden cut of the working-fluid flow through one of its tubes. Thus, an extreme case was considered in which the convective heat transfer from the tube wall to the working fluid was suddenly cut. The 2D analysis was carried out using a finite-volume method and with the assumption that the material is a thermo-elastic continuum. The analysis showed that the critical stress values were achieved relatively quickly.

(Keywords: steam boilers, evaporators, heat transfer, numerical methods)

0 UVOD

Obravnavan je dejanski dogodek v termoelektrarni Kakanj, in sicer v njegovi enoti 7 z močjo 230 MW. V decembru leta 2000 je tam nastala okvara na cevi uparjalnika parnega kotla, ki je bila več ali manj usmerjena vzdolžno. Deformacija je bila največja na višini cevi 17 in 18 metrov [1]. Inženirji v elektrarni so mnenja, da se je zgodila kot posledica zastoja delovnega medija v poškodovani cevi. Zares je bil tu ob demontaži poškodovane cevi najden material, ki je zapiral šobo na izhodu uparjalnikove cevi. Material je bil tam puščen po napaki med remontom sistema šob. V nadaljevanju je bil opazen stalen problem zagotovitve uravnovešenega pretoka delovne tekočine skozi cevi uparjalnika v kotlu, potrjen z merjenjem z ultrazvočnim inštrumentom. Rezultati kažejo odstopanja v toku delovne tekočine v območju ± 60 % od imenske vrednosti [1]. Poleg težav zagotovitve ustaljenega pretoka delovne tekočine so se slabšali pogoji delovanja uparjalnika zaradi razpoke v toplotno zaščitnem materialu v delu uparjalnika, posebno na stropu zgorevalne komore.

0 INTRODUCTION

A real event that occurred in the thermal power plant Kakanj, i.e., in its thermal unit 7, with a power of 230 MW, was analysed. In December 2000, there was a breakdown of the steam boiler's evaporator tube, which was more or less deformed lengthways. The deformation was the largest at tube heights of 17 and 18 meters [1]. Engineers in the plant assumed that it happened due to a cut in the working-medium flow in a damaged tube. Indeed, while disassembling the damaged tube, a material was found, which blocked a nozzle at the inlet of the evaporator tube. The material was left behind by mistake during an overhaul of the nozzle system. In addition, there was a constant problem regarding provision of a balanced working-fluid flow through the evaporator tubes in this boiler, which was confirmed by measurements using ultrasonic instrument. The results showed certain deviations in the working-fluid flow reaching ± 60 % of the nominal value [1]. Besides the problem with the provision of a balanced working-fluid flow, the evaporator working conditions were worsened due to a lack of heat-protection material in some parts of the evaporator, especially at the ceiling of the flame

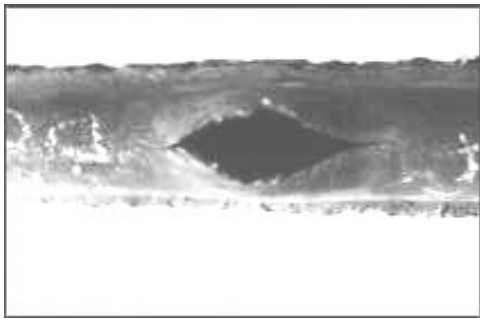

Sl. 1. *Poškodovana cev*
Fig. 1. *Damaged tube*

Slika 1 prikazuje poškodbo cevi, nastalo v območju najvišjih temperatur zaradi zaustavitve pretoka delovne tekočine. Delovna tekočina je demineralizirana voda, ki vstopa v uparjalnik v stanju nasičene kapljevine. Vzdolž cevi se stanje tekočine nadalje spreminja prek stanja mokre pare v nasičeno paro.

Postopek uparjanja vode v uparjalniku parnega kotla je urejen tako, da je nasičena voda gnana iz rezervoarja uparjalnika skozi cevi uparjalnika v uravnovešenem toku. Nadaljnje gretje v uparjalniku vodi v postopno uparjanje nasičene vode, dokler se v celoti ne upari v nasičeno paro. Točka celotne preobrazbe iz kapljevite v parno fazo se imenuje kritična točka in je za ta uparjalnik približno 18 metrov. Tipično za to območje je nenadno povišanje temperature stene, kateremu sledi postopno povišanje temperature v smeri toka pare. Hkrati pade vrednost koeficienta prenosa toplote na strani delovne tekočine. Območje intenzivnega uparjanja nasičene vode, to je območje mokre pare, ima značilno visoko vrednost koeficienta prenosa toplote na strani delovne tekočine, to je 10 kW/m^{2}K [2].

Teoretično (v ustaljenem stanju) kritična točka vedno zavzame isto vrednost. V resničnih razmerah v elektrarni se kritična točka premika. Če pomični gradient ni prevelik, je pričakovati, da toplotne napetosti, povzročene s tem pomikanjem, niso nad dovoljeno mejo.

Premik kritične točke navzgor ali navzdol lahko povzročijo različni razlogi. Za primer: upočasnitev pare delovne tekočine skozi cevi uparjalnika vodijo k znižanju kritične točke proti dnu kurišča kotla. Do izredne situacije pride v primeru celotne in trenutne ustavitve toka pare delovne tekočine v cevi, ko kapljevina delovne tekočine uparja zelo hitro. To je napovedano stanje v numerični simulaciji.

1 MATEMATIČNI MODEL

1.1 Vodilne enačbe

Glede na zgoraj navedeno je uporabljen dvorazsežni napetostni postopek. V vodilnih enačbah

chamber. Figure 1 illustrates the tube damage that occurred in the maximum temperature zone as a consequence of a cut in working-fluid flow. The working fluid is a decarbonized water, which enters the evaporator in the state of a saturated liquid. Along the tube this state is subsequently followed by the states of wet and then saturated steam.

The process of water evaporation in the steam-boiler evaporator is thus organized so that saturated water is forced from the steam drum through the tubes in a balanced flow. Further heating in the evaporator leads to gradual evaporation of the saturated water until it completely evaporates into saturated steam. The point of complete transformation from the liquid phase to the gas phase is the so-called critical point, and for this boiler it is above 18 meters. Typical for this area is a sudden increase in tube-wall temperature, which is then followed by a gradual temperature increase in the steam flow direction. At the same time, the heat-transfer coefficient decreases on the working-fluid side. The area of intensive evaporation of saturated water, i.e., the wet steam zone, has a significantly high heat transfer coefficient on the working fluid side e.g., 10 kW/m^{2}K [2].

Theoretically (in the steady state), the critical point always takes the same position. However, in real plant conditions the critical point is movable. If the moving gradient is not too large, it can be expected that the thermal stresses caused by this movement are not above the allowed limit.

Different reasons can lead to displacement of the critical point upwards or downwards. For example, a slow down of the working-fluid stream through the evaporator pipes leads to a lowering of the critical point towards the boiler flame chamber bottom. An extreme situation occurrs in the case of a complete and immediate interuption of the working-fluid stream in the pipe when the total liquid working fluid evaporates very quickly. This is an anticipated situation in the numerical simulation.

1 MATHEMATICAL MODEL

1.1 Governing equations

Based on the above, the 2D strain concept was adopted. In the governing equations of linear

gibalne količine in ohranitve energije so zanemarjene prostorninske sile in deformacijsko delo. Tako imajo enačbe v dvorazsežnem kartezijevem koordinatnem sistemu obliko:

momentum and energy conservation the volume forces and the deformation work were neglected. Thus, in the Cartesian 2D coordinate system the equations are:

$$\frac{\partial}{\partial\tau}\int_V \rho\frac{\partial u}{\partial\tau}dV = \int_S \left\{\left[2\mu\frac{\partial u}{\partial x}+\lambda\left(\frac{\partial u}{\partial x}+\frac{\partial v}{\partial y}\right)-3\ K\ \beta\ \Delta T\right]n_x+\mu\left(\frac{\partial u}{\partial y}+\frac{\partial v}{\partial x}\right)n_y\right\}dS \quad (1)$$

$$\frac{\partial}{\partial\tau}\int_V \rho\frac{\partial v}{\partial\tau}dV = \int_S \left\{\mu\left(\frac{\partial v}{\partial x}+\frac{\partial u}{\partial y}\right)n_x+\left[2\mu\frac{\partial v}{\partial y}+\lambda\left(\frac{\partial u}{\partial x}+\frac{\partial v}{\partial y}\right)-3\ K\ \beta\ \Delta T\right]n_y\right\}dS \quad (2)$$

$$\frac{\partial}{\partial\tau}\int_V \rho\ c_p\ T\ dV = \int_S (k\frac{\partial T}{\partial x}n_x + k\frac{\partial T}{\partial y}n_y)\ dS \quad (3),$$

kjer so: V – prostornina, S – robna površina, n_x in n_y – normalni vektorji katezijevih komponent, λ in μ - Lamejevi konstanti, K - elastični modul (λ, μ in K so definirani v viru [3]), c_p – specifična toplota, k – toplotna prevodnost in β - prostorska toplotna razteznost. Prostorski koordinati x in y, kakor tudi čas t so neodvisne spremenljivke, medtem ko so u, v in T odvisne spremenljivke, ki pomenijo kartezijeve komponente pomika (u, v) in temperaturo (T).

where V is volume, S is the system boundary area, n_x and n_y are the Cartesian normal vector components, λ and μ are Lame's constants, K is the elasticity module (λ, μ and K are defined in reference [3]), c_p is the specific heat, k is the thermal conductivity and β is the coefficient of linear thermal expansion. The space coordinates, x and y, as well as the time τ are independent variables, whereas u, v and T are dependent variables representing Cartesian displacement components (u, v) and temperature (T) respectively.

1.2 Robni pogoji

Z namenom podaje popolne matematične razlage problema, so podani Neumannovi robni pogoji za enačbo gibalne količine na robnem območju, podane so sile, kakor je prikazano spodaj:

1.2 Boundary conditions

In order to give a full mathematical explanation of the problem, boundary conditions of the Neumann type were given to the linear momentum equation at the boundary domain, i.e., the forces were given as shown below:

$$\int_S \mathbf{N}\cdot\mathbf{n}\ \ dS = \int_S \mathbf{f}\ \ dS \quad (4),$$

kjer so: **N** – napetostni tenzor, **n** – vektor v smeri normale, **f** – podan vektor sil na robu S.

Robni pogoji druge in tretje vrste so prav tako uporabljeni v primeru energijske enačbe:

where **N** is the stress tensor, **n** is the normal vector, and **f** is the given force vector on the boundary S.

Boundary conditions of the second and third kind were also used in the case of the energy equation

$$q = -k\frac{\partial T}{\partial n}\ \text{na/on}\ \ S_1 \quad (5)$$

$$k\frac{\partial T}{\partial n} = -\alpha\left(T - T_f\right)\ \text{na/on}\ \ S_2 \quad (6),$$

kjer je q znana vrednost toplotnega toka na delu roba S_1 medtem, ko so na delu roba S_2 podane vrednosti: α – toplotna prestopnost na strani delovne tekočine, T – temperatura stene, T_f – povprečna temperatura delovne tekočine, ki pomeni temperaturo nasičene vode. Prav tako je treba navesti, da je $S=S_1\cup S_2$.

where q is the heat flux value known in the part of the S_1 boundary, whereas the values known in the part of the S_2 boundary are as follows: α is the average convection heat-transfer coefficient on the side of the working fluid, T is the wall temperature, T_f is the the working-fluid average temperature, which, in fact, represents the temperature of the saturated water. Also, it is necessary to note that $S=S_1\cup S_2$.

2 NUMERIČNI IZRAČUNI

2.1 Definiranje računskega območja

Računsko območje (sl. 2) je razdeljeno na 3976 nadzornih prostornin. Za diskretizacijo območja

2 NUMERICAL CALCULATIONS

2.1 Definition of the calculation domain

The calculation domain (shown in Figure 2) was divided in 3976 control volumes. An unstructured

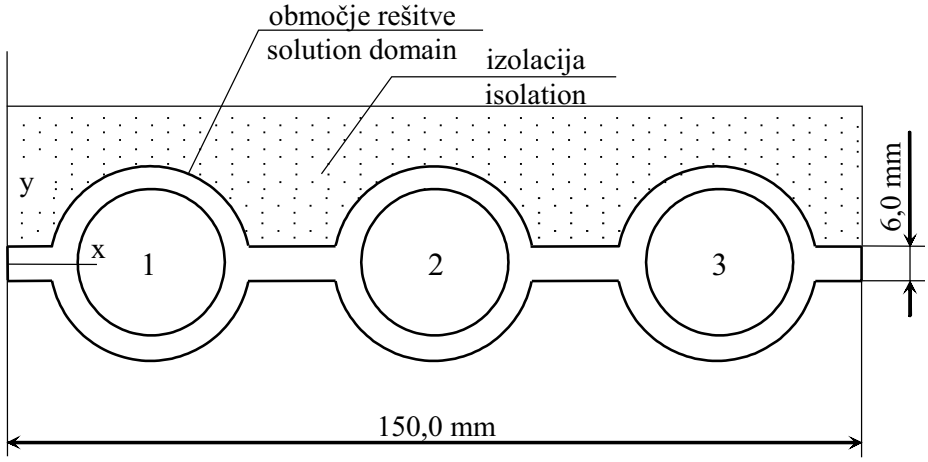

Sl. 2. *Geometrijska oblika računskega območja (notranji premer cevi je 25 mm)*
Fig. 2. *Calculation domain geometry (inner diameter of the tube is 25 mm)*

Preglednica 1. *Snovske lastnosti materiala (15Mo3)*
Table 1. *Physical characteristics of material (15Mo3)*

ρ [kg/m^3]	c_p [J/kgK]	k [W/mK]	β [1/K]	ν -	E [Pa]	σ_g [Pa]
7749	574	40,697	$1{,}3469\cdot10^{-5}$	0,3	$1{,}7163\cdot10^{11}$	$1{,}7163\cdot10^{8}$

je uporabljena nestrukturirana mreža. Opravljena je vozliščna analiza, katere rezultati so prikazani v viru [6]. Izračun je izpeljan na mreži, ki je nekoliko ustreznejša za zagotovitev zahtevane natančnosti spremenljivk *u*, *v* in *T.* Fizikalne lastnosti materiala 15Mo3 (podane v preglednici 1) so vzete za temperaturo 673 K in so štete kot nespremenljive med izračunom. Vrednosti ν, E , σ_g so Poissonov koeficient, Youngov modul elastičnosti, meja elastičnosti.

Za obravnavani problem je uporabljena metoda nadzornih prostornin. Poleg klasičnega numeričnega postopka s programskim orodjem COMET [4] je uporabljena večmrežna tehnika za pospešitev konvergence in za ta namen je ustvarjena preprosta mreža.

2.2 Opis robnih pogojev

Tlak v cevi je bil 18,8 MPa, medtem ko preostali robovi območja niso bili obremenjeni s silo. Tu so različni referenčni podatki za koeficient prenosa toplote za uparjanje vode v navpičnih ceveh, kjer so vrednosti v območju 5 do 29 kW/m^{2}K. Za obravnavani parni kotel je koeficient v mejah od 5 do 10 kW/m^{2}K. V tem delu je vzet koeficient prenosa toplote 7 kW/m^{2}K, z ustrezno temperaturo nasičenosti vode 633 K. Na strani dimnih plinov je podan konstanten toplotni tok 211 kW/m^2, katerega vrednost je dobljena s preizkusom v območju uparjanja vode [5]. Zunanja stena stenskega uparjalnika je obravnavana kot idealno

grid was used for the space discretisation. A grid-independence test was carried out and shown in reference [6]. This calculation used a grid that was somewhat more than necessary for the requested accurateness of the variables *u*, *v* and *T.* The physical properties of the 15Mo3 material (given in Table 1) are determined for 673 K and considered constant during the calculation. The values ν, E and σ_g are Poisson's coefficient, Young's module of elasticity and elasticity limit stress, respectively.

The finite-volume method was applied to the considered problem. Besides a standard numerical proceeding integrated in the COMET software [4], there was also a multigrid technique of accelerating convergence and, for that purpose, two coarse grids were generated.

1.2 Description of boundary conditions

The pressure within the tube was 18.8 MPa, whereas the other boundaries of the domain were free of forces. There are various reference data for the heat-transfer coefficient of water evaporation in vertical tubes, the values of which range from 5 to 29 kW/m^2·K. For this particular steam boiler the coefficient ranges from 5 to 10 kW/m^2·K. In this paper, the adopted heat-transfer coefficient is 7 kW/m^2·K, with a corresponding water-saturation temperature of 633 K. On the flue-gas side a constant heat flux of 211 kW/m^2 was given, and its value was found by an experiment in the water-evaporation zone [5]. The external wall of the wall evaporator is considered as

izolirana. Začetno polje odvisnih spremenljivk *u, v* in *T* je računano za ustaljeno stanje in prej omenjene robne pogoje [6].

V začetnem trenutku $\tau_0 = 0$ sekund je podan robni pogoj $q = 0$ kW/m^2 na notranji strani cevi 2 računskega območja, prikazanega na sliki 2. Preostali robni pogoji se niso spreminjali med izračunom. Testni izračun je pokazal, da se pomembni dogodki pojavijo med prvimi desetimi sekundami, medtem ko je dosežen ustaljen koeficient prenosa toplote po 600 sekundah.

Upoštevajoč navedeno dejstvo je izbran časovni korak $\delta\tau = 1$ sekund za prvih deset sekund izračuna. Za nadaljnjih petdeset sekund je uporabljen časovni korak $\delta\tau = 5$ s. Koraki $\delta\tau = 10$ sekund in $\delta\tau = 20$ sekund so uporabljeni do poteka opazovanega časovnega obdobja. Izračun prenosa toplote je opravljen do poteka opazovanega časa ob predpostavki, da območje ne dopušča deformacij, ki bi lahko privedle do spremembe oblike ali celo do razpoke. Napetost je računana oziroma obravnavana samo do trenutka, ko je najvišja ustrezna napetost v območju višja od napetosti materialove meje elastičnosti.

2.3 Rezultati izračunov

Iz rezultatov izračuna je mogoče dobiti veliko pomembnih informacij. Najzanimivejši so: temperatura v območju v posameznih časih, čas za dosego ustaljenega stanja prenosa toplote in čas za dosego elastične meje napetosti. Kot primer je na sliki 3 prikazano temperaturno polje v območju v začetnem času, po 6 sekundah in po 600 sekundah.

Očitno je (sl. 3), da po 600 sekundah začetni robni pogoj $q = 0$ kW/m^2 privede začetno ustaljeno polje v novo ustaljeno stanje. To ima za posledico postopek prenosa toplote na sosednje cevi skozi povezujoče membranske plošče. Najvišja temperatura v materialu cevi po 600 sekundah je 1593 K, kar je pod tališčem (1809 K). Potrebna hitrost lokalnega gretja materiala je lahko ponazorjena s temperaturno spremembo v odvisnosti od časa v robnem vozlišču, ležečem na zunanjem premeru cevi 2 (sl. 4a). Razvidno je, da je ustaljeno stanje skoraj doseženo po 600 sekundah.

Po drugi strani je dejanska napetost računana na temelju Misesove hipoteze ob uporabi vrednosti prej izračunanih glavnih napetosti. Časovna sprememba dejanske napetosti je prikazana na sliki 4b. Ta sprememba se prav tako nanaša na robno vozlišče, ležeče na zunanjem premeru cevi 2. Preglednica v diagramu podaja računane dejanske napetosti v MPa in kaže, da je elastična meja napetosti dosežena po 6 sekundah.

Slika 5 prikazuje porazdelitev normalnih napetosti v ceveh (po šestih sekundah), ki s strižnimi napetostmi določajo napetostno stanje v območju.

ideally insulated. The initial field of dependent variables *u, v* and *T* was calculated for the stationary state and the previously mentioned boundary conditions [6].

In the initial moment $\tau_0 = 0$ sec., a boundary condition $q = 0$ kW/m^2 was set within the tube No.2 of the calculation domain, shown in Figure 2. The other boundary conditions remained unchanged during the calculation. The testing calculations showed that important events occur in the first 10 sec., whereas stationary heat transfer is achieved after 600 sec.

Based on this fact, the time interval $\delta\tau = 1$ sec. was chosen in the first 10 sec. In the next 50 sec. the interval was $\delta\tau = 5$ sec. Intervals $\delta\tau = 10$ sec. and $\delta\tau = 20$ sec. were used until the end of the observed time interval. The heat-transfer calculation was carried out until the end of the observed time interval, providing the domain has not suffered deformations that would cause a change of shape – or even cracking. The stresses were only calculated or considered until the moment when a maximum equivalent stress appearing in the domain is somewhat above the stress on the material elasticity limit.

2.3 Results of calculations

It is possible to get a lot of important information from the calculation results. The most interesting results are the temperature within the domain at particular time points, the time period to reach the heat-transfer stationary state, and the time period to reach the stress on the elasticity limit. Thus, for example, Figure 3 shows the temperature fields in the domain at the initial moment, after 6 sec., and after 600 sec.

It is obvious (Figure 3) that after 600 sec. the initial boundary condition $q = 0$ kW/m^2 brings the stationary temperature field into a new stationary state. This results in a heat-transfer process carried out by conduction towards neighbouring tubes through connecting membrane plates. The maximum temperature of the tube material after 600 sec. is 1593 K, which is below the melting temperature of iron (1809 K). The velocity needed for local heating of the material can be illustrated by the temperature change over time at the boundary node located on the external diameter of tube No.2 (see Figure 4a). It is clear that the stationary state is almost reached after 600 sec.

On the other hand, the effective stress was calculated on the basis of Mises's hypothesis, using the values of previously calculated main stresses. The change of effective stress over time is shown in Figure 4b. This change also refers to the boundary node located on the external diameter of tube No. 2. The table within the diagram gives the calculated effective stresses in MPa, and shows that the elasticity limit stress is reached after 6 sec.

Figure 5 shows the distribution of normal stresses in the tubes (after six seconds), which together with the shear stresses define the stress

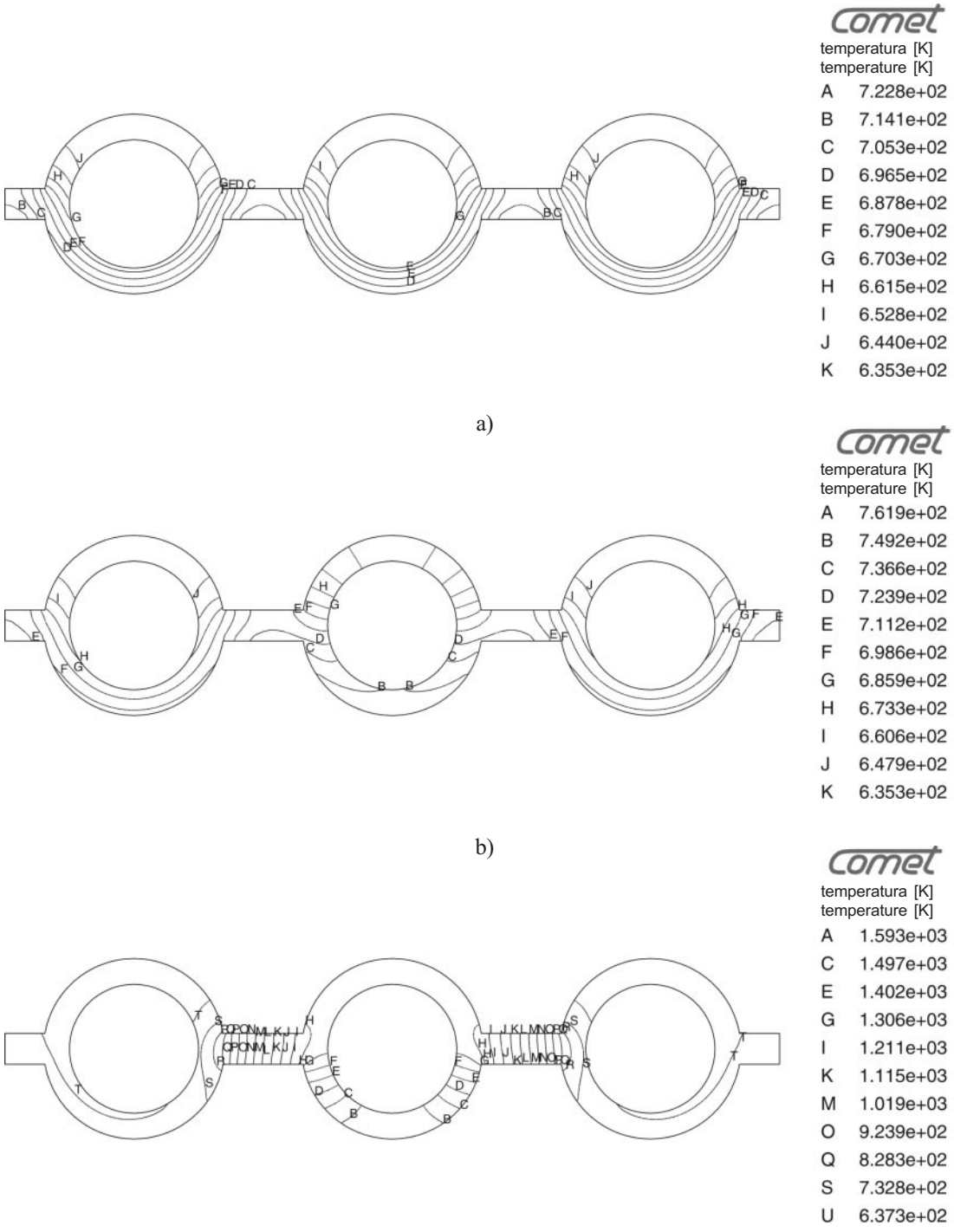

Sl. 3. *Temperaturno polje za: a) τ =0 sekund, b) τ =6 sekund in c) τ =600 sekund*
Fig. 3. *Temperature field for: a) τ =0 sec, b) τ =6 sec and c) τ =600 sec*

Kakor je razvidno, je najvišja vrednost vzdolžnih napetosti (S_{zz}) -197 MPa v robnem vozlišču, postavljenem na zunanjem premeru cevi št. 2. V tem vozlišču ima prav tako najvišjo vrednost dejanska napetost. Normalna napetost (S_{yy}) 113 MPa ima prav tako znatno visoko vrednost vzdolž stene notranje cevi nasproti zvarjene membranske plošče.

state in the domain. As we can see, the maximum value of the axial stress (S_{zz}) is -197 MPa at the boundary node located on the external diameter of tube No. 2. At this point the effective stress also has its maximum value. The normal stress (S_{yy}) of 113 MPa also assumes a very high value along the internal tube wall, opposite to the welded membrane plate.

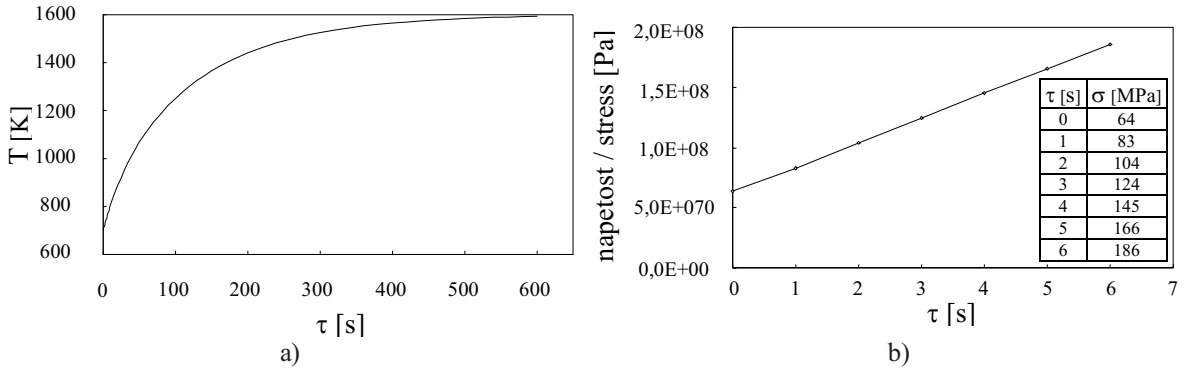

τ [s]	σ [MPa]
0	64
1	83
2	104
3	124
4	145
5	166
6	186

Sl. 4. *a) – Temperaturna sprememba v vozlišču, ležečem na zunanjem premeru zamašene cevi, b) – vrednost primerjalne napetosti med prvimi 6 sekundami*

Fig. 4. a) - *Temperature change at the boundary node located on the external diameter of the blocked tube, b) - Equivalent stress values within the first 6 sec*

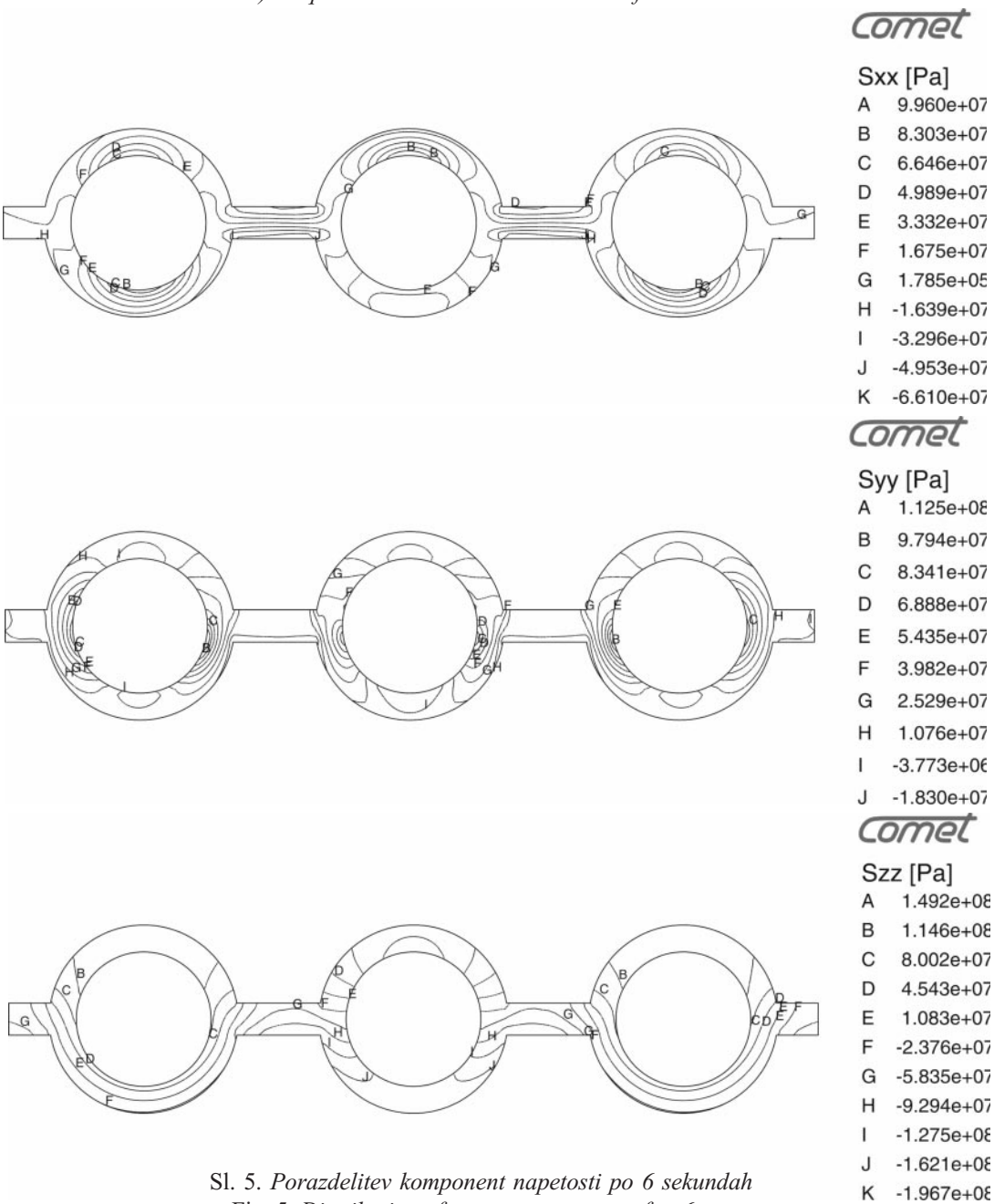

Sl. 5. *Porazdelitev komponent napetosti po 6 sekundah*

Fig. 5. *Distribution of stress components after 6 sec*

3 SKLEP

Numerični izračuni kažejo, da je modeliran pojav zelo hiter. Upoštevajoč, da nimamo možnosti za avtomatično intervencijo, pojava ne moremo pravočasno preprečiti. Pojav ima za posledico razpoko cevi, ustavitev delovanja parnega kotla in zato celotne termoelektrarne.

Numerični izračuni ponujajo številne pomembne parametre, ki določajo dogodek. Ti parametri so: stanje prehodne periode ustaljenega prehoda, najvišja temperatura materiala v razpočeni cevi in čas dosega elastičnih mejnih napetosti. Numerični model je lahko na splošno uporabljen za analize s podobnimi pojavi v proizvodnem postopku.

Med remontom termoelektrarne je pogosta praksa (in prav tako potreba) najetje inštitucij, ki se ukvarjajo s preiskavo materialov. Vsekakor je po zgoraj navedenih dogodkih preiskava vedno obvezna.

Nazadnje je jasno, da informacije o vrednostih in porazdelitvah temperatur in napetosti v materialu omogočajo boljšo diagnostiko posameznega primera. V nasprotju z drugimi metodami zagotavljajo numerični izračuni več informacij ob manjšem trudu ob uporabi sodobnih numeričnih algoritmov in programov, pri čemer ni nujno potrebno uporabiti hitrih računalnikov. Kot primer je izračun v tem delu opravljen z osebnim računalnikom s hitrostjo 233 MHz. V prihodnosti bo razvoj modela najverjetneje usmerjen v numerično modeliranje termoplastičnosti, gibajoče mreže itn.

3 CONCLUSIONS

Numerical calculations show that the modelled process is very fast. Bearing in mind that there is no possibility of automatic intervention, the process cannot be prevented in time. This results in the tube cracking, shutting down of the steam boiler, and, as a result, of the whole of the thermal power plant.

A numerical calculation offers a number of important parameters that determine such an occurrence. These parameters are as follows: the state transition period, the maximum temperature of the material in the broken tube and the time to reach the elasticity limit stress. The numerical model can be widely applied in the analyses of similar occurrences in production processes.

During the periods of thermal power plant overhauls, there is a need to involve institutions dealing with material examination. Indeed, such examinations are obligatory after the above-mentioned occurrences.

Finally, it is clear that information on values and on the distribution of temperatures and stresses in a material enables a better diagnosis of a particular problem. As opposed to other methods, the numerical calculation provides more information for less effort by using modern numerical algorithms and software, but does not necessarily require fast computers. For example, the calculation in this paper was carried out using a PC with a 233-MHz processor. In the future, the development of the model would most probably go in the direction of numerical modelling of themoplasticity, moving grids, etc.

4 LITERATURA
4 REFERENCES

[1] TE Kakanj (1980) Projektna i pogonska dokumentacija.

[2] Stošić, N. (1987) Kotlovi, Mašinski fakultet, Sarajevo.

[3] Demirdžić, I., A. Ivanković (1998) Lecture notes for the course Finite Volume Stress Analysis, *Imperial College*, London.

[4] COMET (1998), User manual, *ICCM*, Hamburg.

[5] Radovanović, P. (1989) Utvrđivanje realnih radnih uslova i njihov uticaj na radni vijek metala pregrijačkog sistema a posebno na radni vijek membranskih zidova drugog promajnog cuga kotla 230 MW TE Kakanj, *Institut za nuklearne nauke "Boris Kidrič"*, Beograd.

[6] Neimarlija, N. (1999) Analiza temperaturnih polja i termalnih napona na karakterističnim vezama dva ili više zidnih pregrijača pare u kotlovima membranskog tipa, magistarski rad, *Mašinski fakultet u Sarajevu*.

Naslova avtorjev: mag. Namir Neimarlija
Termoelektrana Kakanj-Ćatići
72240 Kakanj, BiH
nnamir@bih.net.ba

prof.dr. Nagib Neimarlija
Mašinski fakultet u Zenici
Ul. Fakultetska 1
72000 Zenica, BiH
nagibn@mf-ze.unsa.ba

Author's Addresses: Mag. Namir Neimarlija
Termoelektrana Kakanj-Ćatići
72240 Kakanj, BiH
nnamir@bih.net.ba

Prof.Dr. Nagib Neimarlija
Faculty of Mechanical Eng. Zenica
Ul. Fakultetska 1
72000 Zenica, BiH
nagibn@mf-ze.unsa.ba

Prejeto: 16.4.2004
Received:

Sprejeto: 2.12.2004
Accepted:

Odprto za diskusijo: 1 leto
Open for discussion: 1 year

Osebne vesti
Personal Events

Prof. dr. Matija Tuma, ob odhodu v pokoj

17.7. 1938 se je rodil deček, ki so mu dali ime Matija. Ko je dovolj zrasel, je šel v osnovno šolo, potem v klasično gimnazijo, kjer je leta 1956 maturiral in se nato vpisal na Fakulteto za strojništvo v Ljubljani. Že med študijem ga je mikalo področje energijskih pretvorb in termodinamike, zato si je za mentorja pri diplomskem delu izbral prof. Ranta. Leta 1962 je diplomiral, iz razširjene diplome pa je leta 1964 v Strojniškem vestniku objavil svoj prvi članek o vplivu na temperature predgretega zraka in vrste goriva na eksergijski izkoristek parnih kotlov. Kot mlad diplomirani inženir strojništva se je po služenju vojske zaposlil v tovarni Rog in tu oral ledino na področju konstruiranja transportnih naprav v proizvodnji. 1966 se je z ženo in malim sinom preselil v Švico, kjer je bil v firmi Brown Boveri v Badnu do 1973 leta zaposlen kot projektant v oddelku za velike parne turbine. Svojo kariero v tem koncernu je končal kot vodja skupine za tehniko postrojenj. V tistem času so v Sloveniji gradili JE Krško, zato se je želel vrniti domov in sodelovati pri izgradnji. Krška jedrska elektrarna je njegovo prošnjo za zaposlitev zavrnila. Zanj je bila to sreča v nesreči saj je zaradi zavrnitve odšel v službo na Švicarsko tehniško visoko šolo, ETH v Zürichu v ustanovo, ki se ponaša s 14 Nobelovimi nagrajenci. Tu je delal kot višji asistent in kljub pedagoškim obveznostim v petih letih doktoriral s področja termodinamike in prenosa toplote.

V Švici se je družil z slovenskimi izseljenci. Skupaj so ustanovili fundacijo "Pro cultura slovenica". Matija je fundaciji dal ime in napisal pravila v skladu s švicarskimi zakoni. Fundacija, ki finančno podpira šolanje zamejskih Slovencev v materinem jeziku, obstoja še danes. V tistem času je dejavno spremljal dogajanja med Slovenci v Avstriji, Italiji in na Madžarskem ter v bran rojakov pisal članke v zamejske, slovenske in švicarske časopise. Bil je med ustanovitelji slovenskega dopolnilnega pouka za otroke v Zürichu. Zanimivo je, da je njegova žena prevzela pouk slovenskih otrok - ob sredah popoldne, ko švicarske šole nimajo pouka.

Rad je hodil v hribe. Ljubezen do planin je podedoval po svojem starem očetu dr.Henriku Tumi, znanem gorniku, zavednem Slovencu in buditelju narodne zavesti. Bil jo zelo povezan z dejavnostjo slovenskega izseljeniškega planinskega društva Triglav. Povzpel se je na 19 štiritisočakov, tudi na Mont Blanc, Monte Roso in Matterhorn. Nekatere vzpone je opisal in svoja doživetja objavil v Planinskem vestniku v člankih Kako me je osvojil štiritisočak in Grozo izzivam, v dušo jo vabim. Zanimivi so tudi njegovi članki z opisi gora, ki nosijo enako ime kot je njegov priimek. To je gora Piz Tuma v Švici in Torre Tuma v Argentini, ki je dobila ime po njegovem starem očetu.

V Švici se je zakoncema Tuma rodil še en sin. Bolj, ko sta sinova odraščala, bolj ga je obhajal dvom ali ostati v Švici ali oditi domov in omogočiti, da otroci ostanejo Slovenci. Z ženo sta se odločila, da se vrnejo v domovino. Povratek ni bil lahek. Zopet se je domovina obnašala mačehovsko. Zaman je oddal 26 vlog za službo. V nekaterih vlogah celo ni upal napisati, da je doktor znanosti. Končno je dobil zaposlitev v tovarni Lek na časopisni oglas, Potrebe po delavcih, s katerim so iskali primernega brezposelnega tehnologa.

Konec leta 1982 se je Matija predvsem iz družinskih razlogov odločil, da se ustali. Zaposlil se je kot izredni profesor na Fakulteti za strojništvo, kjer je že honorano predaval nekatere predmete s področja energetike. S svojim delom je pomembno zaznamoval razvoj Katedre za energetsko strojništvo, Fakultete za strojništvo in celotne energetike v Sloveniji. Leta 1986 je postal predstojnik Katedre za energetsko strojništvo in to, s kratkimi presledki, ostal vse do upokojitve. Leta 1993 je bil izvoljen v naziv redni profesor. Bil je dekan fakultete od leta 1995 do leta 1997. Leta 1994 je postal član Sveta za visoko šolstvo vlade Republike Slovenije, 1995 nacionalni koordinator za področje Energetika pri ministrstvu za znanost in tehnologijo in leta 2000 član Sveta za znanost in tehnologijo Republike Slovenije. Bil je član nadzornih svetov v več podjetjih in v tujini tudi član Znanstvenega sosveta VGB, Nemčija. Upokojil se je 30.9.2004 po skoraj dvaištiridesetih letih delovne dobe.

Kljub številnim odgovornim zadolžitvam je Matija bogato prispeval na pedagoškem, raziskovalnem in strokovnem področju energetskega strojništva. Njegovi sodelavci smo občudovali njegovo predanost, saj delovnega časa sploh ni poznal. Predaval je na diplomskem in podiplomskem

študiju, bil je mentor šestim doktorjem, trinajstim magistrom in sedeminosemdesetim diplomantom.Dva njegova kandidata sta dobila Prešernovo nagrado. Spisal je dva univerzitetna učbenika, ki sta izšla v več izdajah. Širše področje njegovega raziskovalnega in strokovnega dela bi lahko zaobsegli z izrazom premene energij, posebej pa bi morali poudariti klasične in jedrske elektrarne, plinske in parne turbine ter smotrno rabo energije v industriji. Objavil je petinpetdeset znanstvenih člankov, od tega petintrideset v tujih revijah in štiriindvajset v revijah s količnikom vplivnosti po SCI, veliko število strokovnih člankov, ter znanstvenih in strokovnih referatov, do upokojitve skupaj stoosemnajst člankov in referatov.

Obseg Matijevega strokovnega dela je izjemen. Sodeloval je z vsemi slovenskimi termoelektrarnami, s številnimi podjetji, ki imajo energetsko intenzivno proizvodnjo ter z vladnimi inštitucijami. Njegovo delo na strokovnem področju obsega stooseminsedemdeset poročil.

V COBISS-u izkazuje skupaj petstoštirideset enot, med katerimi je, razen že naštetih del, tudi preko petdeset poljudnih člankov, več intervjujev, polemike, itn.

Sodelavci smo ga osebno, kot človeka, doživljali predvsem kot vodjo Laboratorija za termoenergetiko, predstojnika Katedre za energetsko strojništvo in vodjo raziskovalne skupine. Njegov prirojeni čut za sodelovanje in pravičnost je omogočal ustvarjalno klimo v skupinah, ki jih je vodil, pri tem pa je bilo vedno dovolj prostora, da smo se vsi podrejeni sodelavci lahko uveljavljali v okviru svojih sposobnosti. Ko je leta 1986 prevzel predstojništvo katedre, so bili na katedri štirje doktorji znanosti, ob njegovem odhodu v pokoj jih je enajst, od tega sedem visokošolskih učiteljev. Na izrazito človeško plat vodenja in uveljavljeno ustvarjalno klimo v skupini kaže tudi dejstvo, da v praktično dvajsetih letih njegovega vodenja katedre niti enkrat ni prišlo do osebnih trenj ali napetosti med člani. Kot vodja raziskovalne skupine je omogočil v skupini oblikovati okolje nadpovprečne ustvarjalnosti, saj je tudi Ministrstvo za šolstvo znanost in šport ocenilo delo programske skupine, ki jo je vodil, kot nadpovprečno dobro, kar je zagotovilo financiranje v naslednjem obdobju.

Vsi njegovi sodelavci želimo, da bi se kljub upokojitvi Matija čim večkrat vračal na fakulteto, da bi z nami še naprej sodeloval in nam pomagal s svojimi nasveti in izkušnjami. Predvsem pa Matiji želimo, da bi v upokojitvi našel nove cilje in izzive, ter jih koristno uporabil v svoje zadovoljstvo. Naj se skupaj velikokrat nasmejemo pomenu misli, ki jo je sam večkrat hudomušno izrekel: ni toliko bistvena velikost pokojnine, bolj bistveno je, kolikokrat jo dobiš.

prof.dr. Janez Oman

Prešernove nagrade za leto 2004

UNIVERZITETNA PREŠERNOVA NAGRADA
Marko Thaler

Naslov dela: Napoved energije v daljinskih energetskih sistemih
Mentor: prof.dr. Alojz Poredoš
Somentor: akad.prof.dr. Igor Grabec

Marko Thaler se je rodil leta 1981 v Ljubljani. Kot Zoisov štipendist je po končani Srednji šoli za strojništvo Ljubljana, nadaljeval izobraževanje na univerzitetnem študijskem programu Fakultete za strojništvo. V zadnjem letniku dodiplomskega študija je pričel z razvojem lastnega programskega paketa za napovedovanje rabe energije in optimalno krmiljenje daljinskih energetskih sistemov, imenovanega INTELPRED, ki je bil na strokovnih konferencah, tako doma kot v tujini, sprejet z velikim zanimanjem energetske stroke. Za svoje študijske dosežke je kot najboljši študent prejel številna priznanja. Svojo študijsko pot sedaj nadaljuje kot mladi raziskovalec na podiplomskem študiju Fakultete za strojništvo, Univerze v Ljubljani.

Nagrajena naloga, izdelana pod mentorstvom prof.dr. Alojza Poredoša in akad. prof.dr. Igorja Grabca, obravnava problem napovedovanja časovnih vrst rabe energije v daljinskih energetskih sistemih in možno rešitev z uporabo lastno razvitega empiričnega modela napovedovanja. Zasnova modela je podobna simuliranim nevronskim mrežam. Model omogoča napoved rabe energije na osnovi samoorganizacije podatkov o preteklem delovanju sistema in predvidenih prihodnjih vrednostih nekaterih spremenljivk postopkov. Pri tem nudi osnovo za optimalno krmiljenje daljinskih energetskih sistemov, preko analize ekonomskega tveganja.

1. FAKULTETNA NAGRADA
Uroš Rosa

Tema: Razvoj šasije športnega vozila
Mentor: doc.dr. Marko Nagode
Somentor: prof.dr. Matija Fajdiga

Uroš Rosa se je rodil 16. decembra 1978 v Kopru. Po končani osnovni šoli se je vpisal na Gimnazijo Koper, ki jo je s prav dobrim uspehom končal leta 1997. Sledil je vpis na Fakulteto za strojništvo v Ljubljani. V tretjem letniku je izbral smer Konstruuiranje in gradnja strojev – modul vozila. V času

srednješolskega in univerzitetnega izobraževanja je bil Zoisov štipendist, poleg tega pa je opravljal različna dela od pomoči v proizvodnji in sodelovanja pri izdelavi orodij za vakuumiranje plastike, do poučevanja računalniškega risanja, anketiranja in tržnih raziskav. Pomemben mejnik v času študija predstavlja projekt "Student roadster"; to je projekt izdelave prototipnega športnega avtomobila na osnovi Peugeot 406. Kot ustanovni član je na projektu že od začetka zadolžen za obliko vozila in konstrukcijo šasije.

Oktobra leta 2003 se je kot mladi raziskovalec zaposlil na Fakulteti za strojništvo v Ljubljani in pod mentorstvom prof.dr. Matije Fajdiga vpisal podiplomski študij. V Laboratoriju za vrednotenje konstrukcij raziskovalno dela na področju metod vrednotenja konstrukcij in skrbi za nadaljevanje in uspešno zaključitev projekta "Student roadster".

V delu je predstavljen celovit razvoj šasije športnega avtomobila "Student roadster". Uroš Rosa je na osnovi izčrpnega pregleda ECE priporočil in raziskave obstoječih zamisli športnih vozil najprej določil tehnične in ekonomske kriterije za vrednotenje šasije. Upošteval je tudi omejitve zaradi uporabe nekaterih sklopov vozila Peugeot 406 v novem vozilu. V delu je zasnoval in optimiral obliko vozila, ergonomijo potniškega prostora, dovoljeno torzijsko togost, največjo upogibno deformacijo in faktor učinkovitosti lahkosti gradnje do te mere, da nova šasija po izpolnjevanju kriterijev celo presega lastnosti nekaterih avtomobilov srednjega cenovnega razreda. Zaradi omejitev maloserijske gradnje in uporabe cenenih jeklenih profilov predstavlja delo pomemben dosežek. Iz opravljenega dela je objavil dva znanstvena prispevka na konferenci IAT'03, na Fakulteti za strojništvo je bila organizirana odmevna predstavitev projekta in razstava, projekt pa je bil deležen tudi velike medijske pozornosti in pozornosti študentov. Uroš Rosa je s svojo zavzetostjo, smislom za skupinsko in raziskovalno delo ter prenašanjem znanja na mlajše študente odločilno prispeval k razvoju smelo zastavljenega projekta.

2. FAKULTETNA NAGRADA
Jure Smrekar

Naslov: Neželjeni dinamični pojavi v hladilnem stolpu in njihov vpliv na kvaliteto obratovanja termoelektrarne
Mentor: izr.prof.dr. Janez Oman
Somentor: izr.prof.dr. Brane Širok

Jure Smrekar je bil rojen 9. aprila 1980. leta v Ljubljani. Obiskoval je osnovno šolo Adolfa Jakhla v Zalogu po kateri se je leta 1995 vpisal na Gimnazijo Ledina. V času obiskovanja osnovne in srednje šole je intenzivno treniral namizni tenis v katerem je dosegel vidne rezultate na republiški in mednarodni ravni. Opravljen ima tudi izpit za republiškega sodnika. Po končani maturi se je leta 1999 vpisal na Fakulteto za strojništvo v Ljubljani in junija leta 2004 dobil naziv univerzitetnega diplomiranega inženirja. Med študijem na Fakulteti za strojništvo je bil proglašen za najuspešnejšega študenta univerzitetnega študija v letu 2002/2003.

Že v času študija je pričel z raziskovanjem na področju energetskega strojništva in je soavtor treh prispevkov objavljenih na mednarodnih konferecah. Sodeloval je pri razvoju enote za pozicioniranje na Turboinštitutu v Ljubljani, opravil 2. delovno prakso v Laboratoriju za termoenergetiko na fakulteti, udeležil se je dvotedenskega tečaja energetikov v Nemčiji in med drugim prejel tudi štipendijo mestne občine Ljubljana za nadarjene študente.

Sedaj je mladi raziskovalec, zaposlen na Fakulteti za strojništvo v Ljubljani.

Kandidat Jure Smrekar je v izbor za Prešernovo nagrado predložil delo z naslovom Neželjeni dinamični pojavi v hladilnem stolpu in njihov vpliv na kvaliteto obratovanja termoelektrarne. Osnovna ideja je, kako z merilnimi in statističnimi metodami poboljšati delovanje hladilnih stolpov in s tem povečati izkoristke in moči termoelektrarn. Povzel je metodo, ki izhaja iz končanega evropskega projekta Copernicus in sloni na meritvah temperatur in masnih pretokov vode in zraka v hladilnem stolpu. Sistem meritev je nadgradil z statističnimi modeli, s katerimi je preko eksergijske analize povezal lokalne in integralne lastnosti delovanja hladilnih stolpov. Pokazal je, da je z razporejanjem masnega pretoka vode tako, da porazdelitev vode v stolpu prilagajamo lokalnim hitrostim hladilnega zraka, mogoče vplivati na zmanjšanje generacije entropije in s tem povečati izkoristek hladilnega stolpa. Raziskal je parametre, ki pomembno vplivajo na kakovost obratovanja in predlagal ter utemeljil nekatere izboljšave za povečanje integralne učinkovitosti stolpa. Predstavljena metoda omogoča hitro oceno možnih ukrepov za izboljšanje prenosa toplote v stolpu, kar je pogoj za povečanje izkoristka hladilnega stolpa ter povečanje moči termoelektrarne.

3. FAKULTETNA NAGRADA ZA SKUPINSKO DELO
Vasja Ravbar, Željko Pelengić

Naslov: Razvoj in uporaba opto-mehatronskega sistema za določitev reliefa majhnih predmetov
Mentor: doc.dr. Janez Diaci
Somentor: doc.dr. Ivan Polajnar

Žejko Pelengić se je rodil 3.5.1979 v Šempetru pri Gorici. Po končani osnovni šoli se je v šolskem letu 1993/94 vpisal na Srednjo tehniško šolo v Novi Gorici in jo leta 1998 sklenil z uspešno opravljeno maturo. Istega leta se je kot redni študent vpisal na Fakulteto za strojništvo v Ljubljani v univerzitetni študijski program. Študij je uspešno končal septembra

2004 z diplomsko nalogo »Projektorji strukturirane svetlobe za optične meritve majhnih sprememb površine« pod mentorstvom doc.dr. Janeza Diacija.

Vasja Ravbar se je rodil 20.11.1979 v Šempetru pri Gorici. Obiskoval je osnovno šolo Frana Erjavca v Novi Gorici, ki jo je v šolskem letu 1993/94 zaključil z odličnim uspehom. Šolanje je nadaljeval na Tehniškem šolskem centru Nova Gorica, kjer je leta 1998 maturiral. Istega leta se je vpisal na Univerzo v Ljubljani – Fakulteto za strojništvo. Študij je končal z uspešnim zagovorom diplomske naloge »Razvoj algoritma določitve reliefa majhnih predmetov«, ki jo je izdelal pod mentorstvom doc.dr. Janeza Diacija in somentorstvom doc.dr. Ivana Polajnarja.

Nagrajenca sta se že v času študija vključila v raziskovalno delo na področju mehantronike in laserske tehnike. Rezultate svojega dela sta samostojno predstavila na dveh domačih konferencah.

Avtorja v delu predstavljata razvoj sistema, ki je zasnovan na metodi optične triangulacije in omogoča merjenje oblike površine majhnih predmetov. Pri tem jima je vodilni cilj razvoja možnost aplikacije razvitega sistema na področju sprotnega spremljanja degradacije tehničnih površin.

V okviru eksperimentalnega dela sta avtorja med drugim razvila in izdelala izviren projektor na podlagi svetlečih diod, za katerega sta pokazala, da omogoča bistveno večjo prilagodljivost osvetljevanja od tržno dosegljivih laserskih projektorjev. Globino teoretične podlage sta izkazala med drugim z izpopolnitvijo algoritma, ki sta ga uporabila za določitev oblike površine, z avtomatskim generiranjem referenčne ploskve iz zajete slike in izbiro optimalne poti rekonstrukcije oblike.

To jima je omogočilo izvedbo eksperimenta, s katerim sta dokazala, da je z njunim sistemom mogoče spremljati postopno degradacijo elektrodnih konic pri uporovnem točkovnem varjenju na stroju po vsakem izvedenem zvaru. Tak ekspriment doslej v dostopni literaturi še ni bil opisan in odpira povsem nove možnosti za raziskave degradacije elektrodnih konic.

Doktorati, magisteriji, diplome

DOKTORATI

Na Fakulteti za strojništvo Univerze v Mariboru sta z uspehom zagovarjala svoji doktorski disertaciji:

dne 11. novembra 2004: **Uroš Župerl,** z naslovom: »Dinamično optimiranje rezalnih pogojev med postopkom frezanja z uporabo hibridnih nevronsko-evolucijskih tehnik« in

dne 22. novembra 2004: **Matjaž Ramšak,** z naslovom: »Večobmočna metoda robnih elementov za dvoenačbne turbulentne modele«.

S tem sta navedena kandidata dosegla akademsko stopnjo doktorja znanosti.

MAGISTERIJI

Na Fakulteti za strojništvo Univerze v Ljubljani je z uspehom zagovarjal svoje magistrsko delo:

dne 12. novembra 2004: **Robert Planinc**, z naslovom: »Izboljšave sistema za rokovanje z jedrskim gorivom«.

Na Fakulteti za strojništvo Univerze v Mariboru je z uspehom zagovarjal svoje magistrsko delo:

dne 11. novembra 2004: **Brigita Tepuš**, z naslovom: "Odstranjevanje dušika iz komunalne odpadne vode".

S tem sta navedena kandidata dosegla akademsko stopnjo magistra znanosti.

DIPLOMIRALI SO

Na Fakulteti za strojništvo Univerze v Ljubljani so pridobili naziv univerzitetni diplomirani inženir strojništva:

dne 29. novembra 2004: Leon NASTAV, Matjaž OBRČ, Marko SEDLAČEK.

*

Na Fakulteti za strojništvo Univerze v Ljubljani so pridobili naziv diplomirani inženir strojništva:

dne 11. novembra 2004: Marko MUZIC, Igor NELEC;

dne 12. novembra 2004: Matjaž DOLINAR, Antonio Pablo JERETINA, Roman LAŠIČ, Jure LONCNAR, Jure OLAJ, Matjaž PAJEK, Borut VEHAR, Simon ZARABEC.

Na Fakulteti za strojništvo Univerze v Mariboru so pridobili naziv diplomirani inženir strojništva:

dne 24. novembra 2004: Franc GAJŠEK, Marko GRMEK, Jožef KOŠČAK, Srečko ŠTEFLIČ, Uroš VRČKOVNIK.

© Strojniški vestnik 50(2004)12,635
Mesečnik
ISSN 0039-2480

© Journal of Mechanical Engineering 50(2004)12,635
Published monthly
ISSN 0039-2480

Recenzenti letnika 2004

Reviewers of 2004 Volume

Strojniški vestnik - Journal of Mechanical Engineering
letnik - volume 50, (2004), številke - numbers 1-12

Tuji recenzenti / International reviewers:

prof.dr. Ryszard A. Białecki, Silesian University of Technology
prof. dr. Kurt Desoyer, Technical University of Vienna
prof. dr. Leszek Dobrzański, Silesian University of Technology
prof. dr. Ivan Filipović, University of Sarajevo
prof. dr. Adolf Frank, Technical University of Graz
prof. dr. Bernard Franković, University of Rijeka
prof. dr. Manfred Geiger, Friedrich-Alexander University
prof. dr. Dusan Gruden, Dr. Ing. h.c. F. Porsche Aktiengesellschaft
dr. E. van der Heide, TNO Industrial Technology
prof. dr. Glenn R. Heppler, University of Waterloo
prof. dr. Horst Herold, Otto-von-Guericke University
prof. dr. Kenneth Holmberg, VTT Industrial Systems
prof. dr. Branko Katalinic, Technical University of Vienna
prof. dr. Božidar Križan, University of Rijeka
prof. dr. Gideon Levy, University of Applied Sciences St. Gallen
prof. dr. Vladimir Medica, University of Rijeka
prof. dr. Andrzej J. Nowak, Silesian University of Technology
prof. dr. Kees Jan Roodbergen, Erasmus University Rotterdam
prof. dr. Victor Starkov, Moscow State Technological University
prof. dr. Luiz C. Wrobel, Brunel University

Domači recenzenti / National reviewers:

prof. dr. Ivan Anžel
prof. dr. Ivo Bajsić
prof. dr. Jože Balič
prof. dr. Miha Boltežar
prof. dr. Franci Čuš
prof. dr. Želimir Dobovišek
doc. dr. Karl Gotlih
prof. dr. Edvard Govekar
prof. dr. Aleš Hribernik
doc. dr. Zoran Kariž
prof. dr. Janez Kopač
prof. dr. Franc Kosel
prof. dr. Janez Kramar
prof. dr. Jurij Krope
prof. dr. Janez Možina
prof. dr. Maks Oblak
prof. dr. Amand Papotnik
doc. dr. Stanislav Pehan
prof. dr. Andrej Polajnar
prof. dr. Alojz Poredoš
prof. dr. Rudolf Pušenjak
prof. dr. Iztok Potrč
dr. Zlatko Rek
doc. dr. Niko Samec
prof. dr. Marko Starbek
prof. dr. Brane Širok
doc. dr. Borivoj Šuštaršič
prof. dr. Matija Tuma

© Strojniški vestnik 50(2004)12,636-638
Mesečnik
ISSN 0039-2480

© Journal of Mechanical Engineering 50(2004)12,636-638
Published monthly
ISSN 0039-2480

Vsebina 2004
Contents 2004

Strojniški vestnik - Journal of Mechanical Engineering
letnik - volume 50, (2004), številke - numbers 1-12

Navodila avtorjem
Instructions for Authors

Članki morajo vsebovati:
- naslov, povzetek, besedilo članka in podnaslove slik v slovenskem in angleškem jeziku,
- dvojezične preglednice in slike (diagrami, risbe ali fotografije),
- seznam literature in
- podatke o avtorjih.

Strojniški vestnik izhaja od leta 1992 v dveh jezikih, tj. v slovenščini in angleščini, zato je obvezen prevod v angleščino. Obe besedili morata biti strokovno in jezikovno med seboj usklajeni. Članki naj bodo kratki in naj obsegajo približno 8 tipkanih strani. Izjemoma so strokovni članki, na željo avtorja, lahko tudi samo v slovenščini, vsebovati pa morajo angleški povzetek.

Vsebina članka

Članek naj bo napisan v naslednji obliki:
- Naslov, ki primerno opisuje vsebino članka.
- Povzetek, ki naj bo skrajšana oblika članka in naj ne presega 250 besed. Povzetek mora vsebovati osnove, jedro in cilje raziskave, uporabljeno metodologijo dela,povzetek rezulatov in osnovne sklepe.
- Uvod, v katerem naj bo pregled novejšega stanja in zadostne informacije za razumevanje ter pregled rezultatov dela, predstavljenih v članku.
- Teorija.
- Eksperimentalni del, ki naj vsebuje podatke o postavitvi preskusa in metode, uporabljene pri pridobitvi rezultatov.
- Rezultati, ki naj bodo jasno prikazani, po potrebi v obliki slik in preglednic.
- Razprava, v kateri naj bodo prikazane povezave in posplošitve, uporabljene za pridobitev rezultatov. Prikazana naj bo tudi pomembnost rezultatov in primerjava s poprej objavljenimi deli. (Zaradi narave posameznih raziskav so lahko rezultati in razprava, za jasnost in preprostejše bralčevo razumevanje, združeni v eno poglavje.)
- Sklepi, v katerih naj bo prikazan en ali več sklepov, ki izhajajo iz rezultatov in razprave.
- Literatura, ki mora biti v besedilu oštevilčena zaporedno in označena z oglatimi oklepaji [1] ter na koncu članka zbrana v seznamu literature. Vse opombe naj bodo označene z uporabo dvignjene številke[1].

Oblika članka

Besedilo naj bo pisano na listih formata A4, z dvojnim presledkom med vrstami in s 3 cm širokim robom, da je dovolj prostora za popravke lektorjev. Najbolje je, da pripravite besedilo v urejevalnilku Microsoft Word. Hkrati dostavite odtis članka na papirju, vključno z vsemi slikami in preglednicami ter identično kopijo v elektronski obliki.

Prosimo, da ne uporabljate urejevalnika LaTeX, saj program, s katerim pripravljamo Strojniški vestnik, ne uporablja njegovega formata. V urejevalniku LaTeX oblikujte grafe, preglednice in enačbe in jih stiskajte na kakovostnem laserskem tiskalniku, da jih bomo lahko presneli.

Enačbe naj bodo v besedilu postavljene v ločene vrstice in na desnem robu označene s tekočo številko v okroglih oklepajih

Enote in okrajšave

V besedilu, preglednicah in slikah uporabljajte le standardne označbe in okrajšave SI. Simbole fizikalnih veličin v besedilu pišite poševno (kurzivno), (npr. *v, T, n* itn.). Simbole enot, ki sestojijo iz črk, pa pokončno (npr. ms^{-1}, K, min, mm itn.).

Vse okrajšave naj bodo, ko se prvič pojavijo, napisane v celoti v slovenskem jeziku, npr. časovno spremenljiva geometrija (ČSG).

Papers submitted for publication should comprise:
- Title, Abstract, Main Body of Text and Figure Captions in Slovene and English,
- Bilingual Tables and Figures (graphs, drawings or photographs),
- List of references and
- Information about the authors.

Since 1992, the Journal of Mechanical Engineering has been published bilingually, in Slovenian and English. The two texts must be compatible both in terms of technical content and language. Papers should be as short as possible and should on average comprise 8 typed pages. In exceptional cases, at the request of the authors, speciality papers may be written only in Slovene, but must include an English abstract.

The format of the paper

The paper should be written in the following format:
- A Title, which adequately describes the content of the paper.
- An Abstract, which should be viewed as a miniversion of the paper and should not exceed 250 words. The Abstract should state the principal objectives and the scope of the investigation, the methodology employed, summarize the results and state the principal conclusions.
- An Introduction, which should provide a review of recent literature and sufficient background information to allow the results of the paper to be understood and evaluated.
- A Theory
- An Experimental section, which should provide details of the experimental set-up and the methods used for obtaining the results.
- A Results section, which should clearly and concisely present the data using figures and tables where appropriate.
- A Discussion section, which should describe the relationships and generalisations shown by the results and discuss the significance of the results making comparisons with previously published work. (Because of the nature of some studies it may be appropriate to combine the Results and Discussion sections into a single section to improve the clarity and make it easier for the reader.)
- Conclusions, which should present one or more conclusions that have been drawn from the results and subsequent discussion.
- References, which must be numbered consecutively in the text using square brackets [1] and collected together in a reference list at the end of the paper. Any footnotes should be indicated by the use of a superscript[1].

The layout of the text

Texts should be written in A4 format, with double spacing and margins of 3 cm to provide editors with space to write in their corrections. Microsoft Word for Windows is the preferred format for submission. One hard copy, including all figures, tables and illustrations and an identical electronic version of the manuscript must be submitted simultaneously.

Please do not use a LaTeX text editor, since this is not compatible with the publishing procedure of the Journal of Mechanical Engineering. Graphs, tables and equations in LaTeX may be supplied in good quality hard-copy format, so that they can be copied for inclusion in the Journal.

Equations should be on a separate line in the main body of the text and marked on the right-hand side of the page with numbers in round brackets.

Units and abbreviations

Only standard SI symbols and abbreviations should be used in the text, tables and figures. Symbols for physical quantities in the text should be written in Italics (e.g. *v, T, n,* etc.). Symbols for units that consist of letters should be in plain text (e.g. ms^{-1}, K, min, mm, etc.).

All abbreviations should be spelt out in full on first appearance, e.g., variable time geometry (VTG).

Slike

Slike morajo biti zaporedno oštevilčene in označene, v besedilu in podnaslovu, kot sl. 1, sl. 2 itn. Posnete naj bodo v kateremkoli od razširjenih formatov, npr. BMP, JPG, GIF. Za pripravo diagramov in risb priporočamo CDR format (CorelDraw), saj so slike v njem vektorske in jih lahko pri končni obdelavi preprosto povečujemo ali pomanjšujemo.

Pri označevanju osi v diagramih, kadar je le mogoče, uporabite označbe veličin (npr. *t, v, m* itn.), da ni potrebno dvojezično označevanje. V diagramih z več krivuljami, mora biti vsaka krivulja označena. Pomen oznake mora biti pojasnjen v podnapisu slike.

Vse označbe na slikah morajo biti dvojezične.

Za vse slike po fotografskih posnetkih je treba priložiti izvirne fotografije ali kakovostno narejen posnetek. V izjemnih primerih so lahko slike tudi barvne.

Preglednice

Preglednice morajo biti zaporedno oštevilčene in označene, v besedilu in podnaslovu, kot preglednica 1, preglednica 2 itn. V preglednicah ne uporabljajte izpisanih imen veličin, ampak samo ustrezne simbole, da se izognemo dvojezični podvojitvi imen. K fizikalnim veličinam, npr. *t* (pisano poševno), pripišite enote (pisano pokončno) v novo vrsto brez oklepajev.

Vsi podnaslovi preglednic morajo biti dvojezični.

Seznam literature

Vsa literatura mora biti navedena v seznamu na koncu članka v prikazani obliki po vrsti za revije, zbornike in knjige:

[1] Tarng, Y.S., Y.S. Wang (1994) A new adaptive controler for constant turning force. *Int J Adv Manuf Technol* 9(1994) London, pp. 211-216.

[2] Čuš, F., J. Balič (1996) Rationale Gestaltung der organisatorischen Abläufe im Werkzeugwesen. *Proceedings of International Conference on Computer Integration Manufacturing,* Zakopane, 14.-17. maj 1996.

[3] Oertli, P.C. (1977) Praktische Wirtschaftskybernetik. *Carl Hanser Verlag,* München.

Podatki o avtorjih

Članku priložite tudi podatke o avtorjih: imena, nazive, popolne poštne naslove, številke telefona in faksa ter naslove elektronske pošte.

Sprejem člankov in avtorske pravice

Uredništvo Strojniškega vestnika si pridržuje pravico do odločanja o sprejemu članka za objavo, strokovno oceno recenzentov in morebitnem predlogu za krajšanje ali izpopolnitev ter terminološke in jezikovne korekture.

Avtor mora predložiti pisno izjavo, da je besedilo njegovo izvirno delo in ni bilo v dani obliki še nikjer objavljeno. Z objavo preidejo avtorske pravice na Strojniški vestnik. Pri morebitnih kasnejših objavah mora biti SV naveden kot vir.

Rokopisi člankov ostanejo v arhivu SV.

Vsa nadaljnja pojasnila daje:

Uredništvo
STROJNIŠKEGA VESTNIKA
p.p. 197
1001 Ljubljana
Telefon: (01) 4771-137
Telefaks: (01) 2518-567
E-mail: strojniski.vestnik@fs.uni-lj.si

Figures

Figures must be cited in consecutive numerical order in the text and referred to in both the text and the caption as Fig. 1, Fig. 2, etc. Figures may be saved in any common format, e.g. BMP, GIF, JPG. However, the use of CDR format (CorelDraw) is recommended for graphs and line drawings, since vector images can be easily reduced or enlarged during final processing of the paper.

When labelling axes, physical quantities, e.g. *t, v, m,* etc. should be used whenever possible to minimise the need to label the axes in two languages. Multi-curve graphs should have individual curves marked with a symbol, the meaning of the symbol should be explained in the figure caption.

All figure captions must be bilingual.

Good quality black-and-white photographs or scanned images should be supplied for illustrations. In certain circumstances, colour figures may be considered.

Tables

Tables must be cited in consecutive numerical order in the text and referred to in both the text and the caption as Table 1, Table 2, etc. The use of names for quantities in tables should be avoided if possible: corresponding symbols are preferred to minimise the need to use both Slovenian and English names. In addition to the physical quantity, e.g. *t* (in Italics), units (normal text), should be added in new line without brackets.

All table captions must be bilingual.

The list of references

References should be collected at the end of the paper in the following styles for journals, proceedings and books, respectively:

[1] Tarng, Y.S., Y.S. Wang (1994) A new adaptive controler for constant turning force. *Int J Adv Manuf Technol* 9(1994) London, pp. 211-216.

[2] Čuš, F., J. Balič (1996) Rationale Gestaltung der organisatorischen Abläufe im Werkzeugwesen. *Proceedings of International Conference on Computer Integration Manufacturing,* Zakopane, 14.-17. maj 1996.

[3] Oertli, P.C. (1977) Praktische Wirtschaftskybernetik. *Carl Hanser Verlag,* München.

Author information

The following information about the authors should be enclosed with the paper: names, complete postal addresses, telephone and fax numbers and E-mail addresses.

Acceptance of papers and copyright

The Editorial Committee of the Journal of Mechanical Engineering reserves the right to decide whether a paper is acceptable for publication, obtain professional reviews for submitted papers, and if necessary, require changes to the content, length or language.

Authors must also enclose a written statement that the paper is original unpublished work, and not under consideration for publication elsewhere. On publication, copyright for the paper shall pass to the Journal of Mechanical Engineering. The JME must be stated as a source in all later publications.

Papers will be kept in the archives of the JME.

You can obtain further information from:

Editorial Board of the
JOURNAL OF MECHANICAL ENGINEERING
P.O.Box 197
1001 Ljubljana, Slovenia
Telephone: +386 (0)1 4771-137
Fax: +386 (0)1 2518-567
E-mail: strojniski.vestnik@fs.uni-lj.si